The Role of the Endoplasmic Reticulum Stress Transducer Ire1 during Photoreceptor Differentiation in *Drosophila*

Dina Raquel da Silva Coelho

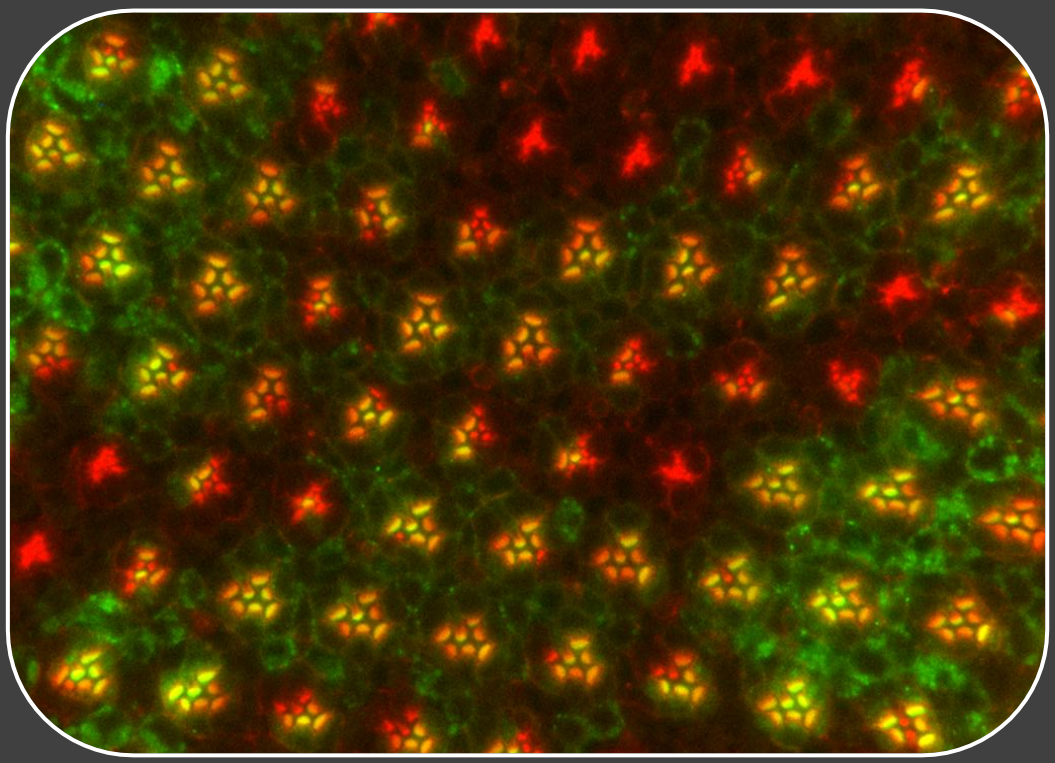

Dissertation presented to obtain the Ph.D degree in Biology

Instituto de Tecnologia Química e Biológica António Xavier | Universidade Nova de Lisboa

Oeiras,
December, 2013

INSTITUTO
DE TECNOLOGIA
QUÍMICA E BIOLÓGICA
ANTÓNIO XAVIER /UNL

Knowledge Creation

The Role of the Endoplasmic Reticulum Stress Transducer Ire1 during Photoreceptor Differentiation in *Drosophila*

Dina Raquel da Silva Coelho

Dissertation presented to obtain the Ph.D degree in Biology

Instituto de Tecnologia Química e Biológica António Xavier | Universidade Nova de Lisboa

Oeiras, December, 2013

INSTITUTO
DE TECNOLOGIA
QUÍMICA E BIOLÓGICA
ANTÓNIO XAVIER /UNL

Knowledge Creation

Oeiras, December, 2013

The Role of the Endoplasmic Reticulum Stress Transducer Ire1 during Photoreceptor Differentiation in *Drosophila*

Dina Raquel da Silva Coelho

ITQB-UNL | Av. da República, 2780-157 Oeiras, Portugal
Tel (+351) 214 469 100 | Fax (+351) 214 411 277

www.itqb.unl.pt

Para a minha Avó Edina.

Acknowledgments

First and foremost I would like to thank my PhD advisor, Pedro Domingos, who took me in the laboratory as an inexperienced master's student and gave me conditions to grow and evolve as a scientist. It was a long journey since Pedro introduced me to the basics in the laboratory until we finally got our paper accepted in a high standard journal. Thank you for pushing me and giving me the motivation that I needed. I feel that my work was completely rewarded and most of the times rewarding, as well. Thank you for supporting me and caring for everybody in the lab.

I want to thank everyone who has helped in my scientific education, but mainly to people in the lab. Fátima Cairrão who showed me molecular biology techniques and Vanya Rasheva who explained me some classical genetics tricks. I appreciate the companionship from girl members of the lab, Nadine, Rita and Tânia.

I am grateful to people who contributed to my paper and provided important results for this thesis: Elisabete Pires, Ana Varela Coelho, Hyung Don Ryoo, Xiaomei Zeng and Fátima Cairrão.

I want also to acknowledgment ITQB, IGC and CEDOC for giving me access to equipment and facilities. In particular I want to acknowledgment Jaime Mota Lab and Cristina Silva Pereira Lab for always sparing reagents and consumables with us and for giving me some precious protocol advices.

I want to acknowledge Gulbenkian Foundation for paying my PhD fellowship and Fundação para a Ciência e Tecnologia for supporting the project through grants PEst-OE/EQB/LA0004/2011, PTDC/BIA-BCM/105217/2008, PTDC/SAU-OBD/104399/2008, and PTDC/ BEX-BCM/1217/2012.

My deepest gratitude is towards my family that made their own my wins and defeats. Thank you for your generosity and for your understanding.

FUNDAÇÃO CALOUSTE GULBENKIAN

FCT

Fundação para a Ciência e a Tecnologia

MINISTÉRIO DA CIÊNCIA, TECNOLOGIA E ENSINO SUPERIOR

Table of contents

List of Figures

Abbreviations

ADP adenosine diphosphate

aPKC: atypical protein kinase C

ARF1: ADP-ribosylation factor 1

Arm: armadillo

Asn: asparagine

ASK1: apoptosis signal-regulating kinase 1

ATF4: activating transcription factor 4

ATF6: activating transcription factor 6

ATP: adenosine triphosphate

BBS: bip-binding site ,

BCL2: B-cell CLL/lymphoma 2

BE: bipartite element

Bip binding immunoglobulin protein

Bp: base pairs

BSA: bovine serum albumin

bZIP: basic leucine zipper domain

cDNA: complementary DNA

CHOP: C/EBP homologous protein

CL: cell lethal

Cnx: calnexin

CRB2: crumbs homolog 2

CRE: cAMP response element

CREBH: cyclic AMP response element binding protein hepatocyte

CTR: c-terminal domain

Dlt: discs-lost

DSHB: developmental studies hybridoma bank

DSS: dextran sodium sulfate

DTT: dithiothreitol

EDAM1: ER degradation enhancer, mannosidase alpha-like 1

EDAM2: ER degradation enhancer, mannosidase alpha-like 2

EGFP: enhanced green fluorescent protein

EGFR: epidermal growth factor receptor

EGUF: eyeless-Gal4 UAS-Flipase

eiF2: eukaryotic translation initiation factor 2

Elav: embryonic lethal abnormal vision

ER: endoplasmic reticulum

Ero1: ER oxidoreductin 1

FATP: fatty acid transporter protein

Flp: flipase recognition target

FRT: flipase recombination target

GADD34: growth arrest and DNA-damage inducible protein-34

GMR: glass multimer reporter

GRP78: 78 kDa glucose-regulated protein

GRP94: 94 kDa glucose-regulated protein

HAC1: homologous to ATF/CREB1

Herp: homocysteine-induced endoplasmic reticulum protein

HR2: hydrophobic region2

HRD1: HMG-CoA reductase degradation protein 1

Hsc3: heat shock cognate 3

HSP40: heat shock protein 40

HSP70: heat shock protein 70

HSP90: heat shock protein90

IKK: inhibitor kβ kinase

Ire1: inositol-requiring enzyme 1

JNK: cJun-N terminal kinase

Kb: kilobase

KEN: kinase extension nuclease

LC-MS: liquid chromatography-mass spectroscopy

LPP: lipid phosphatase phosphohydrolase

MHC: major histocompatibility complex

MyoV: Myosin V

Neo: neomycin

NF-κB: factor nuclear kappa B

ninaA: neither inactivation nor afterpotential A

ninaE: neither inactivation nor afterpotential E (Rhodopsin1 gene)

Nt: nucleotide

PA: phosphatidic acid

Par-3: partitioning defective 3 homolog

pd: pupal development

Pdi: protein disulfide isomerase

Perk: protein kinase (PKR)-like ER kinase

PLD: phosphatidylcholine-hydrolyzing phospholipase D

PP1: protein phosphatase 1

PTEN: Phosphatase and tensin homolog

R1-8: photoreceptor 1-8

Rh1: rhodopsin 1

RIDD: regulated Ire1 dependent decay

RNC ribosome-nascent chain

RNAi: RNA interference

RTW: rhabdomere terminal web

S1P: site 1 protease

S2P: site 2 protease

Ser: serine

SD: standard deviation

SOD1: Super Oxide Dismutase 1

SRP: signal recognition particle

SUMO: small ubiquitin-like modifier

Thr: threonine

TP: translational pausing

TPRs: tetratricopeptide repeats

TRAF2: TNFR-associated factor 2

Trl1: tRNA ligase 1

UAS: upstream activating sequence

UGT: UDP glucose-glycoprotein glucosyl transferase

uORF: upstream open reading frames

UPR: unfolded protein response

UPRE: unfolded protein response element

UTR: untranslated region

USP14: ubiquitin specific protease 14

VCP: Valosin-containing protein (VCP)

Xbp1: X-box binding protein 1

ZA: zonula adherens

Summary

The accumulation of misfolded proteins in the lumen of the endoplasmic reticulum (ER) causes ER stress and activates a homeostatic mechanism termed the Unfolded Protein Response (UPR). The most conserved arm of the UPR is mediated by the ER transmembrane protein Ire1 that removes an unconventional intron from Xbp1 mRNA upon ER stress. Xbp1spliced is an effective transcription factor that up-regulates ER chaperones and enzymes.

This project started with the observation that the ER stress reporter Xbp1-EGFP is activated in the photoreceptors of *Drosophila* eye at mid and late pupal stages, when the morphogenesis of the light sensing organelle (rhabdomere) occurs. I generated Xbp1 null mutations, which I used to investigate the function of the Ire1/Xbp1 signaling during photoreceptor differentiation. I found that Ire1 is required for photoreceptor differentiation and rhabdomere morphogenesis, including delivery of Rhodopsin1 to the rhabdomere and secretion of Spacemaker into the interrhabdomeral space. Xbp1 null mutations do not present the same phenotypes observed in Ire1 mutants. I identified an alternative mechanism for these Xbp1-independent signaling events downstream of Ire1. I found that mRNAs targeted for Regulated Ire1-Dependent Decay (RIDD) are up-regulated in Ire1 mutant eyes, including the mRNA of Fatty acid transport protein (Fatp), a regulator of Rhodopsin1 protein levels. RIDD dependent regulation of Fatp is critical for rhabdomere morphogenesis, since the defects observed in Ire1 mutant photoreceptors are rescued by down-regulation of Fatp by RNA interference and over-expression of Fatp results in phenotypes similar to Ire1 mutants. In addition, I have shown that dysregulation of Fatp in Ire1 mutants results in higher levels of phosphatidic acid and decreasing the levels of phosphatidic acid in Ire1 mutants by expression of Lazaro, an enzyme that converts phosphatidic acid to diacylglycerol, rescues photoreceptor phenotype. Thus, Ire1 regulates the rhabdomere morphogenesis through its RIDD activity, independent of its canonical target Xbp1.

Sumário

A acumulação de proteínas *misfolded* no lúmen do retículo endoplasmático (RE) causa stress celular e ativa um mecanismo homeostático desigando *Unfolded Protein Response (UPR)*. A via de sinalização mais conservada do UPR é mediada por Ire1,uma proteína transmembranar do RE que remove um intrão não conventional do mRNA de Xbp1 em condições de stress no RE. Xbp1spliced é um factor de transcrição eficiente que activa chaperones e enzimas do RE.

Este projecto começou com a observação que o repórter de stress no RE Xbp1-EGFP é ativado nos fotoreceptores do olho de *Drosophila* em fases intermédias e avançadas do desenvolvimento na pupa, aquando da morfogénese do organelo sensível à luz (rabdómero). Após gerar mutantes nulos de Xbp1, investiguei a função da sinalização mediada por Ire1/Xbp1 durante a diferenciação dos photoreceptores. Descobri que Ire1 é necessária para a diferenciação dos fotoreceptores e morfogénse do rabdómero, nomeadamente para o transporte de Rodopsina1 para o rabdómero e para a secreção de Spacemaker para o espaço interrabdomérico. Os mutantes nulos de Xbp1 não apresentam os mesmos fenótipos observados nos mutantes de Ire1. Identifiquei um mecanismo alternativo de sinalização a jusante de Ire1, independente de Xbp1. Descobri que a expressão de mRNAs alvo de Regulated Ire1-Dependent Decay (RIDD) está aumentada em photoreceptores mutantes para Ire1, incluindo o mRNA de Fatp (Fatty acid transport protein), um regulador dos níveis de Rodopsina1. A regulação de Fatp através de RIDD é crítica para a morfogénese do rabdómero já que defeitos observados em photoreceptores mutantes para Ire1 são recuperados através da sob-regulação de Fatp por RNA de interferência e a sobre-expressão de Fatp resulta em fenótipos semelhantes aos observados em mutantes de Ire1. Mostrei ainda que a desregulação de Fatp em olhos mutantes para Ire1 leva a níveis aumentados de ácido fosfatídico e a expressão de Lazaro, uma enzima que converte ácido fosfatidico em diacilglicerol, nos muatntes de Ire1 reverte o fenótipo para

selvagem. Portanto, Ire1 regula a morfogénese do rabdómero através da sua atividade de RIDD, a qual é independente do seu alvo canónico Xbp1.

Introduction

CHAPTER I

1. The Endoplasmic Reticulum

The endoplasmic reticulum or ER is an organelle present in all eukaryotic cells. The ER is organized in an extensive network of flattened sac and branching tubules and its membrane constitutes more than half of the total membrane in the cell, forming a continuum with the nuclear envelope (**Figure1.1**) (Cooper, 2000). The ER is the main cellular storage of intracellular calcium and works as a factory for the synthesis of membrane lipids like phospholipids and cholesterol. The ER is also the entry site for the secretory pathway: all proteins targeted for the plasma membrane, extracellular space and some organelles (the ER itself, the Golgi apparatus, the lysosomes, the endosomes) are imported into the ER from the cytosol, where they are folded and modified (Cooper, 2000).

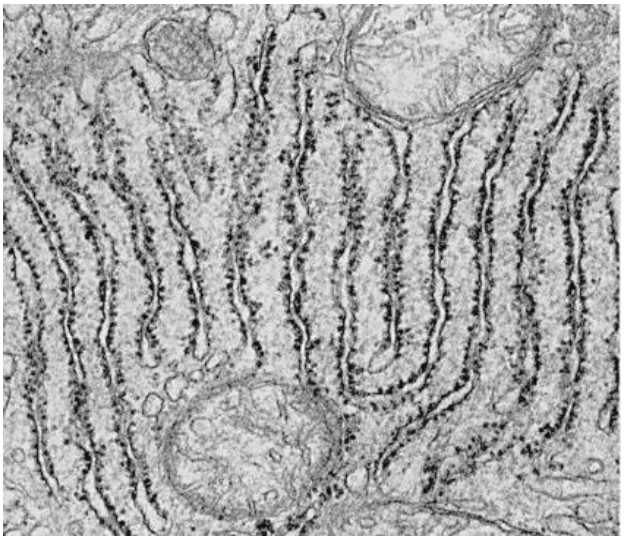

Figure 1.1 The endoplasmic reticulum.

Electron micrograph of ribosomes (black dots) attached to the endoplasmic reticulum. Membrane regions bound by ribosomes are termed rough endoplasmic reticulum.

1.1 Folding and Post-translational Modifications

Proteins can be translocated into the ER after translation by free ribosomes in the cytosol (post-translationally) or during translation by ER membrane bound

ribosomes (co-translationally) (Wickner and Schekman, 2005). In both cases, the unfolded polypeptide transverse the ER membrane through a pore formed by the Sec61 complex (Robson and Collinson, 2006). Co-translational translocation is initiated when a signal recognition particle (SRP) detects a hydrophobic signal sequence in the nascent polypeptide chain and directs it to the ER membrane (Lütcke, 1995). The process of protein synthesis drives the translocation of growing polypeptide chains. Post-translational translocation does not require SRP and the signal sequence is recognized by receptor proteins of the Sec62/63 complex associated with Sec61 in the ER membrane (Ng et al., 1996). In the luminal face of the ER membrane, the chaperone GRP78 binds the polypeptide and pulls it into the ER lumen.

In the ER lumen, polypeptide chains fold into their correct three-dimensional conformation and polypeptides are assembled into multi-subunit proteins (**Figure1.2**). For any protein, the number of possible conformations corresponds to the possible interactions of its amino acid residues, which is determined by the characteristics of its amino acid sequence. During folding, the proteins undergo transient conformational changes until they achieve the most stable conformation and with less free energy, that is called native conformation (Anfinsen and Scheraga, 1975).

To form secondary and tertiary structures, in which residues far apart in the polypeptide chain interact, such as β-sheets or disulfide bonds, the polypeptide must be maintained in a folding competent state. Resident molecular chaperones of the ER bind folding intermediates and facilitate their folding by shielding hydrophobic patches at their surface and avoiding improper interactions with other proteins in the lumen of the ER (Blond-Elguindi et al., 1993; Flynn et al., 1991). Interaction with chaperones consumes ATP and the folding of many secretory proteins is inhibited by depletion of ATP (Dorner et al., 1990). ER chaperones and co-chaperones are classified into several groups according to their cytosolic counterparts: HSP70 class includes Bip/GRP78 (Haas and Wabl, 1983; Munro and Pelham, 1986); HSP90 class, e.g. GRP94/endopasmin (Lee et

al., 1984), DNA-J-like/HSP40 class (Chevalier et al., 2000; Cunnea et al., 2003; Schlenstedt et al., 1995) and GrpE class (Chung et al., 2002). Foldases catalyze protein folding steps to increase their rates, for instance, *cis-trans* peptidyl-propyl isomerases catalyze the cis-trans isomerization of peptidyl-propyl bonds (Price et al., 1991; Spik et al., 1991).

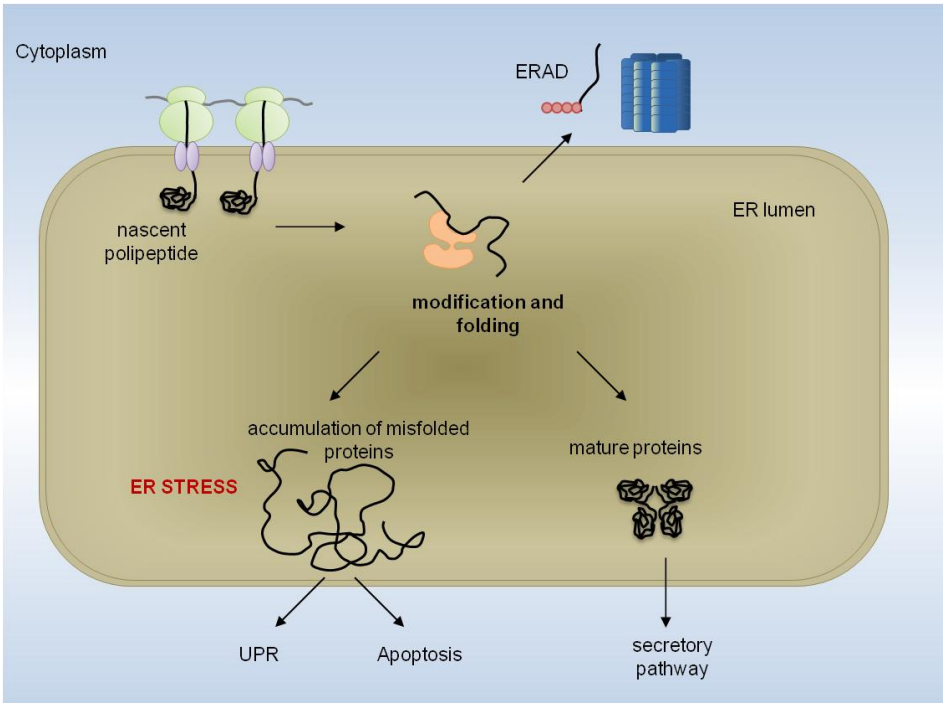

Figure 1.2. The endoplasmic reticulum is the entry site for the secretory pathway.

Proteins are translocated into the ER lumen, where chaperones and folding enzymes assist in the folding of the nascent polypeptide. Correctly folded proteins are transported to the Golgi and proceed in the secretory pathway *en route* to the plasma membrane or the extracellular space. Proteins that are unable to achieve a native conformation are dislocated into the cytoplasm and degraded by the ubiquitin/proteasome system, a process known as ER-associated degradation (ERAD). Under certain conditions, misfolded proteins accumulate in the ER and cause ER stress. The Unfolded Protein Response (UPR) is activated as an adaptative mechanism to ER stress. In case of overwhelming ER stress the cell dies by apoptosis.

The ER is also the site where proteins undergo covalent modifications, such as disulfide bond formation, lipidation, initial stages of glycosylation, and addition of glycolipid anchors to plasma membrane proteins. Disulfide bond formation between the side chains of cysteine residues (S—S) has an important role in the structure of secreted and membrane surface proteins. Pdi (Protein disulfide isomerase) catalyses the formation of disulfide bond and Ero-1 (ER oxidoreductin 1) reconverts Pdi into its reduced form (Freedman, 1989; Frand and Kaiser, 1998).

Nascent polypeptides are glycosylated (N-linked glicosilation) while they are translocated into the ER. An oligosaccharide with 14 sugars is transferred to the side chain of an asparagine residue in the consensus sequence Asn-x-Ser/Thr by a membrane bound oligosaccharyl transferase (Hubbard and Ivatt, 1981; Kornfeld and Kornfeld, 1985). Some proteins require N-linked glycosylation for proper folding in the ER. One arm of the ER quality control, the calnexin/calreticulin machinery, monitors the folding status by interaction with sugar residues in folding intermediates (Ellgaard and Helenius, 2003). After addition of the core oligosaccharide, two glucoses are sequentially removed by glucosidase I and glucosidase II. The monoglycosilated glycan of unfolded proteins interact with the lectins calnexin and calreticulin, retaining them in the ER. When a third glucose is removed from the glycan, the protein dissociates from calnexin/calreticulin and can leave the ER. However, if the protein is still unfolded, UGT (UDP glucose-glycoprotein glucosyl transferase) adds another glucose residue and the unfolded protein goes through another cycle of interaction with calnexin/calreticulin. An unfolded protein undergoes continuous cycles of de- and re-glucosylation, and maintains an affinity for calnexin and calreticulin until it has achieved its fully folded state.

1.2 ER-Associated Degradation

Proteins that fail to fold into their native conformation are targeted to the ER associated degradation (ERAD) pathway (**Figure1.3**). Proteins marked as terminally misfolded are dislocated to the cytoplasm, where they are degraded by the ubiquitin-proteosome system (Claessen et al., 2012; Smith et al., 2011). ERAD machinery includes chaperones that extract misfolded proteins from the pro-folding machinery, a complex in the ER membrane which coordinates and drives protein dislocation across the membrane, and ubiquitination/deubiquitination proteins and proteosome in the cytoplasm. Damaged ER compartments and aggregated misfolded proteins might also be eliminated by autophagy (Bernales et al., 2006). Autophagy is a survival response linked to adaptation to starvation that involves the sequestration of substrates in autophagosomes and fusion with lysosome containing hydrolases. ERAD and autophagy might be coordinated processes, with autophagy being up-regulated upon proteasome impairment (Nedelsky et al., 2008).

Depending on the topology of the substrate, *i. e.,* misfolded domains in the ER lumen, membrane, or cytosolic compartments of the protein, a distinct ERAD pathway is engaged. Studies in yeast and metazoan have revealed a great complexity and diversity of key ERAD components and adaptor proteins for some model substrates. The transmembrane complexes associated with E3 ubiquitin ligases have a central role and are common to all pathways (Carvalho et al., 2006; Denic et al., 2006; Gauss et al., 2006a). E3 ubiquitin ligases have a variable number of transmembrane domains, a cytoplasmic RING domain and catalyze substrate ubiquitylation (Gardner et al., 2000). E3 ligase complexes organize the machinery that coordinates events on both sides of the ER membrane. The prototipycal E3 ligase is Hrd1 (HMG-CoA reductase degradation protein 1) in yeast or HRD1, its mammalian homolog. Hrd1 over-expression is sufficient to promote the degradation of ER luminal proteins (Carvalho et al., 2010). Hrd1 is active in an oligomeric complex, whose assembly is regulated by

Usa1. However Usa1 is not required for the degradation of some subtracts and a mammalian homolog has not be identified (Carvalho et al., 2006).

Adaptor proteins in the E3 ligase bound complex determine substrate specificity by recruiting misfolded proteins to the membrane. The most well characterized adaptor protein is Hrd3 in yeast and its counterpart SEL1 in mammals. Hrd3 binds misfolded proteins, a interaction that is facilitated by a large luminal domain with multiple tetratricopeptide repeats (TPRs) (Gauss et al., 2006b). Housekeeping chaperones such as Bip can also work as adaptor proteins and delivery proteins to the E3 ligase complexes.

The E3 complex members Derlins have a function which is not fully understood. Yeast Der1p is a multi-pass transmembrane protein that interacts with Hrd1p and Hrd3p as well as with substrates (Gauss et al., 2006a; Carvalho et al., 2006) and are likely protein adaptors. In mammals, Derlin1, Derlin2 and Derlin3 may form homo- and heterodimers, giving rise to the hypothesis that they form (part of) a protein conducting channel (Bagola et al., 2011). Derlins are inactive members of the rhomboid family of proteases that conserve a membrane-embedded hydrophilic domain and can interact with translocation machinery via its C-terminus (Greenblatt et al., 2011). Derlins recruits p97/VCP to functional ERAD complexes for the extraction of misfolded secreted proteins from the cytoplasmic face of the ER membrane (Ye et al., 2004).

The modification of a substrate with ubiquitin can recruit either one of two multiprotein complexes that extract the protein from the ER membrane: the ATPase Cdc48 (p97/VCP in metazoans) or the 19S lid complex of the proteasome (Kalies et al., 2005; Stolz et al., 2011). The core of each complex consists of a ring-shaped, hexameric ATPase of the AAA family and ATP hydrolysis generates the energy necessary for protein dislocation across the membrane and unfolding. 19C docks to the Sec61 channel at the ER membrane (Kalies et al., 2005; Ng et al., 2007). Proteins might be retro-translocated via this channel and delivered directly to the proteasome, which pulls the protein from the ER membrane.

In the cytoplasm, p97 recruits peptide N-glycanase (PNGase) to remove N-linked oligossacharides moiety from substrates before they enter the proteosome (Hirsch et al., 2003). P97 also recruits a de-ubiquitinase YOD1.

The mechanism of ERAD is best understood for the case of luminal glycoproteins. As glycoproteins attempt to achieve their native conformation entering the calnexin/calreticulin cycle, mannosidases mediate competing reactions that remove mannoses residues from the glycan moiety (Ruddock and Molinari, 2006). Removal of a α1,2-linked mannose from the A chain, the only acceptor for UGT-catalyzed protein re-glucosylation, abrogates interaction with calnexin/calreticulin and thus prevents defective folding glycoproteins from entering futile cycles in the calnexin/calreticulin cycle. The kinetics of the de-mannosidase reaction is slow thus only proteins that fail to mature in a timely manner are marked as 'misfolded proteins', a mechanism known as the mannose timer (Helenius, 1994).

In mammals, over-expression of EDEM1 (ER degradation enhancing mannosidase-like Protein 1) enhances the rate of ERAD by accelerating the release of defective folding polypeptides from calnexin (Molinari et al., 2003; Oda et al., 2003). Possibly EDEM1 recognizes proteins marked as misfolded and deliver them to the retro-translocation complex in the membrane. The core component of the E3 complex SEL1L (Hrd3) forms a complex with glycan-binding lectins Yos9p in yeast and OS-9 and XTP3-B in mammals to recruit misfolded proteins ((Bernasconi et al., 2008; Christianson et al., 2008; Denic et al., 2006; Gauss et al., 2006)). EDEM3 (or yeast Htm1p) functions as a exomannosidase that exposes a terminal α(1,6)-bonded mannose in glycoproteins, a commitment step required for effect degradation, which is recognized by Yos9p/OS-9/XTP3-B ((Clerc et al., 2009; Hosokawa et al., 2009; Quan et al., 2008)). To facilitate retro-translocation ER enzymes help processing ERAD substrates, for example ERdj5 can reduce disulfide bonds of aberrantly linked proteins and alleviate compact folds and accelerates ERAD rate when overexpressed (Ushioda et al., 2008).

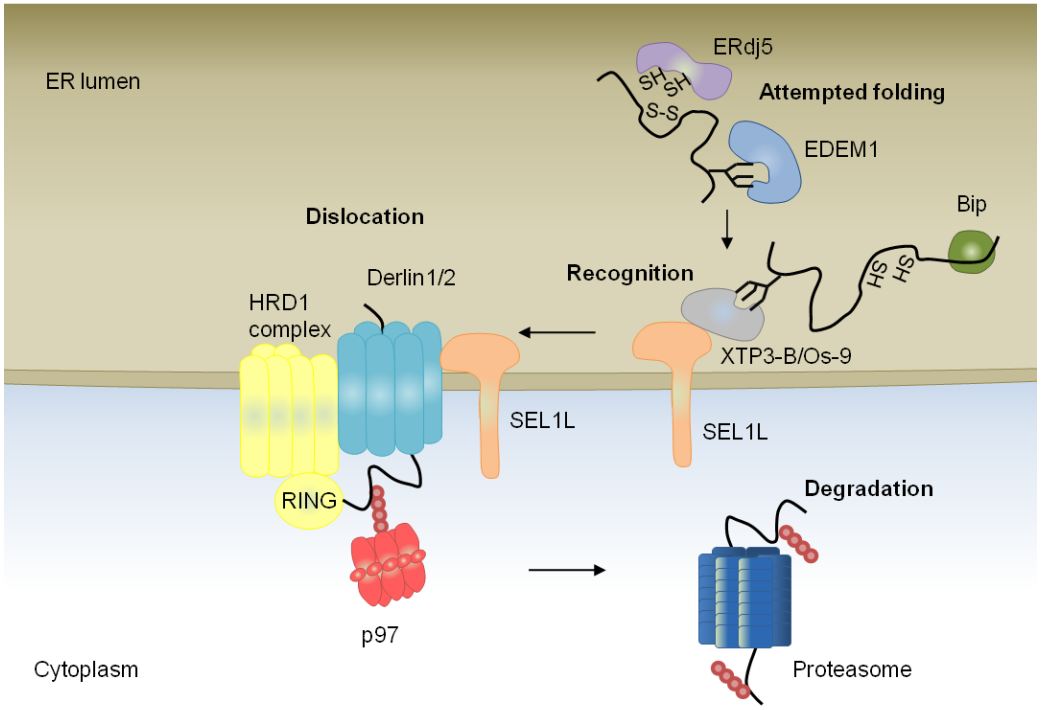

Figure 1.3 The events and components of ERAD.

The key steps of ERAD for a luminal glycoprotein in metazoans. See text for details. Adapted from Smith et al., 2011.

1.3 ER stress and Unfolded Protein Response

A number of cellular stress conditions such as low ATP levels, redox stress or abnormal ER calcium content may perturb protein maturation in the ER and interfere with ER folding capacity. Mutations in the amino acid sequence may render some proteins incompetent to fold and lead to their constitutive retention in the ER (Malhotra and Kaufman, 2007). Many physiological processes may challenge the ER by representing a constant or fast source of large amounts of proteins in the ER (Moore and Hollien, 2012). This is the case of differentiation of highly secretory cells, such as the pancreatic β-cells, that produce insulin in

response to sucrose stimulation. The imbalance between the ER folding capacity and the burden of incoming proteins into the ER leads to the accumulation of misfolded/unfolded proteins in the lumen of the organelle and causes ER stress. Adaptation to ER stress is mediated by the engagement of the Unfolded Protein Response or UPR (Hetz, 2012; Ron and Walter, 2007). The UPR terms a collection of integrated signaling pathways triggered by ER-localized transmembrane receptors, with luminal portions that sense stress in the ER and cytoplasmatic effector portions that interact with the transcriptional or translational apparatus. The UPR changes expression of proteins related to nearly every aspect of the secretory pathway.

The UPR was first described in yeast, where a single ER transmembrane protein, Ire1 (inositol-requiring enzyme 1), mediates one linear pathway (Mori et al., 1992). In higher eukaryotes the UPR gained complexity and is mediated by three ER transmembranar sensors: pancreatic ER kinase (PKR)-like ER kinase (Perk), activating transcription factor 6 (ATF6) and Ire1 (Harding et al., 2002) The outcomes of the three UPR pathways are temporally coordinated: first the general rate of translation is attenuated to reduce the load of protein synthesis into the ER and prevent further accumulation of unfolded proteins; second, genes encoding ERAD components are up-regulated to increase the retro-translocation and degradation of misfolded proteins from the ER; and third, genes encoding ER chaperones and enzymes are up-regulation to enhance the ER folding capacity.

If UPR mechanisms are insufficient to overcome ER stress and restore ER homeostasis, cells undergo apoptosis (Rasheva and Domingos, 2009). Chronic ER stress and deleterious effects of the UPR have been involved in the pathology of human diseases, such as cancer, diabetes, neurodegenerative disorders and inflammation (Wang and Kaufman, 2012). Therefore there has been increasing interest in controlling ER stress pathways and discover new therapeutic targets to treat diseases.

1.4 Ire1 Signaling

Ire1 is the most evolutionarily conserved arm of the UPR, with homologs in yeast, plants, worms, flies and vertebrates (Cox et al., 1993; Koizumi et al., 2001; Mori et al., 1993a; Shen et al., 2001; Wang et al., 1998). Ire1 is a type I ER-resident transmembrane protein with an ER luminal dimerization domain and a cytoplasmic domain with Ser/Thr kinase and endoribonuclease activities (Shamu and Walter, 1996; Tirasophon et al., 1998; Liu et al., 2002).

In the budding yeast the only known substrate of Ire1 is the mRNA of the bZIP transcription factor Hac1 (**Figure1.4**) (Cox and Walter, 1996; Mori et al., 1996; Nikawa et al., 1996). Under normal conditions, Hac1 mRNA is not translated due to a translational attenuation exerted by the base pairing between the 5'UTR and a 262bp intron (Rüegsegger et al., 2001). In case of ER stress, Ire1 oligomerizes and activates its RNase domain by autophosphorylation (Liu et al., 2000; Papa et al., 2003; Shamu and Walter, 1996; Welihinda and Kaufman, 1996). Activated Ire1 recognizes a double stem loop in the intron of Hac1 mRNA and cleaves it twice, leading to the excision of the 252bp intron (Sidrauski and Walter, 1997) A tRNAse ligase, Trl1, joins both ends of the exons (Sidrauski et al., 1996). This unconventional splicing has two consequences: release of the translational repression of Hac1 mRNA and introduction of a new C-terminus during translation that transforms Hac1spliced into an effective transcription factor (Chapman and Walter, 1997; Cox and Walter, 1996). The functional homolog of Hac1 in mammals, worms and flies is Xbp1 (Calfon et al., 2002; Yoshida et al., 2001a); Ryoo et al., 2007; Souid et al., 2007). The intron spliced by Ire1 in Xbp1 mRNA has only 26bp in mammals (or 23bp in *Drosophila*) and does not exert a translational repression. Xbp1 unspliced mRNA is translated under normal conditions but originates a inhibitor of the UPR, which is rapidly degraded (Calfon et al., 2002; Yoshida et al., 2006). Xbp1 spliced protein comprises the original N-terminal DNA binding domain plus an alternative C-terminal domain encoding for a potent trans-activation domain, which is

introduced upon a frame-shit during translation of the spliced Xbp1 mRNA. So far, the ligase that joins the ends of Xbp1 spliced mRNA was not identified.

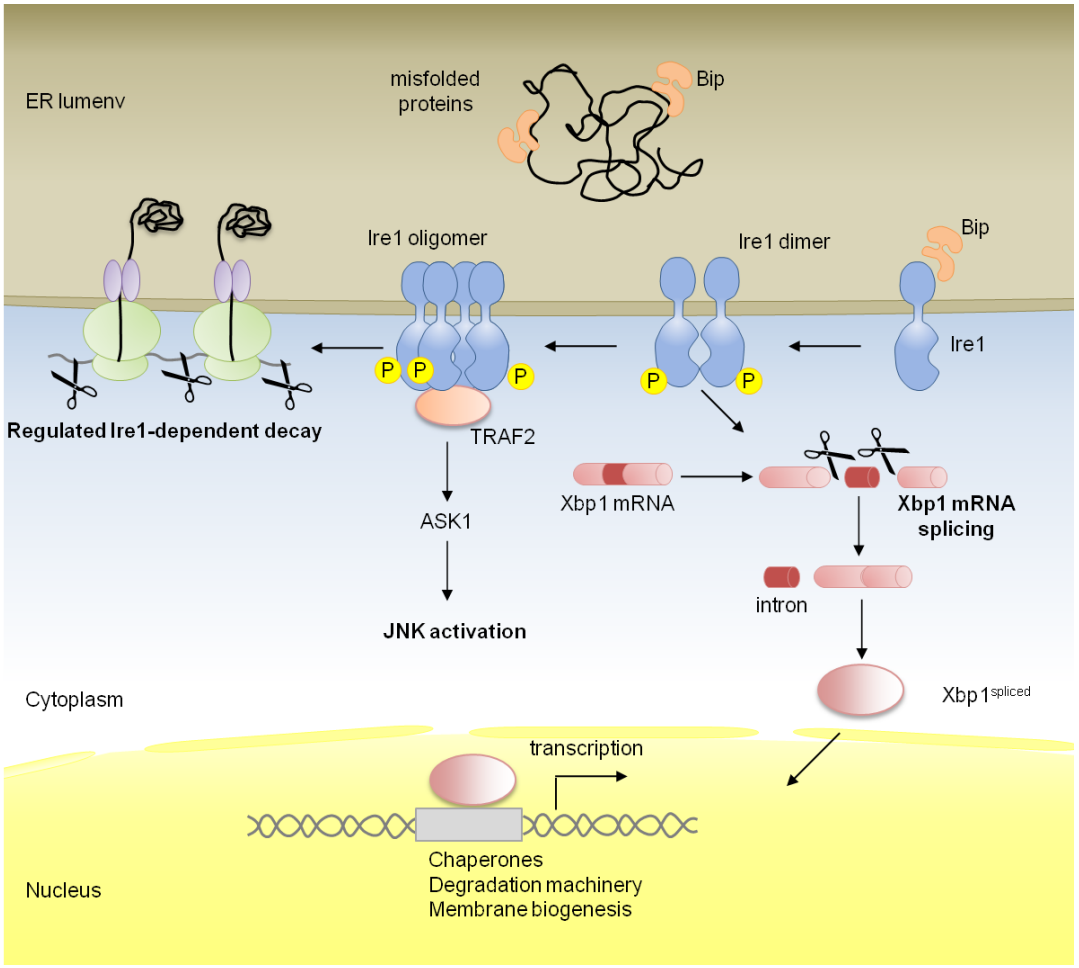

Figure 1.4 Ire1 signaling.

Mechanism of Ire1 activation in stressed cells entails dimerization in the plane of the membrane, nucleotide binding, trans-autophosphorylation and activation of RNase domain. Higher order oligomers might form upon additional stress stimulli. Activated Ire1 mediates the splicing of Xbp1 mRNA in higher eukaryotes or Hac1 in yeast. Excision of the intron results in a frame-shift in Xbp1 transcript and the production of a potent transcription factor. Xbp1spliced has a bZIP domain and regulates UPR target genes that promote protein folding in the ER lumen, ER-associated degradation (ERAD) of misfolded proteins and ER biogenesis. Ire1 can also act by alternative means. Phosphorylated Ire1 associates with TRAF2 and initiates the JNK pathway via ASK1. JNK signaling is associated with insulin resistance and cell death. Ire1 degrades mRNAs localized to the ER membrane through its RNase activity leading to a reduction in proteins imported into the ER lumen.

Spliced Hac1 binds the unfolded protein response element (UPRE) containing the consensus sequence CAGCGTG and Xbp1spliced binds promoters containing CRE (cAMP response element)-like elements [GATGACGTG(T/G)NNN(A/T)T] (Mori et al., 1992, 1998; Clauss et al., 1996). Genetic profiling and genetic analyses reveled that Hac1/Xbp1 control the expression of genes related to the UPR including chaperone induction, up-regulation of ERAD machinery, membrane biogenesis and ER quality control (Lee et al., 2003; Shaffer et al., 2004). In mammals, Xbp1 coordinates the expression of unexpected cell type specific targets linked to cell differentiation, signaling and DNA damage (Acosta-Alvear et al., 2007).

Mechanism of ER stress sensing by Ire1

The mechanism by which the ER luminal domain of Ire1 senses misfolded proteins remains somewhat enigmatic. It has been known that the ER chaperone Bip binds to Ire1 and maintains it in an inactive monomeric state under normal conditions (Bertolotti et al., 2000; Okamura et al., 2000). The model suggested that Bip is a negative regulator of Ire1 activity; and under stress conditions, Bip is mobilized to misfolded proteins allowing Ire1 to multimerize and autophosphorylate on its cytosolic domain. However, mutagenesis analysis showed that variants of Ire1 that do not bind Bip respond normally to stress, leading to the proposal that Bip binding is more important for preventing inappropriate activation of Ire1 rather than eliciting activation by ER stress (Kimata et al., 2003).

Recently the resolution of the crystal structure of the ER luminal domain of yeast and human Ire1 protein brought new insights about the mechanism of Ire1 activation (Credle et al., 2005; Zhou et al., 2006). The luminal domain of yeast Ire1 displays a MHC-like groove and mutations in the amino acids of the groove or in the dimerization interface, abrogate the ability of Ire1 to engage the UPR (Credle et al., 2005). This observation led to the speculation that misfolded proteins may directly bind to the luminal domain of yeast Ire1, facilitating its

oligomerization. *In vitro* studies show that yeast Ire1 binds to a constitutively misfolded form of carboxypeptidase Y through its luminal groove and peptide binding causes Ire1 oligomerization (Gardner and Walter, 2011). A more direct model of activation has now gained strength: first Bip dissociates from Ire1 leading to its dimerization and then direct binding of unfolded proteins to Ire1 luminal domain may contribute to cluster formation and engage full ribonuclease activity (Kimata et al., 2007).

Additional studies with mammalian Ire1 suggest that this mechanism of ER stress sensing might not be conserved. The MHC-like groove of mammalian Ire1 might be too narrow to accommodate an unfolded peptide, as indicated by the crystal structure (Zhou et al., 2006). Furthermore, Ire1 mutants for Bip binding become active even under unstressed conditions and the luminal domain of mammalian Ire1 did not interact with unfolded proteins in an *in vitro* assay (Oikawa et al., 2009). It may be that regulation of mammalian Ire1 depends on Bip dissociation and not on the ligation of misfolded proteins, contrary to the yeast counterpart.

Activation and Regulation of Ire1 RNase activity

The sequential steps of Ire1 activation - oligomerization, autophosphorylation and RNase activitation - have been known for some time. The recent crystal structure models of Ire1 cytosolic domain elucidated the molecular mechanism of its activation, in particularly explaining the coupling of Kinase and RNase activities.

The cytosolic domain of yeast Ire1 was crystallized in an activated state with bound ADP-Mg and phospharylated at the kinase activation loop (**Figure 1.5**). The crystal structure revealed a typical bilobed protein kinase domain, with the ATP-binding site in the cleft between the N-lobe and C-lobe, and an atypical RNase domain formed exclusively by alpha helices, named the KEN (*k*inase *e*xtension *n*uclease) domain. The KEN domain is contiguous and fused to the C-lobe of the kinase domain (Lee et al., 2008). Dimerization of yeast Ire1 in

symmetric back-to-back dimers, creates a cleft with the RNase catalytic active site. Dimers may assemble into rodshaped oligomers with a helical symmetry. In oligomers, the phosporyilated activation loop is ordered, and contributes to a stable active conformation by forming salt bridges with residues in *cis* (Korennykh et al., 2009).

The crystal structure of a cytoplasmatic portion of dephosphorylated human Ire1α bound to ADP further supported the previous data from yeast Ire1 and added new details. The model for human Ire1 predicted a face-to-face dimer with the ATP binding pockets facing each other and the activation loops juxtaposing, in a position favoring trans-autophosphorylation (Ali et al., 2011). The face-to-face dimer is predicted to be an intermediate state that precedes the back to back activated state described in yeast.

Association into high order oligomers reinforces RNase activity, as suggested by cooperative activation of the Ire1 RNase *in vitro* and stabilization of the RNase active site in crystallized oligomers (Li et al., 2010). The RNA binding cavity created by two RNase domains accommodates only one RNA stem loop and the docking is probably asymmetric. Both Ire1 monomers participate in the recognition of the stem loop but only one active site, with the catalytic residues H1061 and Y1043 is used (Korennykh et al., 2011a).

Cofactors bind the ATP-binding pocket of the Ire1 kinase and modulate the RNase activity and oligomerization of Ire1. Following dimerization, the alpha C-helix moves into an active conformation, enabling productive ATP docking and phosphorylation (Korennykh et al., 2009, 2011b). ADP, which is the natural co-factor, modulates the position of the alpha C-helix. ADP and synthetic molecules as APY29 may induce a 200-fold increase in the RNase activity (Korennykh et al., 2011b). A screen to identify new Ire1 modulators identified flavonoids as activators of the RNase activity. The most potent flavonoid activator of RNase activity was quercitin, which binds to a deep buried hydrophobic pocket at the dimer interface and might further stabilize dimers (Wiseman et al., 2010).

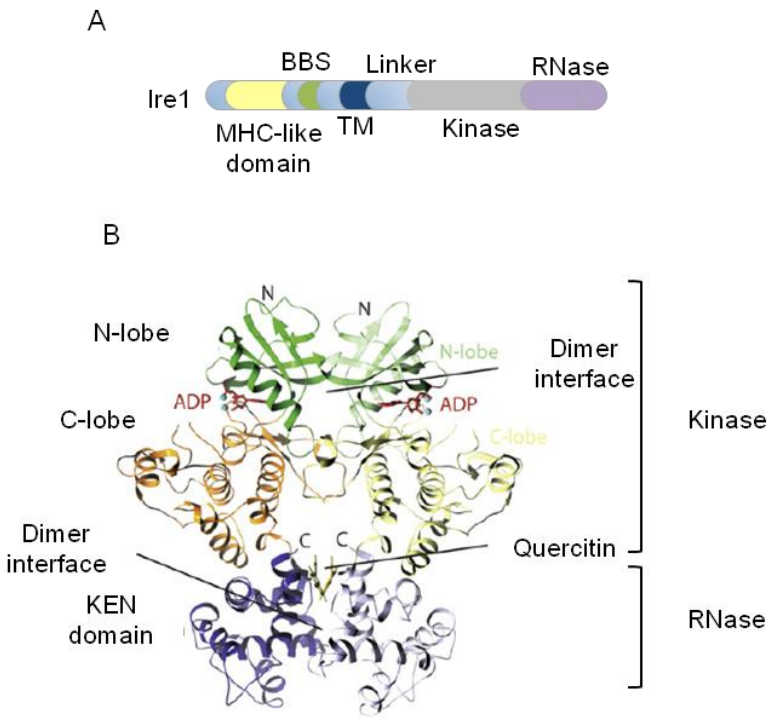

Figure 1.5 Structure of Ire1.

(A) A schematic representation of the yeast Ire1 structure indicating the kinase and RNase domains, BiP-binding site (BBS), the MHC-like domain, linker region and transmembrane region (TM).
(B) Crystal structure of the cytoplasmic domain of yeast Ire1 bound with ADP and quercetin. One dimer is represented and the interfaces between the monomers are indicated. The N- and C-terminal lobes of the kinase domain are green and orange, respectively, and the KEN domain (containing the RNase activity) is blue. Adapted from Wiseman et al., 2010.

Besides promoting stronger Ire1 self association, autophosphorylation may have a role in shutting down Ire1 after ER adaptation. Yeast cells with kinase inactive Ire1 have defects in the deactivation of Ire1, causing chronic ER stress (Rubio et al., 2011). Phosphorylation may serve as a timer to count the duration of the Ire1 signaling and hiper-phosphorylation may help to the disassembly of Ire1 signaling complexes. The existence of this timer is observed in human

Ire1, where oligomers disassemble concomitantly with Ire1 dephosphorylation, even if the source of stress has not been mitigated (Li et al., 2010). After inactivation, Ire1 enters a refractive state in which Ire1 no longer responds to ER stress.

Targeting of Hac1/Xbp1 mRNA to Ire1

To be unconventionally spliced by Ire1, Hac1/Xbp1 mRNA must reach the ER surface where Ire1 is localized. The mechanism of recruitment of the Hac1/Xbp1 mRNA to the ER membrane seems to differ considerably between yeast and mammals. Under non-stressed conditions, unspliced Hac1 mRNA is found mostly in the cytoplasm, in association with stalled ribosome. Upon ER stress, Hac1 mRNA is recruited to Ire1 clusters in the ER membrane, in a process that depends on translational repression of Hac1 mRNA and on a bipartite element (BE) at its 3' UTR (Aragón et al., 2009). Disruption of Ire1 dimerization interfaces, prevented cluster assemble of Ire1 and impaired Hac1 mRNA targeting to the ER. Robust Ire1 oligomerization and Hac1 mRNA targeting serves to concentrate both key UPR components into *foci* and ensure efficient RNA processing.

In mammals, Xbp1 mRNA localization to the ER membrane is independent of Ire1 and does not require secondary structures on unspliced Xbp1 mRNA (Yanagitani et al., 2009). The unspliced Xbp1 mRNA is translated under normal conditions and originates a polypeptide that associates with membranes through a hydrophobic region at its C-terminus (the hydrophobic region2 - HR2) (**Figure 1.6**). The HR2 is a conserved region predicted to form a α-helice that has propensity to interact with membrane lipid bilayers (Yanagitani et al., 2009). Presumably, upon unspliced Xbp1 mRNA translation the HR2 on the nascent polypeptide associates with the ER membrane and brings the Xbp1 mRNA-ribosome-nascent chain (RNC) complex to the vicinity of Ire1, facilitating Ire1-mediated splicing.

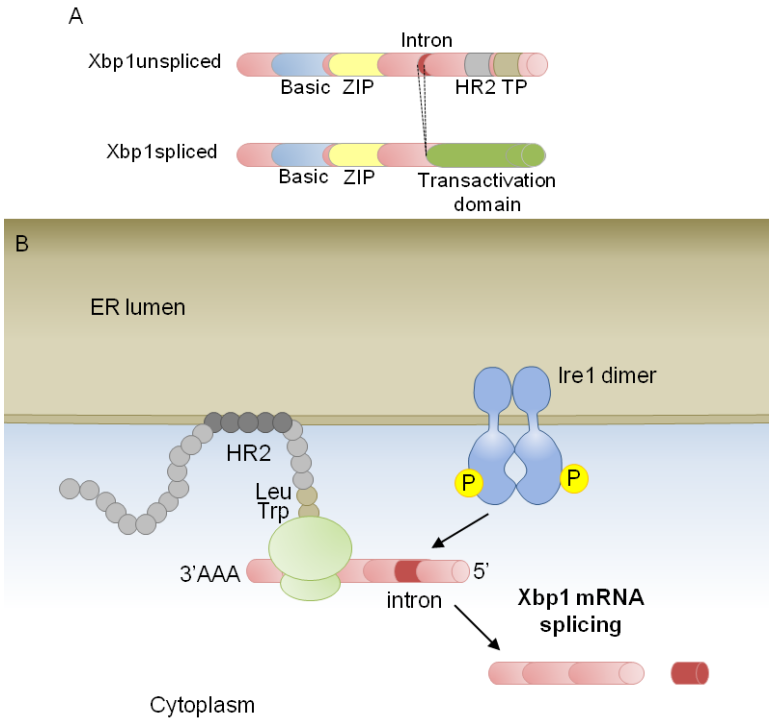

Figure 1.6 Recruitment of Xbp1 mRNA to the ER membrane in mammals.

(A) Structure of Xbp1 unspliced and Xbp1 spliced. ZIP, Leu zipper. TP, Translational pausing domain. HR2, hydrophobic region 2.
(B) Xbp1 unspliced mRNA originates a translational pausing through its domain TP (Translational Pausing) domain, giving time for the hydrophobic region (HR2) to target the unspliced Xbp1 mRNA to the ER membrane.

The HR2 is only 53 amino acid distant from the STOP codon. Before the Xbp1 unspliced polypeptide is released from the RNC, a translational pause stabilizes the complex and gives time for its recruitment to the ER membrane (Yanagitani et al., 2011). The C-terminal region (CTR) in the Xbp1 unspliced - with conserved Leu and Trp at positions 246 and 256,respectively, in humans – is essential for elongation pausing when the HR2 portion of the Xbp1 unspliced polypeptide protrudes from the ribosome exit tunnel (Yanagitani et al., 2011).

The mechanism underlying Xbp1 mRNA targeting to the ER was not yet addressed in *Drosophila*. VISTA analysis for comparative genome analysis shows that the 3'UTR of Xbp1 mRNA is conserved in four *Drosophila* species, raising the possibility that the 3'UTR has affinity for Ire1. The Kyte and Doolittle

hydrophobicity scale predicts a region similar to mammalian HR2 in the *Drosophila* unspliced Xbp1 protein. In addition the conserved Leu and Trp of the CTR are also present. These Xbp1 features may have an important physiologic role, taking into account that addition of yeast 3′UTR and mammalian CTR and HR2 coding regions to a *Drosophila* ER reporter increased greatly its sensitivity (Sone et al., 2013).

Xbp1-independent Ire1 functions

In contrast to budding yeast, where Ire1 and Hac1 are in a linear pathway, in metazoans Ire1 has several signaling functions besides nucleolytic cleavage of Xbp1 mRNA. Non-overlapping defects in Ire1 or Xbp1 mutants in *C.elegans* first evidenced the existence of Ire1 alternative roles (Shen et al., 2005). Ire1 is thought to regulate apoptosis, autophagy, and ERAD through interaction with cytoplasmic partners and independently of its RNase activity (Hetz and Glimcher, 2009). However other targets of Ire1 kinase activity besides Ire1 itself are unknown until date (Korennykh and Walter, 2012).

The cytosolic domain of Ire1 interacts with Traf2 (TNFR-associated factor 2), and activates ASK1 (Apoptosis signal-regulating kinase1), triggering the JNK (cJun-N terminal kinase) pathway (Urano et al., 2000; Nishitoh et al., 2002). This Ire1/Traf2 interaction may lead to the activation of apoptosis under irreversible ER stress (Mauro et al., 2006). Activated Ire1 may also instigate cell death by sequestrating IKK (inhibitor kβ kinase) in a complex with Traf2 (Hu et al., 2006). IKK is a negative regulator of the NF-kβ (factor nuclear kappa B) pathway, associated with inflammation. Ire1 and NF-kβ induce TNF expression and promote cell death in a caspase-8-dependent manner (Hu et al., 2006).

Ire1 may also control levels of autophagy under ER stress through activation of the JNK pathway (Ogata et al., 2006). The phosphorylation of the anti-apoptotic BCL2 (B-cell CLL/lymphoma 2) at the ER by JNK stimulates autophagy, by modulating the activity of Beclin1. BCL2 forms a complex with Beclin1 and dissociation of this association induces autophagy (Pattingre et al., 2009). In a

yeast two-hybrid screen, Ire1 physically interacts with the ubiquitin specific protease 14 (USP14), and this association is inhibited by ER stress (Nagai et al., 2009). Moreover, inactive Ire1 interacts with ERAD components, such as Derlin, SEL1 and HRD1. USP14, which is recruited to the ERAD machinery via interaction with inactive Ire1, inhibits ERAD through deubiquitination-independent mechanism (Nagai et al., 2009). Inactive Ire1 may form a macromolecular complex that sequestrates/inactivates ERAD under non-stressed conditions.

Regulated Ire1-dependent decay (RIDD)

A genome-wide analysis in the budding yeast to find specific mRNA substrates cleaved *in vitro* by Ire1 RNase or degraded in the absence of the Trl1 tRNA ligase only retrieved Hac1, supporting that Hac1 is an exclusive target of Ire1 RNase (Niwa et al., 2005). Computational simulations in mammals searching for mRNAs with structural and regulatory elements similar to Xbp1 (overlapping long open reading frames and Ire1 cleavage sites flanking a short intron) did not identify other mRNAs demonstrating the singularity of the pathway (Nekrutenko and He, 2006). However a report using *Drosophila* S2 cells uncovered a novel function for Ire1 RNase with a broad range of mRNA substrates and independent of Xbp1. The group of Jonathan Weissman found through gene profiling that a subset of mRNAs are degraded during ER stress by a mechanism that is dependent of Ire1 but not Xbp1 (Hollien and Weissman, 2006). The degraded mRNAs encoded mostly proteins with signal peptide/transmembrane domains that would represent an additional challenge to the ER folding machinery under ER stress. This mechanism was named RIDD, for regulated Ire1 dependent decay, and was later described also in mammalian cells and in the fission yeast *S. pombe,* which lacks any Hac1/Xbp1 homologue (Cross et al., 2012, Hollien et al., 2009; Kimmig et al., 2012). While in *Drosophila* cells RIDD down-regulates many RNAs by 5-10 fold, in mammals the magnitudes of expression changes were small, twofold or less for many targets (Hollien and Weissman, 2006; Hollien et al., 2009).

The mechanism of targeting mRNAs to RIDD seems to have diverged throughout evolution (Hollien, 2013). In *Drosophila*, RIDD has a broad scope of targets and there is a strong correlation between interaction of a mRNA with the ER membrane and the extension of its degradation by RIDD (Gaddam et al., 2013; Hollien and Weissman, 2006). In fact, deletion of the signal peptide from a known RIDD target prevents its degradation and conversely, addition of a signal peptide to GFP is sufficient to promote its degradation by RIDD. One interesting exception is the mRNA of PlexinA, which although is strongly associated with ER membrane is protected from RIDD and is continuously translated even during ER stress (Gaddam et al., 2013). PlexinA mRNA has regulatory upstream ORFs, in similarity with Gadd34, which are necessary for its protection from RIDD.

In mammalian cells, RIDD targets are enriched for mRNAs containing a cleavage site with a consensus sequence (CTGCAG) and a predicted secondary structure very similar to the conserved Ire1 recognition loop in Xbp1 mRNA (Han et al., 2009; Hur et al., 2012; Oikawa et al., 2010). Deletion of the stem loop or mutagenesis of the conserved bases abrogated RIDD (Oikawa et al., 2010). The presence of Ire1 recognition sites in many RIDD substrates suggests that mammals have evolved sequence specificity to better control the transcripts that are subjected to degradation. In *Drosophila*, the mRNA encoding Smt3, a homologue of SUMO (small ubiquitin-like modifier) is cleaved by RIDD on a stem loop structure despite not being stably associated to the ER membrane (Moore et al., 2013).

Under conditions of overwhelming ER stress or chronic low level stress (e.g. expression of a mutant folding variant or treatment with 10nM thapsigargin), mRNAs encoding secretory cargo proteins and resident ER proteins and other secretory organelle proteins start to decay (Han et al., 2009). ER chaperone Bip and Golgi localized glycosylating enzyme Gyltl1b are targets of RIDD. Unmitigated ER stress may deplete important cell surface proteins or secretory pathway proteins by continuous decay and promote apoptosis. In fact, expression of wild-type Ire1 in *xbp1*$^{-/-}$ mouse embryonic fibroblasts triggers apoptosis, but

expression of Ire1 kinase active/RNase dead mutants do not induce apoptosis, arguing that an active RNase is required to induce pro-apoptotic signals (Han et al., 2009).

The two Ire1 functions, RIDD and Xbp1 splicing, can be uncoupled *in vitro*, allowing better understanding of the physiological output of each pathway. $Ire1^{I642G}$ mutant has an enlarged kinase pocket that prevents autophosphorylation and activation of the RNase. The need for ATP binding can be bypassed by 1NM-PP1, an ATP analog that binds specifically to the designed pocket of $Ire1^{I642G}$ and activates the RNase by an allosteric mechanism (Papa et al., 2003). Addition of the 1NM-PP1 is sufficient to induce Xbp1 splicing when $Ire1^{I642G}$ is overexpressed, even in the absence of ER stress. However RIDD function can only be engaged by 1NM-PP1 in the presence of ER stress, suggesting different activation modes of Ire1 (Han et al., 2009; Hollien et al., 2009). Other compounds, known as KIRAs (kinase inhibiting RNase attenuators) can bypass the need for autophosphorylation to activate wild-type Ire1, stimulating Xbp1 splicing and tempering RIDD (Han et al., 2009).

ATF6 Signaling

The second arm of the UPR in metazoans is ATF6, an ER localized type II transmembrane protein, whose cytosolic domain encodes a transcription factor (**Figure 1.7**) (Haze et al., 1999; Wang et al., 2000; Yoshida et al., 2000) ATF6 is retained in the ER by interaction with Bip and calnexin, that bind to its luminal domain (Shen et al., 2002; Hong, 2004). Upon ER stress, underglycosylation of ATF6 prevents interaction with calnexin and dissociation of Bip uncovers Golgi localization signals on ATF6. ATF6 is then translocated to the Golgi, where is cleaved sequentially by resident proteases S1P (site 1 protease) and S2P (site 2 protease) (Ye et al., 2000). The cytosolic fragment is released and moves to the nucleus, where activates gene expression through a bZip domain.

ATF6 is more sensitive to perturbations of redox equilibrium in the ER than other UPR mediators. ER stress reduces intermolecular disulfide bonds between

ATF6 oligomers and induces its dissociation. In the monomeric form, ATF6 can more easily be translocated to the Golgi (Nadanaka et al., 2007).

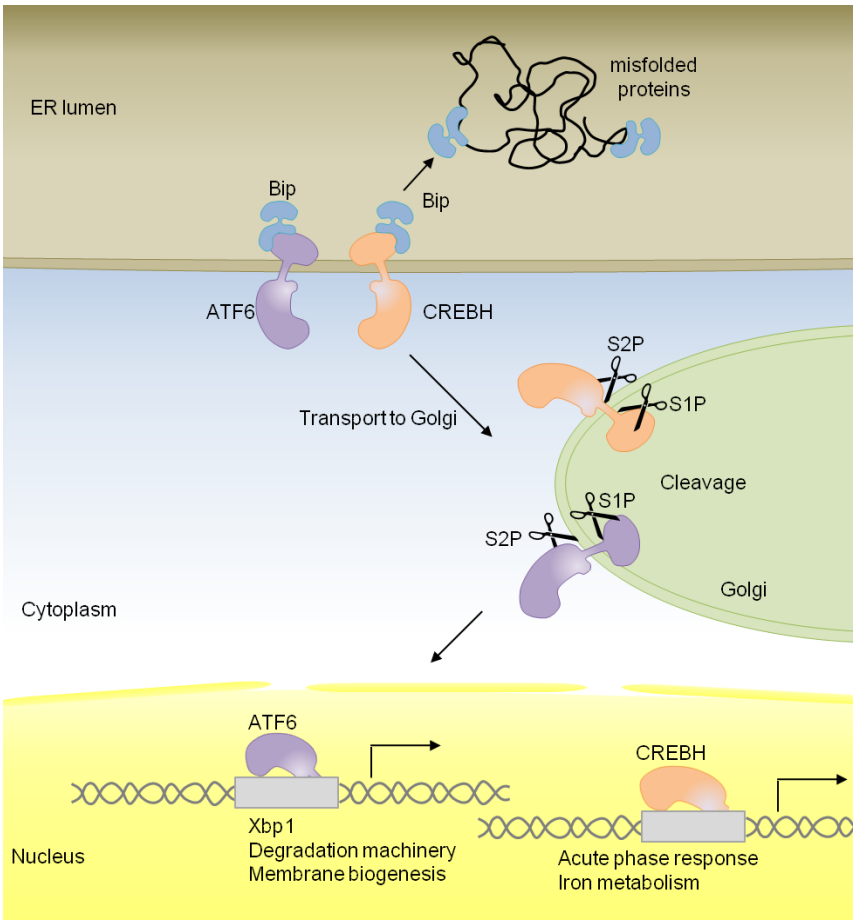

Figure 1.7 ATF6 and CREBH signaling.

ATF6 localizes to the ER, where it is retained by binding with Bip in the luminal domain. ER stress disrupts association with Bip and ATF6 is trafficked in COPII vesicles to the Golgi. Sequential cleavage by the site-1-protease (S1P) and the site-2-protease (S2P) releases the 50kb cytosolic domain of ATF6 and allows its import into the nucleus. ATF6 shares homology with CREBH in hepatocytes, which is also regulated by Bip in the ER and cleaved by proteases in the Golgi apparatus in response to stress. CREBH activate acute-phase response genes that encode secreted proteins involved in inflammation.

ATF6 binds to the ATF/CRE element and the ER stress response elements I and II (ERSE), to induce the transcription of many UPR genes related to ERAD

and folding, for instance *bip*, *xbp1*, *herp*, among others (Yoshida et al., 2003; Kokame, 2000; Yoshida, 1998). ATF6 can form heterodimers with Xbp1, which have higher affinity for UPR elements than either homodimer to promote maximal expression of ER chaperones and degradation machinery (Yamamoto et al., 2007).

Newly identified ATF6 homologs OASIS, CREBH, LUMAN/CREB3, CREB4, BBF2H7 are controlled by ER stress in specific tissues (Bailey and O'Hare, 2007). All are ER-anchored bZip transcription factors that are processed in the Golgi the same way as ATF6 but whose physiological role is poorly characterized. CREBH (cyclic AMP response element binding protein hepatocyte) expressed in hepatocytes induces the expression of hepcidin, both basally and in response to ER stress and inflammation (Vecchi et al., 2009). CREBH links ER stress to the production of acute phase proteins (serum proteins that are associated with inflammation) (Zhang et al., 2006).

Perk Signaling

The third ER transducer, PERK, is an ER associated type I transmembrane protein with a structure similar to Ire1: a luminal stress sensing domain and a cytoplasmic portion with a protein kinase (**Figure 1.8**). The luminal domains of Ire1 and PERK are phylogenetically related and can be experimentally interchangeable in *S. cerevisae*, where Perk can splice Hac1 (Liu et al., 2000). Like Ire1, Perk binds Bip under non stressed conditions (Bertolotti et al., 2000; Ma et al., 2002). Upon ER stress, Bip dissociates and PERK is activated by trans-autophosphorylation after oligomerization and phosphorylates the α-subunit of the eukaryotic translation initiation factor 2 (eiF2) at Serine 51 (Harding et al., 1999). Phosphorylation of eiF2 inhibits its recycling to an active GTP-bound form. Limiting availability of active eiF2 for translation initiation attenuates global protein synthesis and decreases protein influx into the ER lumen.

Expression profiling in ER stressed PERK knock-out cells or with a Ser51Ala mutation in eiF2α that prevents its phosphorylation showed a defective induction

of UPR genes (Harding et al., 2003; Scheuner et al., 2001) Certain mRNAs escape translational attenuation during ER stress due to the presence of regulatory upstream open reading frames (uORFs) in their 5' UTRs. Conditions that limit eIF2 activity lead to ribosome skipping the inhibitory uORFs so that downstream ORFs can be translated. ATF4 or its yeast homolog Gcn4 are translationally induced by phosphorylation of eiF2α (Lu et al., 2004; Vattem and Wek, 2004). ATF4 is a transcription factor responsible for activating genes involved in amino acid metabolism and protection from oxidative stress, including CHOP (C/EBP homologous protein) and Gadd34 (growth arrest and DNA-damage inducible protein-34), besides other targets overlapping with ATF6 and Xbp1 (Harding et al., 2000; Jiang et al., 2004; Ma et al., 2002b). Other stress signaling pathways triggered by amino acid starvation, double-stranded RNA accumulation or haem depletion also converge on eif2α phosphorylation, activating the so called integrated stress response, which share common targets (Harding et al., 2003).

The levels of phosphorylated eIF2α must be tightly regulated to avoid permanent damage to the cell. Dephosphorylation of eIF2α is mediated by CReP (constitutive repressor of eiF2 phosphorylation) and Gadd34 (Jousse et al., 2003; Connor et al., 2001; Novoa et al., 2001). CReP is constitutive expressed and encodes the substrate subunit of Protein Phosphatase 1 (PP1). GADD34 also promotes eIF2α dephosphorylation in complex with PP1, and works in a negative feedback loop to downregulate PERK signaling (Brush et al., 2003; Ma and Hendershot, 2003; Novoa et al., 2003).

Activation of PERK occurs in a reversible manner and PERK is rapidly dephosphoryilated after ER homeostasis is restored, allowing the fast recovery from translational attenuation (Bertolotti et al., 2000; Jousse et al., 2003). The HSP40 co-chaperone p58IPK is up-regulated by ATF6 during late phases of the UPR to inhibit PERK activity by binding to its kinase domain (van Huizen, 2003; Yan et al., 2002)

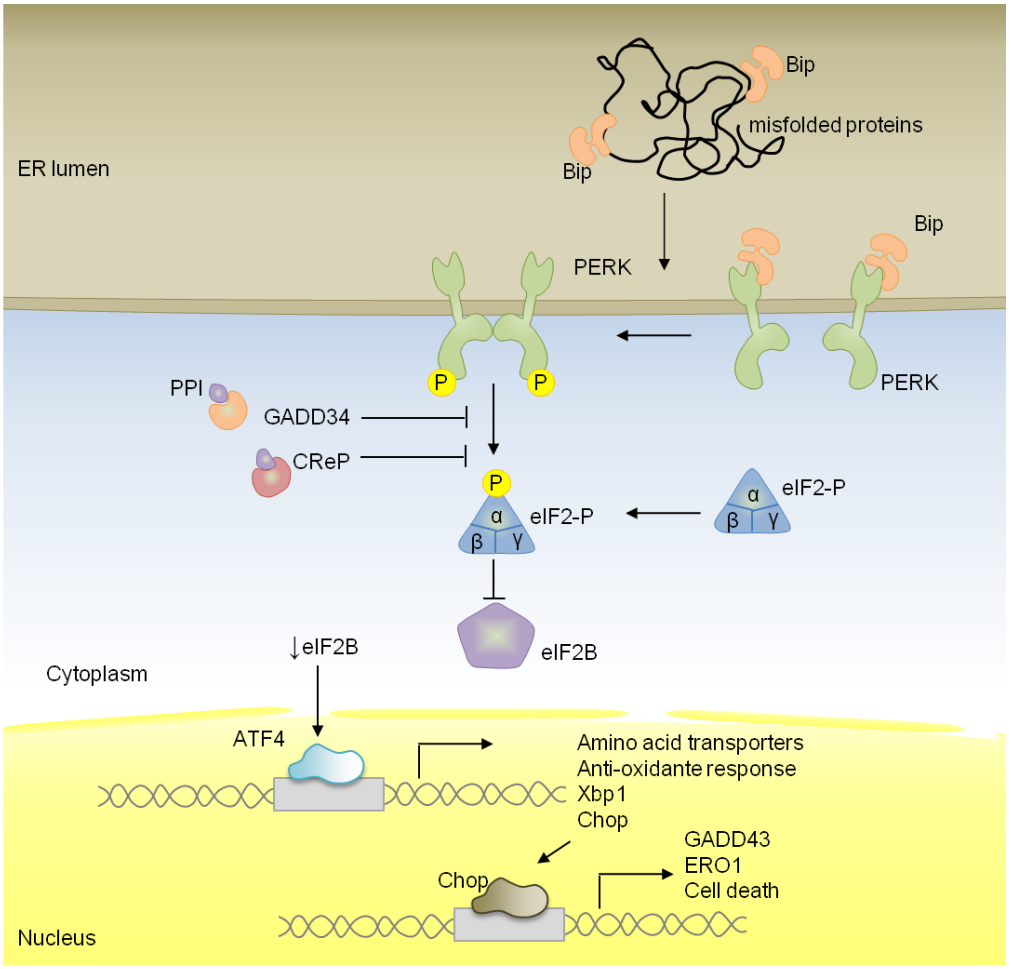

Figure 1.8. PERK signaling.

In response to endoplasmic reticulum (ER) stress, Bip dissociates from PERK luminal domain, allowing PERK to dimerize and be activated by trans-autophosphorylation. PERK phosphorylates the α subunit of eukaryotic translation initiation factor-2 (eIF2) on Ser51, attenuating global protein translation by inhibition of eIF2B complex. Lower global protein synthesis reduces ER unfolded protein load but also affects gene transcription. eiF2 phosphorylation selectively increases the translation of ATF4, which under normal conditions is inhibited by conserved upstream open reading frames. The ATF4 protein up-regulates Xbp1, the proapoptotic transcription factor (CHOP) and genes encoding amino acid transporters and genes that protect against oxidative stress. The target genes of CHOP include GADD34 that dephosphorylates eIF2α and ER oxidase-1 (ERO1) that promote protein folding within the ER lumen. GADD34 associates with protein phosphatase I (PPI) to dephosphorylate eIF2α and relieve PERK dependent translation attenuation in a negative-feedback circuit. A constitutive phosphatase CReP contributes to repress eiF2α phosphorylation and balance Perk activity.

Ire1α or *xbp1* knock-out mice embryos present growth retardation and fetal liver hipoplasia and die after 12.5 days of gestation (Reimold et al., 2000; Zhang et al., 2005). Because the liver becomes the main hematopoietic organ in the fetus, Ire1 or Xbp1 knock-out mice have reduced numbers of red blood cells but can still differentiate erythroid and myeloid lineage cells. Ire1α is required in a later step of the lymphoid differentiation for the immunoglobulin gene rearrangement and formation of the B cell receptor in pro-B and pre-B cells (Zhang et al., 2005). In the adult, splicing of Xbp1 by Ire1 is necessary for the terminal differentiation of mature B-cell into antibody secreting plasmocytes (Iwakoshi et al., 2003; Zhang et al., 2005). Introduction of Xbp1 into B cell lineages is sufficient to induce plasma-cell differentiation and Xbp1 deficient B cells are defective in secreting antibodies *in vivo* upon antigenic stimulation (Reimold et al., 2001).

The targeted expression of Xbp1 in the liver of *xbp1*$^{-/-}$ embryos rescues viability, but mice present severe defects in exocrine pancreas and salivary glands that compromised secretion of digestive enzymes (Lee et al., 2003). Pancreatic acinar cells of the *xbp1*$^{-/-}$*; liver*^{xbp1} mice have a poorly developed ER with few, disorganized cisternae, and immature zymogen granule precursors located in the ER lumen. The failure in the ER expansion of pancreatic exocrine cells during the embryonic development is consistent with Xbp1 role in membrane biogenesis and phospholipid synthesis (Shaffer et al., 2004; Sriburi et al., 2004). The liver is a secretory organ that produces the lipoprotein particles that transport lipids to other tissues and Xbp1 is necessary for hepatic lipogenesis. A Xbp1 conditional knock-out in the liver of adult mice reduces plasma cholesterol and triglycerides due to a down-regulation of lipogenic genes (So et al., 2012).

Deletion of *xbp1* or *ire1β* in intestinal epithelial cells causes increased ER stress and exacerbated colitis induced by dextran sodium sulfate (DSS), a toxin that disrupts mucosal barrier function (Bertolotti et al., 2001; Kaser et al., 2008). Xbp1 deletion in the intestine also impairs mucosa defense to bacterial oral

infection, as a result of Paneth cells dysfunction and apoptosis and lack of bactericidal killing activity (Kaser et al., 2008). Single-nucleotide polymorphisms within the *xbp1* gene locus on chromosome 22q12.1 are a risk factor for human inflammatory bowel diseases, Crohn's disease and ulcerative colitis (Kaser et al., 2008).

Ire1α and *xbp1* knock-outs mice do not have phenotype in the endocrine pancreas (Iwawaki et al., 2010; Lee et al., 2005). However, several experiments *in vivo* and *in vitro* point for a role of the Ire1/Xbp1 pathway during insulin maturation in the ER. Pancreatic β-cells deficient for Xbp1 are inefficient to process and secrete insulin (Lee et al., 2011). Analysis of the morphology of Islets of Langerhans lacking Xbp1 reveals a highly disorganizated structure and abnormal β–cells with fewer insulin granules and distended ER (Lee et al., 2011). These observations are in agreement with Xbp1 being required for expression of ER chaperone genes such as *bip* (Hspa5), *ERdj4* (Dnajb9), and *p58IPK* (Dnajc3).

Perk deficient mice are viable but present growth retardation and have defects in the pancreas and skeleton formation (Zhang et al., 2002). Pancreatic acinar cells of *perk*$^{-/-}$ mice have a distended and fragmented ER, and undergo increased apoptosis by the fourth post-natal week, a phenotype similar with *xbp1*$^{-/-}$*; liver*^{xbp1} mice. The inappropriate production of digestive enzymes causes maldigestion of lipids in Perk$^{-/-}$ mice (Harding et al., 2001; Zhang et al., 2002). *perk*$^{-/-}$ mice show deficient mineralization and impaired formation of skeleton due mostly to osteoblasts defects. Compact bone is formed by type I collagen and other components of the extracellular matrix, which are secreted by osteoblasts. Perk$^{-/-}$ osteoblasts have distended and fragmented ER filled with an electron-dense material that corresponds to unprocessed procollagen (Zhang et al., 2002).

Deletion of Perk leads to progressive degeneration of pancreatic β-cells, deregulation of glucose metabolism and early onset diabetes (Harding et al., 2001; Zhang et al., 2002). In humans, Perk loss-of-function mutations are associated with the autossomal recessive Wolcott-Rallison syndrome, a particular

severe form of type I diabetes, characterized by early failure of β-cells and dependence of insulin at the age of three years (Delépine et al., 2000). The Perk-eiF2α pathway has a homeostatic role in β-cells physiology coordinating pro-insulin translation with pro-insulin folding in the ER. Disruption of the eIF2α phosphorylation site removes the translational control of pro-insulin levels in the ER and causes a diabetic phenotype in mice secondary to ER dysfunction, defective trafficking of pro-insulin, oxidative stress and apoptosis of β-cells (Back et al., 2009; Scheuner et al., 2005).

ATF6α and ATF6β single knock-out mice are viable and develop normally, contrary to the double knock-out which is embryonic lethal. CREBH, the ATF6 homolog specific of the liver, was found to regulate the expression of genes involved in lipogenesis, fatty acid oxidation and lipolysis under conditions of metabolic stress (Zhang et al., 2012; Yamamoto et al., 2007).

Unresolved ER stress caused by high fat or high glucose diet might be associated with metabolic dysfunctions, such as diabetes and fatty liver disease. Obesity induces ER stress in hepatocytes and adipocytes and activates Ire1, which contributes to development of diabetes through JNK signaling (Ozcan et al., 2004). JNK is known to suppress signaling downstream of the insulin receptor. Insulin resistance and glucose homeostasis is ameliorated in obese mice by chemical chaperone that decrease ER stress further suggesting that unresolved ER stress contributes to diabetes pathogenesis (Ozcan et al., 2006). Ablation of any of the three UPR arms in mice treated with thapsigargin causes persistent ER stress and induces a fatty liver phenotype originated by CHOP mediated suppression of key metabolic genes, as C/EBPα. Xbp1spliced binds the promoter of the key lipogenic enzymes Dgat2, Scd1, and Acc2 and induces their expression in mice feed with a high carbohydrate diet (Lee et al., 2008a). Xbp1 liver deficiency provokes Ire1α hyperactivation, which further contributes to the hipolipogenic phenotype. Therefore it seems that UPR signaling pathways cooperate to protect against ER stress related deregulation of lipid metabolism (Rutkowski et al., 2008)

Ire1 plays an important role controlling glucose metabolism and regulating β-cells homeostasis. Ire1α is phosphorylated in response to transient exposure to high glucose and down-regulation of Ire1α signaling reduces insulin biosynthesis (Lipson et al., 2006). Chronic treatment of β-cells with high levels of glucose hyperactivates Ire1 and correlates with a decrease of insulin mRNA expression and shut-down of Xbp-1 splicing and Ero1a induction (Lipson et al., 2008). Ire1α cleaves Insulin 1 and Insulin2 mRNA at several specific sites, which are similar in sequence to Ire1 splice sites in Xbp1 mRNA (Han et al., 2009). Chronic stimulation of β-cells with high glucose concentrations might impose insurmountable levels of ER stress and promote the shift from a protective response to a deleterious. Islets from mice heterozygous for Ire1 are more resistant to chronic high glucose and had higher gene expression for both Insulin1 and Insulin2, thus deletion of Ire1 might be beneficial for the organism in case of diabetes type II models.

The high mutation rate in malignant cells and low oxygen and glucose supplies in tumors affect protein folding and cause ER stress. Activation of the UPR was already reported in various human cancers, promoting tumor growth and survival (Ma and Hendershot, 2004). In models of mammary carcinoma, Perk facilitates tumour growth by protecting against oxidative DNA damage caused by accumulation of reactive oxygen species (Bobrovnikova-Marjon et al., 2010). Inhibition of Ire1 leads to a reduction in angiogenesis, lower blood perfusion and decreased tumour growth rate, and was consistent with a prolonged survival in mice implanted with glioma cells (Auf et al., 2010). Knock-down of Xbp1 compromises the growth of transplantable tumours in nude mice because tumour cells had reduced capacity to survive under hypoxic conditions (Romero-Ramirez et al., 2004)

Activation of the UPR is observed in numerous neurodegenerative diseases, for example amyotrophic lateral sclerosis, Parkinson's disease, Huntington's disease, prion related disorders, Alzheimer's disease, Pelizaeus-Merzbacher, multiple sclerosis and Retinitis Pigmentosa (Lin et al., 2008; Wang and Kaufman,

2012). The role of the UPR in neurodegeneration progression is not fully understood as findings are specific for each disease model. Aβ accumulation in neurons, which underlies the pathogenesis of Alzheimer's disease at least in part, was found to induce the increased expression of ER chaperones in cell culture. (Ferreiro et al., 2006) Moreover, depletion of Ask1 in cultured neurons confer resistance to Aβ cytotoxicity, suggesting that the Ire1-ASK1-JNK pathway is implicated in Aβ mediated cell death (Kadowaki et al., 2005). Specific deletion of Xbp1 in the nervous system of a murine model of amyotrophic lateral sclerosis delayed the onset of the disease upon stimulation of higher levels of autophagy and decreased accumulation of mutant SOD1 (Super Oxide Dismutase 1) aggregates (Hetz et al., 2009). It is possible that induction of ER stress in neurodegenerative diseases is a consequence of proteasome clogging, as a common feature of these diseases is the accumulation of misfolded proteins and formation of cytoplasmic protein aggregates (Bence et al., 2001).

The Ire1/Xbp1 branch of the UPR has a protective role mechanism against retinal degeneration in *Drosophila and rat* models of Retinitis Pigmentosa (Ryoo *et al*, 2007). In this disease, photoreceptors (visual sensory cells) degenerate over time and affected individuals usually show night blindness, followed by loss of peripheral and central vision (Berson, 1996). About 30% of autossomal dominant Retinitis Pigmentosa cases are caused by mutations in Rhodopsin, the light sensing protein present in photoreceptors. Equivalent mutations in the major Rhodopsin of the *Drosophila* eye (Rhodopsin1), also lead to progressive retinal degeneration. Rhodopsin1 displays 22% amino acid identity with human Rhodopsin (Colley *et al*, 1995). Mutations in the transmembranar or extracellular domains of Rhodopsin1 interfere with its normal folding (Colley *et al*, 1995; Kurada and O'Tousa, 1995), causing severe ER stress in the photoreceptors and apoptosis via mediators not yet identified (Davidson and Steller, 1998).

2. Morphogenesis of the *Drosophila* eye

The *Drosophila* eye is composed of 800 well-organized and repeated units, termed ommatidia (**Figure 1.9A**). Each ommatidium has 8 photoreceptor cells, 4 cone cells, 2 primary pigment cells and is surrounded by a hexagonal lattice of 12 accessory cells, including secondary and tertiary pigment cells and cells of the bristle (**Figure 1.9C-D**) (Wolf and Ready, 1993). A dioptric apparatus formed by the cornea (a transparent chitinous cuticle) and the pseudocone (an extracellular fluid secreted by the cone cells) focuses light into the photoreceptor cluster below (**Figure 1.9C**). The pigment cells optically isolate ommatidia, shielding photoreceptors from stray light coming from adjacent ommatidia.

Each ommatidium comprise six outer photoreceptors (R1-R6) arranged in an irregular trapezoid pattern and two inner photoreceptors (R7/8) (Cook and Desplan, 2001; Mollereau and Domingos, 2005). (**Figure 1.9B,D**) Outer and inner photoreceptors have different morphological and functional proprieties. Outer photoreceptors express exclusively Rhodopsin1 (Rh1) and are responsible for vision in dim light and motion detection, being the functional equivalent to rods in the vertebrate eye. Outer photoreceptors span the entire depth of the retina and project their axons into the first optic lobe, the lamina. The inner photoreceptors are responsible for color vision and correspond to cones in the vertebrate retina. The R7 expresses one UV-absorbing Rhodopsin, Rh3 or Rh4. R8 expresses one of three Rhodopsins, Rh3, Rh5 or Rh6, which absorb UV, blue or green light, respectively. R7 and R8 span half of the retina, and are organized in tandem, with R7 localizing on the top of R8 along the distal-proximal axis of the retina. R7/8 axons terminate in different layers of the medulla, the second optic lobe.

Based on the Rhodopsin type expressed, three ommatideal subtypes can be distinguished (Cook and Desplan, 2001). Ommatidia of the dorsal rim area of the eye express Rh3 both in R7 and R8 and are specialized in polarized light detection. The pale ommatidea express Rh3 in R7 and Rh5 in R8 and represent less than 30% of the total ommatidia. The remaining 70%, the yellow ommatidia,

express Rh4 in R7 and Rh6 in R8. Pale and yellow ommatidia are randomly distributed over the retina.

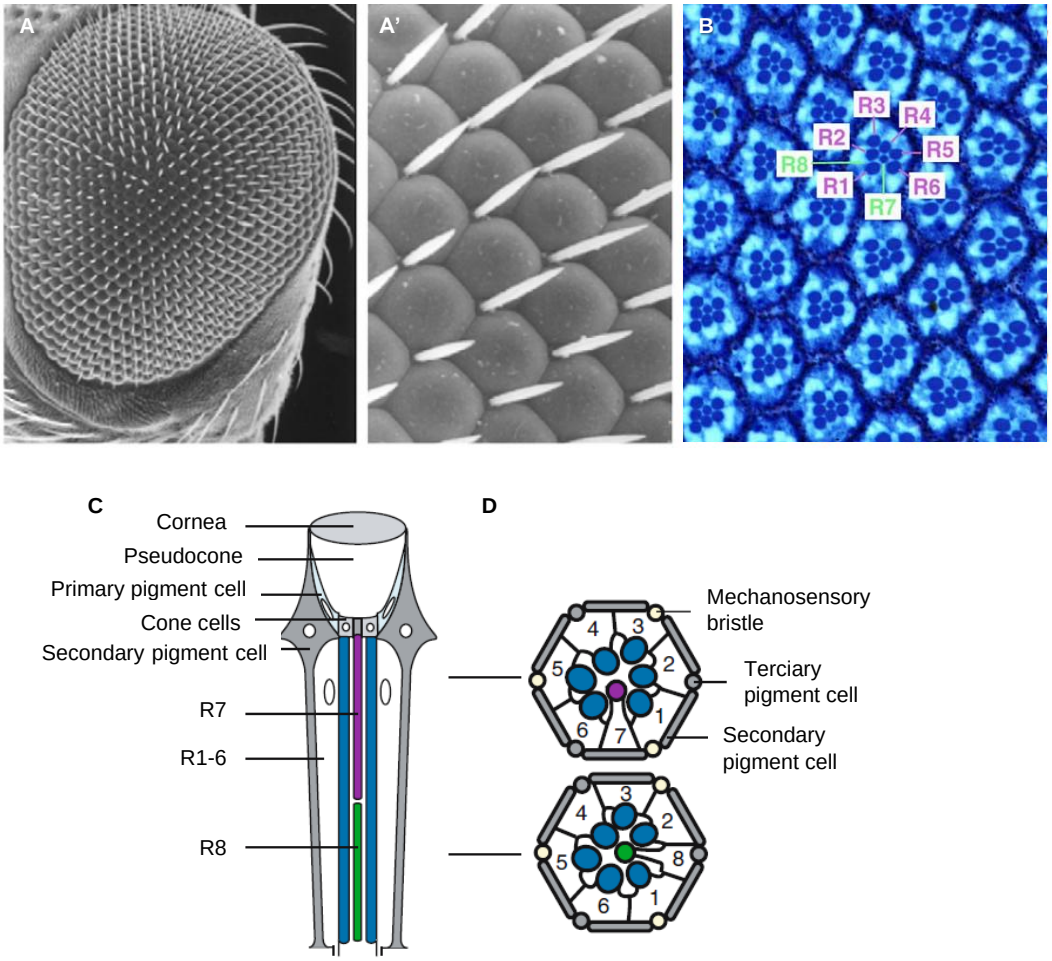

Figure1.9 The structure of the *Drosophila* compound eye.

(A) Scanning electron micrograph of an eye of the adult fly. (A' higher magnification) Adapted from Knust, 2007.
(B) A tangential section through a wild-type eye. Each photoreceptor cell numbered from R1 to R8 can be recognized by the dark rhabdomere. In an ommatidium, rhabdomeres are arranged in a stereotype trapezoid pattern.
(C) Single ommatidium at an horizontal view showing acessory cells.
(D) Cross-sections through the distal and proximal regions of the ommatidium. Rhabdomeres are represented by blue circles and photoreceptor cell bodies are numbered. R8 has a proximal position and R7 has a distal position in the ommatidium.
Adapted from Wang and Montell, 2007.

The photosensitive compartment of the photoreceptors in *Drosophila* named rhabdomere, is made by 30,000–50,000 microvilli closely packed together, each 2μm long and with 60nm in diameter (**Figure 1.10A,B**). Rhodopsins, light-sensitive channels and other components of the phototransduction machinery localize at the expanded membrane of the rhabdomere, while the nucleus and cellular organelles reside in the cell body of the photoreceptor (Hardie, 2012; Katz, 2009; Montell, 2012; Wang and Montell, 2007). The light sensitive structure of vertebrate cones, the outer segment, has a quite similar morphology (array of packed apical membranes) but a different origin (cilia) (**Figure 1.10C**) (Salvini-Plawen and Mayr, 1977). The rhabdomere is connected to the cell body of photoreceptors through a peduncle, the stalk, equivalent to the inner segment in vertebrates. Each microvillus of the rhabdomere has an axial F-actin microfilament linked to the membrane by cross bridges of an unconventional myosin, ninaC (Kumar and Ready, 1995).

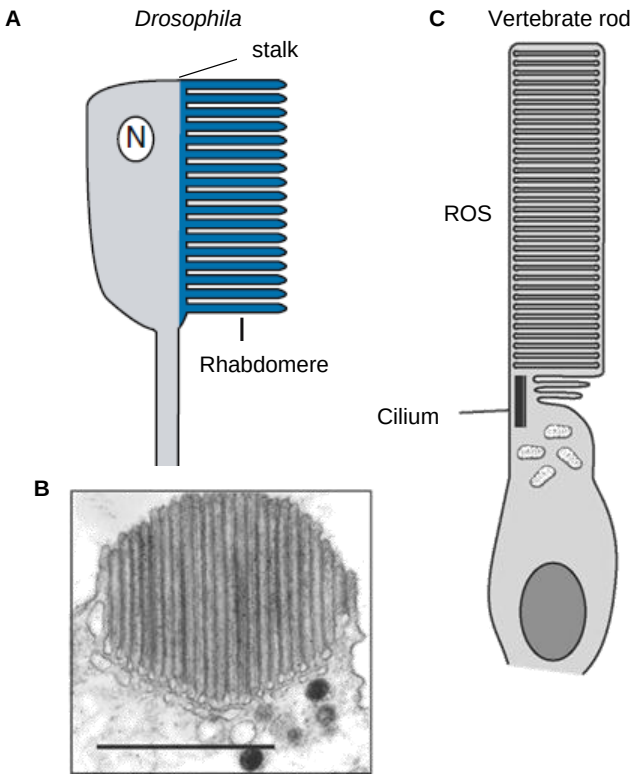

Figure 1.10. The photoreceptive membranes in *Drosophila* and vertebrates.

Photoreceptors maximize absorption of light through cylindrical light-guiding structures with a very high density of membrane containing rhodopsin. (A) *Drosophila* rhabdomere is 100μm long and is formed by tightly packed microvilli, each 1–2μm long and 60 nm in diameter. The stalk connects the rhabdomere to the cell body of the photoreceptor.
(B) Electron micrograph of the rhabdomere.
(C) Vertebrate rod outer segments (ROS) contain stacks of around 1,000 membranous discs and are connected to the cell body by a narrow cilium. Adapted from Hardie et al., 2001.

Drosophila, the housefly and some mosquitos have an open rhabdom architecture where rhabdomeres are separated at the center of each ommatidium, forming a lumen between them (interrhabdomeral space) (Land and Fernald, 1992). In contrast, bees, beetles and other mosquitoes have a closed rhabdom architecture, in which rhabdomeres within each ommatidium are fused to each other, thus sharing the same visual axis. The open rhabdom architecture of the eye has evolutionary advantages because individual rhabdomeres function as independent guide lights and each ommatidium perceives 7 different picture points, increasing greatly sensitivity without compromising the resolution ((Katz, 2009; Moses, 2006). The optical angles between the individual rhabdomeres in one ommatidium are identical to those between adjacent ommatidia to ensure visual connectivity (Kirschfeld, 1967). In addition, all six rhabdomeres that share the same field of view target the same lamina cartridge - principle of neural superposition (Kirschfeld, 1973).

Photoreceptors are recruited from a single layer epithelium in the eye imaginal disc into the developing ommatidium during the third larval instar (Ready et al., 1976). When development in the pupa starts, photoreceptors are organized in clusters of 8 cells that must undergo dramatic morphological changes to give rise to the differentiated photoreceptors of the adult (Cagan and Ready, 1989). During pupation photoreceptors rotate by 90º, its apical membrane is extended to accommodate the phototransduction machinery of the rhabdomere and the interrhabdomeral space arises.

2.1 Apical/Basolateral Specification

In the first half of pupal development, photoreceptors are relatively undifferentiated epithelial cells with apical and basolateral domains separated by a belt-like structure, *zonula adherens* (ZA), encircling the apex of the cell (**Figure 1.11A,B**). Markers of cell polarity are segregated differently to each domain of the photoreceptor plasma membrane (Knust, 2007). The establishment of the apical-basolateral polarity in early pupal photoreceptors depends on Bazooka, the fly

homolog of Par-3 (Partitioning defective 3 homolog), which localizes to the ZA in the first half of pupal development (Hong et al., 2003). In Bazooka mutant photoreceptors, Armadillo staining is severely disrupted and Discs lost (Dlt) labeling becomes fragmented, randomly positioned, or lost at 37% and 47% pupal development (pd), indicating that the ZA and the apical domain are not formed.

In the second-half of pupal development, apical markers like members of the Crumbs complex are excluded from the apex of the apical domain, where the rhabdomere will take shape, and relocalize to the subapical domain (region in proximity to the ZA) to specify the stalk (**Figure 1.11B,C**) (Pichaud and Desplan, 2002). Bazooka is essential for the proper patterning of rhabdomere and stalk membranes and localizes to the rhabdomere in the second-half of pupal development. At 70% pupal development Bazooka recruits PTEN (Phosphatase and tensin homolog), a lipid phosphatase that promotes phosphatidylinositol (3,4,5)-triphosphate degradation, to the ZA (Pinal et al., 2006; von Stein et al., 2005). In PTEN mutants, rhabdomeres are absent, misshapen or splitted by segments of Crumbs/Dlt positive (stalk-like) membrane and Akt1 is up-regulated in the apical membrane (Pinal et al., 2006). Presumably phosphatidylinositol (3,4,5)-triphosphate dependent Akt1 activation is important for controlling the precise localization of Crumbs and Dlt within the photoreceptor apical membrane.

Once the apical domain is subdivided, the rhabdomere elongates along the proximal-distal axis of the retina and the stalk membrane increases its length (Pichaud and Desplan, 2002) (**Figure 1.11 C**). Crumbs is necessary for rhabdomere and stalk growth, but the two functions are mechanistically distinct as different domains of Crumbs protein are required and the interacting partners of Crumbs are different. Crumbs is a conserved transmembrane protein with a large extracellular domain, composed of 29 epidermal growth factor (EGF)-like repeats and four laminin A globular domain-like repeats and a short 37-amino acid long intracellular domain (Tepass et al., 1990). Crumbs PDZ domain on the intracellular side binds Stardust, which in turn recruits Dlt and Lin7 to the

complex, forming a scaffold complex at the stalk membrane (Bachmann et al., 2001, 2008; Bhat et al., 1999). Crumbs mutant photoreceptors show severe defects at 50% pd: the ZA is fragmented and dispersed and rhabdomeres are 50% shorter and confined to the distal region of the retina (Pellikka et al., 2002). The intracellular domain of Crumbs is sufficient to rescue the elongation of the rhabdomere and membrane juxtaposed region of the intracellular domain is responsible for maintaining the integrity of the ZA during the elongation process (Izaddoost et al., 2002; Johnson et al., 2002).

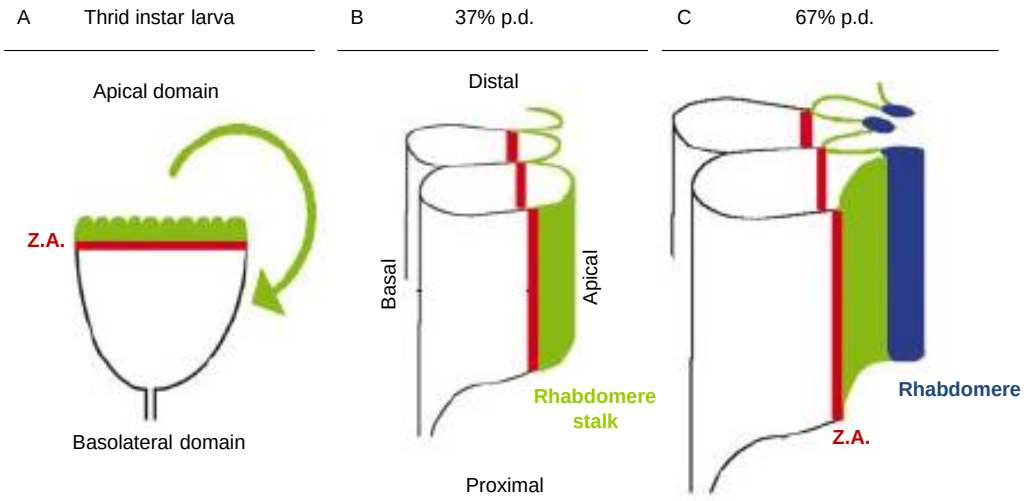

Figure 1.11 Differentiation of photoreceptors in the pupa and markers of cell polarity.

The apical membrane of the photoreceptors is in green, the *zonula adherens* (za) is in red, and the basolateral membrane is in black. The most apical part of the photoreceptors (rhabdomere) is in blue. The proteins Crumbs, Stardust, Discs lost, β_H-spectrin, Bazooka, Protein kinase C and DPA-6 are present in the green areas; Armadillo, Canoe, Pyd and spectrins in the red areas; and Lethal giant larvae, Discs large, Scribble and myosin II in the black areas.
(A) Third-instar eye disc. Apical domains of photoreceptors face the retinal surface and are held together by the ZA (red).
(B) 37% pupal development (p.d.). Apical domains turn by 90º and face each other.
(C) 67% p.d. The apical domain is subdivided into rhabdomere and stalk. ZA anchors photoreceptors to the retinal surface and to the retinal floor. At this stage Crumbs is excluded from the rhabdomere and Bazooka re-localizes to the rhabdomere.
Adapted from Izaddoost et al., 2002.

Crumbs links to the cellular skeleton component β_H-spectrin to regulate the length of the stalk. Lack of β_H-spectrin *per se* causes shortening of the stalk membrane and trans-heterozygous mutants for Karst (gene encoding βH-spectrin) and Crumbs have stalk much shorter than wild-type or heterozygous Crumbs mutants, suggesting that these two proteins cooperate to control the formation of the stalk (Pellikka et al., 2002).

The FERM domain in the cytoplasmic domain of Crumbs interacts with Yurt, a negative regulator of Crumbs function during stalk growth (Laprise et al., 2006). In photoreceptors lacking Yurt, the stalk membrane is expanded, a phenotype similar to that observed upon over-expression of Crumbs or over-expression of its extracellular domain (Pellikka et al., 2002). The complex of Crumbs with β_H-spectrin should stabilize the stalk membrane by decreasing the rate of endocytosis, contributing to its growth. Yurt has a homolog in vertebrates, Mosaic eyes, which negatively regulates the function of CRB2, one of the human orthologs of Crumbs. In zebra-fish lacking CRB2 the extension of the inner segment, the functional equivalent of the stalk membrane in the fly, is shorter (Omori and Malicki, 2006).

2.2 Formation of the Interrhabdomeral Space

When the interrhabdomeral space opens around 55% pd, the apical domain of photoreceptors is clearly divided into rhabdomere and stalk (**Figure 1.12A,B**). Two independent genetic screens to find factors necessary for the formation of the interrhabdomeral space, identified Spacemaker/Eyes Shut, a proteoglycan-related protein with 14 EGF-like repeats and four Laminin G domain. Secretion of Spacemaker by photoreceptors generates an extracellular matrix that separates the rhabdomeres within the same ommatidium and creates the interrhabdomeral space (Husain et al., 2006; Zelhof et al., 2006). Other gene identified in the screen and that belongs to the same complementation group is Prominin (Zelhof et al., 2006). Prominin is a five spanning transmembrane protein that recruits

Spacemaker to the rhabdomere and stalk surfaces to avoid improper adhesion between different rhabdomeres.

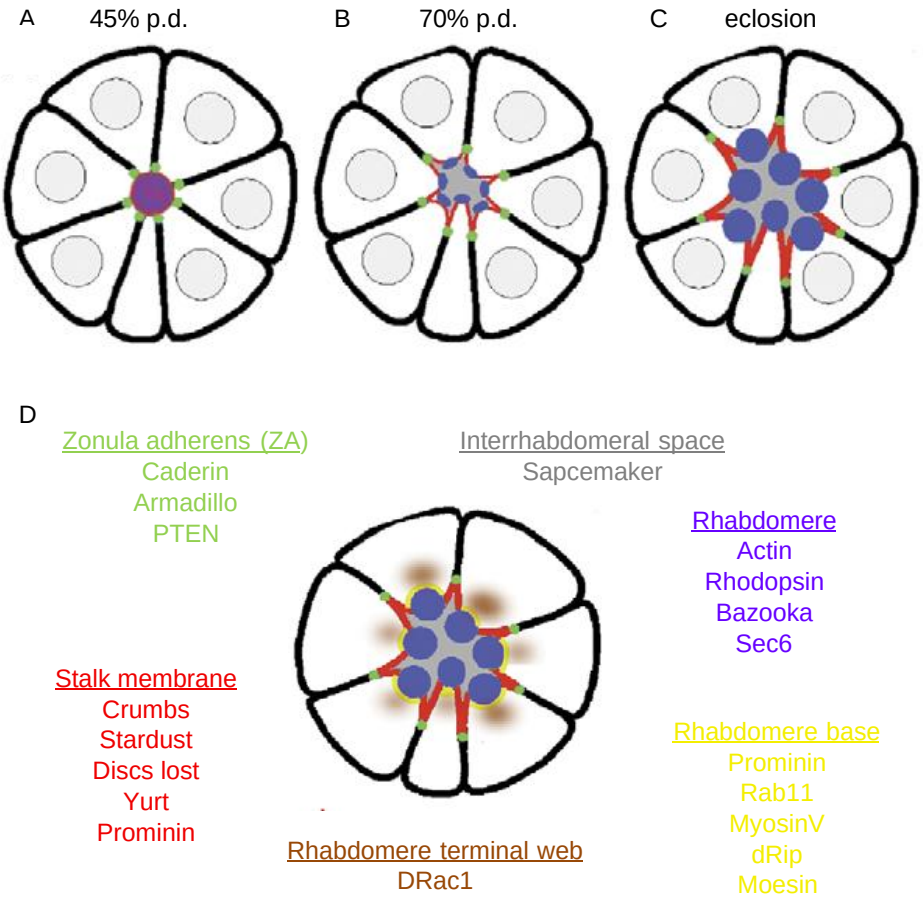

Figure 1.12 Formation of the interrhadomeral space and morphogenesis of the rhabdomere in the pupa.

ZA is in green, the rhabdomere is in blue, the stalk is in red, the rhabdomere base is in yellow and the rhabdomere terminal web is in brown.
(A-C) Schematic representation of photoreceptors at 45% and 70% pupal development and at eclosion. The interrhabdomeral space (dark grey) opens between the photoreceptors and rhabdomeres increase in size during development in the pupa.
(D) Schematic representation of an adult ommatidium, with the localization of proteins mentioned in the text indicated by the colour.
Adapted from Knust, 2007.

In Spacemaker loss-of-function mutants, residual Spacemaker was confined to the stalk membrane and did not penetrate between the rhabdomeres. Moreover, in a mutant of Sec6, a member of the exocyst necessary to the delivery of proteins to the rhabdomere but not to the stalk or to the basolateral membrane, Spacemaker secretion is not affected supporting the idea that Spacemaker is secreted through the stalk membrane and then spreads through the interrhabdomeral space (Husain et al., 2006).

The evolutionary step that separates the eye of insects with open rhadomere system from insects with closed rhabdomere system is the expression of Spacemaker (Zelhof et al., 2006). Ectopic expression of Spacemaker in the ocelli, a simple eye with 70-90 photoreceptor located at the vertex of the fly head, is sufficient to induce the formation of an extracellular space surrounding the rhabdomeres.

2.3 Morphogenesis of the Rhabdomere

Rhodopsin is the major membrane protein of the rhabdomere and represents 65% of the rhabdomere protein in *Calliphora* photoreceptors (Paulsen and Schwemer, 1979). In *Drosophila* Rhodopsin1 (Rh1) nulls, the morphogenesis of the rhabdomere is severely deviated from the normal development well before eclosion and retinal degeneration precedes Rh1 light dependent activation in the adult (**Figure 1.13A**) (Kumar and Ready, 1995; Kumar et al., 1997). Besides its role in phototransduction, Rh1 plays a fundamental regulatory role in the establishment of rhabdomere architecture in the pupa.

Rhabdomere morphogenesis starts around 67% of pupal development (**Figure 1.12B**). At 73%pd, the rhabdomere displays long thumb-like projections with regular section and connected at base by hairpin loops (Kumar and Ready, 1995). Rh1 transcription starts around 75-78% pd. Rh1 is first detected in the cell body of the photoreceptor and is then transported to the rhabdomere, and at 84% pd Rh1 is evenly distributed throughout the rhabdomere (**Figure 1.13B-D**)

(Kumar and Ready, 1995). In the late pupa and in the adult Rhodopsin1 show a C-crescent pattern at the base of the rhabdomere (**Figure 1.13B-E**). After the onset of Rh1 expression, at 90% pd, rhabdomeres show a circular section with tightly packed microvilli, and a well defined catacomb like base. In the absence of Rh1, rhabdomeres show a cylindrical section and severe structural defects: the base is an irregular surface of haipins and loops, and sheets of two apposed planar membrane protrude deep into the cytoplasm (**Figure 1.13A**). At 96% pd, rhabdomeres in the Rh1 null mutants start to degenerate and disappear completely by one day post eclosion (Kumar and Ready, 1995).

Donald F. Ready and collaborators found that expression of a dominant negative form of *Drosophila* Rac1 (DRac1), a member of the Rho GTPases family and key regulator of the actin cytoskeleton, impairs the morphogenesis of the rhabdomere and causes a phenotype reminiscent to the one observed in Rh1 nulls (Chang, 2000). A small pulse of constitutive active form of DRac1 at 80% pd is sufficient to rescue the morphogenesis of the rhadbomere in Rh1 null mutants. DRac1 localizes to the base of the rhabdomere in close proximity to the actin cytoskeleton of the rhabdomere at 76% pd. DRac1 acts downstream of Rh1 to organize the cortical actin cytoskeleton at the base of the rhabodomere into a subapical barrier. Targets of DRac1 activity are still unidentified (Chang, 2000).

The actin cytoskeleton at the base of the rhabdomere is known as RTW - rhabdomere terminal web (**Figure1.13A**). A fusion protein between the Moesin actin binding region and GFP highlights bundles of actin microfilaments that extend from the base of the rhabdomere deep into the cytoplasm of the photoreceptor (Chang, 2000). The microfilaments of the RTW are thought to work also as a route for the vectorial trafficking of vesicles to the base of the rhabdomere.

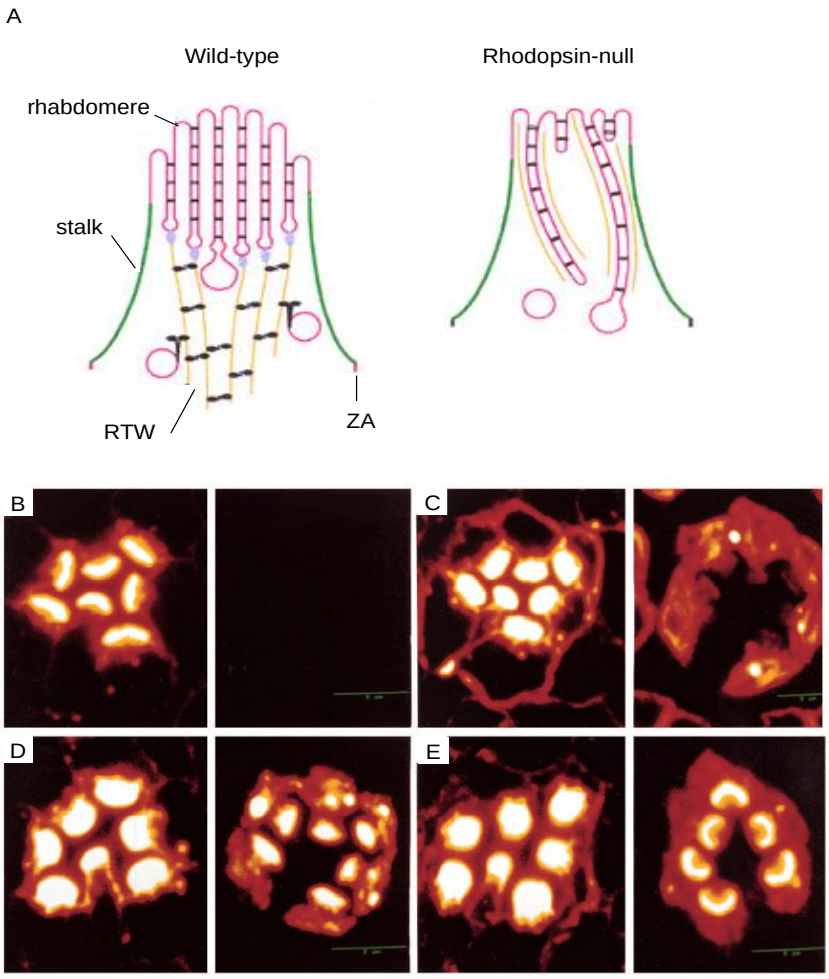

Figure 1.13. Rhabdomere morphogenesis and Rhodopsin1 distribution.

(A) In wild-type flies, a organized rhabdomere terminal web (RTW) sustains the base of the rhabdomere, preventing the expanding rhabdomere from intruding into the cytoplasm. The RTW extends from the base of the rhabdomere into the photoreceptor cytoplasm and is a route for targeted vesicles to the rhabdomere. In rhodopsin null mutants, the RTW fails to organize and the rhabdomere membrane involutes deeply into the photoreceptor. ZA, *zonula adherens*. Adapted from Chang, 2000.
(B-E) Rhabdomere morphogenesis (left panel, stained with rhodamine phalloidin) and Rh1 expression pattern (right panel) in the pupa of wild-type eyes. Source: Kumar and Ready, 1995.
(B) 73% pd. No Rh1 staining is detected although rhabdomere has started to emerge.
(C) 78% pd. Rh1 staining is detected in the cell body and stalk. Little protein appears to localize to the rhabdomere.
(D) 84% pd. Rh1 staining is equally distributed through the entire rhabdomere in outer photoreceptors.
(E) 96% pd. Rh1 concentration shows a crescent gradient with the low levels at the rhabdomere distal tips and highest levels of concentration near the base of the rhabdomere

2.4 Targeted Vesicular Trafficking to the Rhabdomere

Rab11 is a small GTPase that controls membrane fusion at the trans-Golgi network. When Rab11 function is inhibited, vesicles containing Rh1 and other rhabdomere proteins accumulate in the cytoplasm of the photoreceptors, rhabdomeres show reduced size and the interrhabdomeral space is reduced (Satoh, 2005). Rab11 interacts with MyoV (Myosin V), an unconventional motor protein and dRip, an adaptor protein, to form a complex that pulls vesicles through the RTW to the exocytic plasma membrane at the rhabdomere base (Li et al., 2007). When MyoV expression is reduced, ectopic rhabdomere-like structures form at the basolateral membrane of the photoreceptors, demonstrating that MyoV is responsible for targeting the secretory vesicles to the apical membrane (Li et al., 2007).

Sec6 and Sec5, components of the exocyst, are expressed in the photoreceptors during pupation and seem to be involved in the delivery of proteins to the rabdomere (Beronja, 2005). In yeast, the exocyst promotes the tethering of exocytic vesicles to the plasma membrane in the budding site. In photoreceptor cells, a reduction of Sec6 function leads to the accumulation of vesicles in the cytoplasm and a decrease in the size of rhabdomeres (Beronja, 2005). Importantly, in this mutant the delivery of proteins like Rh1 and Chaoptin to the rhabdomere is impaired, but not delivery of Crumbs to the stalk or delivery of other proteins of the basolateral membrane (Beronja, 2005). Moreover, Sec5 interacts physically with Rab11, and Sec5 interacts with Sec6 suggesting that Rab11 forms a complex with the exocyst to facilitate the targeted delivery of proteins to the rhabdomere.

The trafficking of membrane to the growing apical membrane of photoreceptors has to be tightly regulated and signaling lipids were shown to have a critical role during the morphogenesis of the rhabdomere. Genetic manipulations that originate higher levels of a single species of phosphatidic acid in photoreceptors interfere with the endomembrane system and impair the formation of the rhabdomere (Raghu et al., 2009). In EM, mutant photoreceptors

show smaller rhabdomeres and an accumulation of tubular and vesicular transport intermediates within the cell body (Raghu et al., 2009). These structural defects are mediated by Arf1 (ADP-ribosylation factor 1), a small GTPase that regulates the assembly of membranes along the early secretory pathway (between ER and Golgi, between Golgi cisternae and at the trans-Golgi). Expression of Arf1-GAP, which enhances the hydrolysis of GTP on GTP-Arf1 to GDP-Arf1 and reduces Arf1 activity, rescues rhabdomere defects caused by over-expression of Pld (phosphatidylcholine-hydrolyzing phospholipase D), an enzyme that mediates phosphatidic acid production (Raghu et al., 2009). Manipulation of phosphatidic acid is only critical during a window of time before 70% of pupal development.

The RTW is also a route for endocytic vesicles that participate in the rhabdomere membrane turnover . When endocytosis is inhibited by expression of a dominant negative form of Rab5 during photoreceptors differentiation, the rhabdomere base is disrupted and apposed membranes invade the cytoplasm, a phenotype that resembles the phenotype of Rh1 null mutants (Pinal and Pichaud, 2011). These observations indicate that endocytosis is essential for maintaining the integrity of the interface between the cell body and the rhabdomere base during photoreceptors morphogenesis.

2.5 Rhodopsin1 Biogenesis and Retinal Degeneration

Rh1 is synthesized and processed in the ER, where undergoes post-translational modifications such as binding of chromophore 3-hydroxyretinal and N-linked glycosylation, then is transported through Golgi compartments and is inserted in the phototransducing membranes of the rhabdomere. Mutations that affect rhodopsins maturation or its transport are a dominant cause of retinal degeneration in flies and humans.

Drosophila Rh1 is solely glycosylated at position Asn^{20} (Webel et al., 2000). An Asn→Iso substitution in the N-linked glycosilation consensus sequence abrogates (N20I) Rh1 glycosylation and interferes with biogenesis of both mutant

and wild-type Rh1, which are retained in the ER and Golgi. *Drosophila* expressing N20I Rh1 shows accumulation of rough ER cisternae, a dilated Golgi and small rhabdomeres (Webel 2000). *Drosophila* Calnexin or NinaA null mutants exhibit a similar phenotype (Rosenbaum et al., 2006). The ER quality control lectin Calnexin associates in a stable complex with Rh1 and lack of Calnexin leads to degradation of immature Rh1. NinaA is an exclusive chaperone of Rh1 required for Rh1 exit from the ER, escorting Rh1 along the secretory pathway. In ninaA null mutants, levels of Rh1 are strongly reduced and mature and immature forms are detected due to the accumulation of glycosylated Rh1 inside the ER (Baker et al., 1994a). The central cyclophilin homology domain of NinaA extends to the ER lumen and has peptidyl-prolyl cis-trans isomerase activity that is necessary for proline isomerization in Rh1 molecule (Stamnes et al., 1991).

Polarized transport of Rh1 to the rhabdomere membrane is dependent on a region adjacent to the C-terminus (helix 8) that may act as a binding site for targeting factors. Deletion of helix 8 results in an extra-rhabdomeric distribution of Rh1 and profound alteration of rhabdomere structure. This is a major difference to trafficking of vertebrate rhodopsin, which requires a conserved consensus sequence QVxPA at the very C-terminus (Kock et al., 2009).

3. Aims of the work

In *Drosophila*, Ire1 signaling is activated in the photoreceptors upon expression of Rh1 folding mutants (Ryoo et al., 2007; Griciuc et al., 2010; Kang and Ryoo, 2009) or in ninaA mutations that cause the accumulation of misfolded Rh1 in the ER (Mendes et al., 2009). However, the role of Ire1 signaling during normal photoreceptor differentiation remained unknown. The first study relating Rh1 biogenesis with UPR describes a role for the miR-708, a micro-RNA enriched in the eye of mouse (Behrman, Acosta-Alvear et al. 2011). CHOP up-regulates the transcription of miR-708 during ER stress, and miR-708 targets Rhodopsin mRNA through a binding site on its 3'UTR, decreasing the load of client proteins into the ER and alleviating ER stress.

The rhabdomere comprises over 90% of the total membrane in a photoreceptor (Leonard et al., 1992). The biogenesis of the ER membrane and the processing of all proteins accommodated in the rhabdomere during a very short period of time comprising only a few hours, imposes a huge demand to photoreceptors ER. We hypothesized that the UPR, in particular the Ire1/Xbp1 branch, is activated during the differentiation of photoreceptors in the pupa, where it is necessary to maintain ER homeostasis and to ensure a normal morphogenesis of the rhabdomere. In order to elucidate the putative role of the Ire1/Xbp1 signaling in photoreceptor differentiation, we pursued the following specific aims:

1. Mapping temporal and spatial activation of the Ire1/Xbp1 signaling pathway during eye development using the ER stress reporter Xbp1-EGFP.

2. Determination of Ire1/Xbp1 relevance for rhabdomere morphogenesis during pupal development by analysis of photoreceptor differentiation markers in eye clones of Ire1 or Xbp1 loss-of-function mutants.

4. Generation of Xbp1 null mutants by imprecise excision of P elements in the vicinity of Xbp1 genomic region through genetic crosses with Δ23 transposase and characterization by PCR and sequencing.

3. Identification of Ire1/Xbp1 target genes and effector mechanisms required for rhabdomere morphogenesis.

Ire1 signaling is required for rhabdomere morphogenesis and photoreceptor differentiation in *Drosophila*

CHAPTER II

Summary

The accumulation of misfolded proteins in the lumen of the endoplasmic reticulum (ER) causes ER stress and activates a homeostatic mechanism termed the Unfolded Protein Response (UPR). The most conserved arm of the UPR is mediated by an ER transmembrane protein, Ire1, that removes an unconventional intron from Xbp1 mRNA upon ER stress. Xbp1spliced is an effective transcription factor that up-regulates chaperones and enzymes.

We observed that the ER stress reporter Xbp1-EGFP is strongly activated in photoreceptors of the *Drosophila* eye during late pupation. During pupal development, photoreceptors undergo dramatic morphologic changes that include the morphogenesis of the rhabdomere, a specialized organelle for light detection that comprises 50 000 microvilli.

We analyzed mutant mosaic eyes for Ire1 in the pupa and adult by immunohistochemistry to clarify the role of Ire1 signaling in photoreceptor differentiation. Ire1 mutant clones show an atrophy of rhabdomeres and a collapse of the interrhabdomeral space. Rhodopsin1 (Rh1) and Spacemaker are not efficiently delivered to the apical membrane and accumulate in the cell body of photoreceptor. The ER folding capacity of Ire1 mutant photoreceptors is down-regulated but is sufficient to ensure Rh1 maturation and exit from the ER.

In conclusion, the ER stress sensor, Ire1, is necessary for the morphogenesis of the rhabdomere and when mutated causes the early degeneration of photoreceptors in *Drosophila*.

Introduction

The endoplasmic reticulum (ER) is a membranous organelle where proteins targeted for secretion or for the plasma membrane are folded and processed. The ER balances the load of incoming proteins to its folding capacity, avoiding accumulation of toxic misfolded proteins. Disruption of this balance activates the

Unfolded Protein Response (UPR), a homeostatic mechanism that relieves ER stress (Walter and Ron, 2011).

In higher eukaryotes, the UPR has three parallel branches initiated by different ER transmembrane proteins: protein kinase (PKR)-like ER kinase (Perk), activating transcription factor 6 (Atf6) and inositol-requiring enzyme 1 (Ire1). UPR signaling engages translational and transcription modifications to restore the normal functioning of the ER, including up-regulation of ER chaperones and enzymes, attenuation of the overall translation rate, and stimulation of degradation of misfolded ER proteins (Ron and Walter, 2007). When ER stress is severe and prolonged, or when the UPR protective mechanisms are not sufficient to overcome the causes of ER stress, cells die by apoptosis, a programmed form of cell death (Rasheva and Domingos, 2009).

Ire1 is conserved across all eukaryotes, presenting a luminal domain that detects the accumulation of misfolded proteins in the ER lumem, and a cytoplasmic domain with kinase and RNase activities that trigger downstream signals in the cytoplasm (Liu, 2002; Shamu and Walter, 1996; Tirasophon et al., 1998; Credle et al., 2005; Gardner and Walter, 2011). Activated Ire1 catalyzes the unconventional splicing of a small intron from X-box binding protein 1 (Xbp1) mRNA (or Hac1 mRNA, in yeast) (Sidrauski and Walter, 1997; Calfon et al., 2002; Cox and Walter, 1996). This splicing event causes a frameshit during translation that introduces a new carboxyl terminus in Xbp1 encoding for a trans-activation domain (Calfon et al., 2002; Yoshida et al., 2001). Xbp1 spliced protein is an effective transcription factor with a basic leucine zipper motif that regulates the expression of ER-chaperones and other Ire1/Xbp1 target genes (Acosta-Alvear et al., 2007).

Molecular mechanisms underlying Ire1 pathway of the UPR were first dissected in yeast and ever since UPR activation was extensively reported in cell culture and animal models of many diseases, namely cancer, diabetes and degenerative diseases (Lin et al., 2008). In *Drosophila* models of retinal degeneration, dominant mutations in the extracellular or transmembrane domains

of the major Rhodopsin of the eye, Rhodopsin 1 (Rh1), lead to progressive loss of photoreceptor cells by apoptosis (Colley et al., 1995; Davidson and Steller, 1998). Most of these mutations perturb Rh1 folding in the ER, inducing the expression ER stress markers and activating the UPR (Ryoo et al., 2007). Mediators of the UPR signaling (Xbp1) and components of the ER associated degradation machinery (HRP, EDAM1, EDAM2) have a protective role and delay age related retinal degeneration in these models (Kang and Ryoo, 2009; Ryoo et al., 2007). Despite recent findings, it is unclear if the UPR has a physiological role during the normal development of *Drosophila* eye.

In *Drosophila*, photoreceptors specification begins in the eye imaginal disc, during the third larval instar. After the passage of the morphogenetic furrow, a combination of inductive signals recruits sequentially the 8 photoreceptor cells into each ommatidium: R8 is the first to be specified, then R2/5, R3/4, R1/6, and finally R7 (Ready et al., 1976; Tomlinson and Ready, 1987). R8 starts producing Spitz which activates EGFR receptor in the neighboring cells, and contributes to the differentiation of the other photoreceptors (Freeman, 1996; Yang and Baker, 2001). During pupation, photoreceptors undergo a dramatic morphological change: their apical–basal axis rotates by 90º and their apical membranes expand and originate a stack of photosensitive microvilli (Knust, 2007; Pichaud and Desplan, 2002). These microvilli form the rhabdomere, a specialized organelle of the photoreceptors, where rhodopsins and other components of the visual transduction cascade localize. Concomitantly, photoreceptors belonging to the same ommatidium separate from each other at their apical tips and a lumen arises between their rhabdomeres - the interrhabdomeral space (Husain et al., 2006; Zelhof et al., 2006).

Rh1 synthesis starts at 78% of pupal development (Kumar and Ready, 1995; Kumar et al., 1997). Rh1 is synthesized and core-glycosylated in the ER and then transported in secretory vesicles along polarized actin filaments of the subcortical terminal web to the rhabdomere base (Chang and Ready, 2000). The post-Golgi trafficking of Rh1 is regulated by Rab11 and depends on the activity of the motor

protein MyoV, which forms a complex with dRip and Rab11 (Li et al., 2007). Inhibiting the function of any of these genes compromises Rh1 transport to the apical membrane and leads to its accumulation in the cytosol (Li et al., 2007; Satoh et al., 2005). Sec6, a component of the exocyst, is also involved in the target delivery of Rh1 to the apical membrane of photoreceptors (Beronja et al., 2005). Defective trafficking or biogenesis of Rh1 affects the morphogenesis of the rhabdomere, evidencing the structural role of Rh1 (besides its function in light detection).

The morphogenesis of the rhabdomere comports the synthesis of a huge number of secretory vesicles that deliver membrane and proteins to the rhabdomere. Therefore the ER has to deal efficiently with the high demand for its folding and processing function during the morphogenesis of the rhabdomere in the pupa. We found that the UPR is activated in photoreceptor cells of the eye during late stages of development in pupa. Ire1 signaling is required for photoreceptor differentiation and rhabdomere morphogenesis, including delivery of Rh1 to the rhabdomere and secretion of Spacemaker into the inter-rhabdomeral space.

Materials and Methods

Genetics and Fly stocks

Fly stocks and crosses were maintained on standard cornmeal agar medium, at 25ºC, in a 12 hr light/dark cycle and a relative humidity of 70%. Using these experimental conditions 100% pupation corresponds to 86hr of development in the pupa.

The ER stress reporter uas-Xbp1-EGFP was expressed under the control of the GMR-GAL4 driver for ectopic expression in the eye posterior to the morphogenetic furrow. The *PBac{WH}Ire1*^{f02170} allele was obtained from the Bloomington Stock Center (#18520) and recombined into a *P{neoFRT}82B* chromosome. Recombinants resistant to neomicin and w^+ were selected. Mutant somatic clones were generated by the Flp/FRT technique and Flipase was

expressed under the control of the *eyeless* promoter (Golic, 1991; Newsome et al., 2000). The precise excision of *PBac{WH}Ire1*^{f02170} was carried out by crossing this line to the Δ23 transposase line.

The UAS-Ire1 transgenic line was generated by P-element mediated transformation. The CH322-07H05 genomic construct from P[acman] library was integrated into the genome by ϕC31 integrase-mediated transgenesis (acceptor strain #9752 and attP acceptor site 22A3). The injection of DNA into embryos to establish *Drosophila* transgenic lines was performed by BestGene. w^+ transformants were selected and stable transgenic stocks were established.

Stocks used in the western blot were as following: *yw*, *ninaE*^{17} (Joseph O'Tousa – (Kurada and O'Tousa, 1995)), *ninaA*^{1} (Bloomington #3533 (Ondek et al., 1992)), *ninaA*^{E110V} (Charles Zuker - (Ondek et al., 1992)), and *EGUF;;FRT82B GMR-hid CL /TM2* (for whole eye mutant clones, Bloomington # 5253)

To reduce the fluorescence background from the red pigment, *pWIZ* (transgenic construct carrying RNAi against the *white* gene) was introduced into the genetic background (Sik Lee, 2003).

DTT treatment

Third-instar eye imaginal discs were dissected in PBS and incubated in Schneider's cell medium containing 5mM DTT or mock incubated without DTT for 4hr at room temperature.

Molecular Biology

Genomic DNA was isolated from adult flies using the *High Pure PCR Template Preparation kit* (Roche). Flies were snap frozen in liquid nitrogen and macerated with a motorized pestle in lysis buffer. To confirm the insertion site of *PBac{WH}Ire1*^{f02170} the flanking genomic region was amplified by PCR and sequenced. For each transposon end, a primer specific for the transposon and a primer specific for Ire1 genomic sequence was used: for 3'end, primers 3F1 (5'CAA CAT GAC TGT TTT TAA AGT ACA AA3') and Ire11 (5'CAG CAA CCA

AGA GAC AGAT3'); for 5'end, primers 5R1 (5'TGA CAC TTA CCG CAT TGA CA3') and Ire3 (5'TTC ATT ATT GGC CAA CAG GC3').

The precise excision of *PBac{WH}Ire1*^{f02170} and rescue of Ire1 original sequence was confirmed by PCR and sequencing using primers Ire3 and Ire11.

To clone Ire1 open reading frame, total RNA was extracted from adult flies using High Pure RNA Tissue kit (Roche) and 100ng were used as a template in Revertaid H Minus First Strand cDNA Synthesis kit (Fermentas/Thermo). 2 µl of total cDNA was used in a PCR reaction performed with Phusion polymerase with specific primers for Ire1 Isoform C (Ire9 – 5'CGG GGT ACC TCA ATC CTG CGT TGA AGG TGG3' and Ire12 – 5'GGA AGA TCT ATG GGC AGT CTT AAG AAG TTA CC3'). Ire1 open reading frame was then cloned into *Drosophila* expression vector pUAST using BglII and Acc65I restriction sites.

qRT-PCR

For quantitative reverse transcription-PCR (RT-PCR), total RNA was extracted from heads of 3 days old adults with Trizol and Direct-zol RNA mini-prep (Zymo Research). Samples were then treated with Turbo DNA-free (Ambion) and column purified. cDNA was synthesized with 500ng of total RNA using RevertAid First Strand kit (Thermo/Fermentas). PCR reactions were prepared with SSoFast EvaGreen Supermix (Bio-Rad) and a 1:40 diluition of the cDNA and run in a Bio-Rad Cfx-96 system. All samples were analyzed in triplicates. For each sample, the levels of mRNAs were normalized using rp49 as a loading control. Primers used in qPCR were as follows: GRP78 (Forward: 5'TGT CAC CGA TCT GGT TCT TCA GGC3', Reverse: 5'GTC CCA TGA CCA AGG ACA ACC ATC3'), ninaA (Forward: 5'CGT GGC CAG TGG TCT GAG CTT CAC3', Reverse: 5'CTC CAC CGC CAG AGC CTT ATC CTC3'), rp49 (Forward: 5'AGA TCG TGA AGA AGC GCA CCA AGC3', Reverse: 5'GCA CCA GGA ACT TCT TGA ATC CGG3')

Western blot

Protein extracts were prepared from adult heads homogenized with a motorized pestle in PBT containing protease inhibitors (Roche). Homogenates were sonicated in an ice water bath for 15min and centrifuged at 14000rpm for 10min at 4ºC. Supernant was collected, mixed with SDS loading buffer and boiled at 100ºC (or heated for 37ºC, for Rh1) for 5 min. Samples were loaded into a 4-15% gradient Mini-protean TGX precast gel (Biorad) and transferred into a nitrocellulose membrane (Whatman). Primary antibody mouse anti-Rhodopsin1 (4C5, (DSHB), 1:200), mouse anti-tubulin (12G10, DSHB, 1:15) or rabbit anti-Bip/GRP78 (SPC-180 StressMarq18 Biosciences, 1:1000) were incubated at 4ºC overnight and HRP-conjugated secondary anti-mouse antibody was incubated for 3hr at room temperature. Chemiluminescent detection was carried out using an ECL kit (GE Healthcare Life Sciences).

Immunostaining

To prepare horizontal eye cryosections, adult and pupa heads were embedded in OCT and cut in a cryostat. White pre-pupa (0hr) were collected and aged at 25ºC until the appropriate stage.

Pupal and adult eyes were dissected in PBS, fixed in 1X PBS + 4%formaldehyde for 30min at room temperature and washed 3X in PBT (1X PBS+ 0,3% Triton X-100), 10 min each. Primary antibody was diluted in BBT (1xPBS, 1% BSA, 0.1% Tween 20, 250 mM NaCl) and incubated overnight at 4ºC under gentle agitation. Primary antibodies used in immunohistochemistry were: rat anti-ELAV (7E8A10, DSHB), guinea pig anti-homothorax (Wildonger et al., 2005), guinea pig anti-Runt (Duffy et al., 1991), mouse anti-armadillo (N2 7A1, DSHB), rabbit anti-aPKC (Santa Cruz, sc-216), mouse anti-Crumbs (Cq4, DSHB), mouse anti-spam (21A6,DSHB), mouse anti-Rh1 (4C5, DSHB), mouse anti-tubulin (12G10, DSHB), guinea pig anti-Bip/GRP78 (Hsc-3, Ryoo et al., 2007), rabbit anti-Bip/GRP78 (StressMarq18 Biosciences, SPC-180), rabbit anti-calnexin (Rosenbaum et al., 2006), rabbit anti-ninaA (Baker et al., 1994), mouse

anti-Cut (2B10, DSHB), mouse anti-Rh4. Samples were washed 3X for 10min in PBT and incubated with appropriate secondary antibodies (Jackson ImmunoResearch) in BBT for 3hr at room temperature. Phalloidin-TRITC or Phalloidin-FITC (Sigma) was incubated together with secondary antibodies. Eyes were mounted in glycerol 70% and analyzed in a Zeiss LSM 710 microscope. Measurements of the interrhabdomeral space area were performed using ImageJ. For each pair of adjacent wild-type and Ire1 mutant ommatidia was calculated a ratio and a mean value of the ratio was then obtained.

Results

Ire1 signaling is active during photoreceptor differentiation in-the pupa

To test if the Ire1/Xbp1 signaling pathway is active during the development of the eye, we placed the fusion construct Xbp1-EGFP (Ryoo et al., 2007) under the control of the GMR driver for ectopic expression in all cells of the eye. Xbp1-EGFP is a reporter for ER stress, where EGFP is only in frame with Xbp1 upon Ire1 mediated unconventional splicing of Xbp1. In early stages of development in the larva, Xbp1-EGFP is not activated endogenously in eye imaginal discs **(Figure 2.1A)**. Induction of ER stress by treatment with DTT, a drug that blocks disulfide bond formation and interferes with protein folding in the ER, results in a strong activation of Xbp1-EGFP posterior to the morphogenetic furrow in eye imaginal discs **(Figure 2.1B)**.

Photoreceptors start expressing massively Xbp1-EGFP at 48hr of pupation **(Figure 2.1D)**. This strong activation of the ER stress reporter is specific of photoreceptor cells, which are positive for the neuronal marker Elav, and continues at 72hr pupation **(Figure 2.1E)**.

In the adult eye, the activation of Xbp1-EGFP remains in pigment cells marked by Homothorax but is absent in photoreceptor cells or cone cells **(Figure 2.2)**. These results indicate that the reporter Xbp1-EGFP is specifically activated in photoreceptors cells during mid and late stages of pupal development.

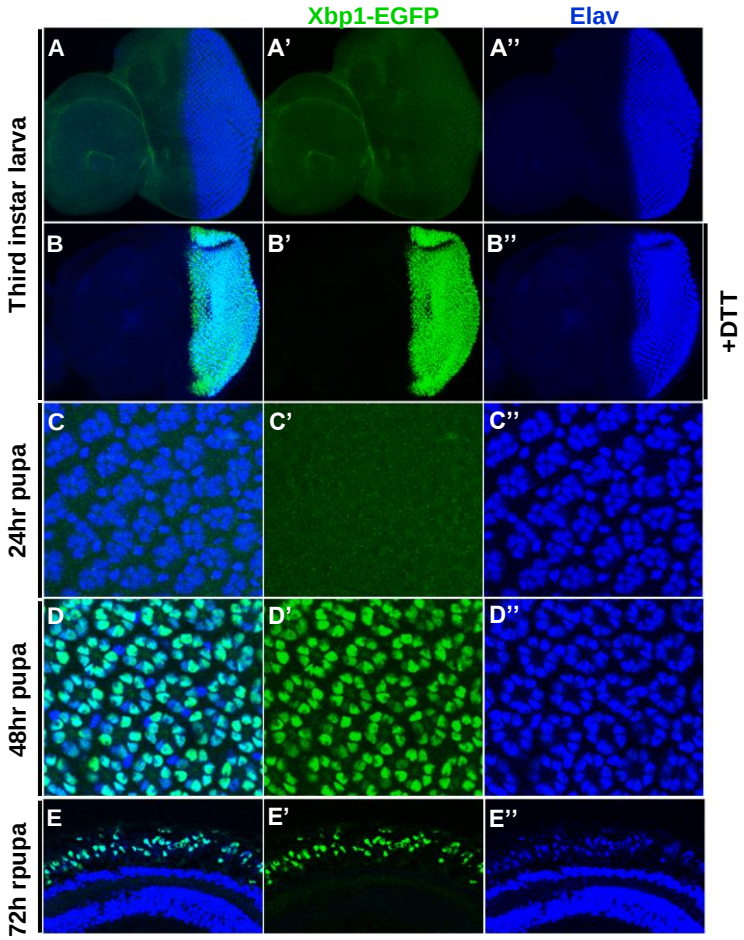

Figure 2.1 The Xbp1-EGFP reporter is activated in the photoreceptors during pupal stages.

The ER stress reporter UAS-Xbp1-EGFP (green) is expressed under the control of GMR-GAL4. Elav (blue) is a neuronal marker expressed in the photoreceptors.
(A) Endogenous GFP expression is not observed in GMR-GAL4 >UAS-Xbp1-EGFP eye/antenna imaginal disc of third-instar larvae.
(B) Culture of GMR-GAL4 > UAS-Xbp1-EGFP imaginal discs in 5 mM DTT for 4hr activates Xbp1-EGFP.
(C) Xbp1-EGFP activation is not observed in photoreceptors at 24hr pupa.
(D) Xbp1-EGFP activation is observed in the photoreceptors at 48hr of pupal development.
(E) Xbp1-EGFP is activated in photoreceptors at 72hr of pupal development.

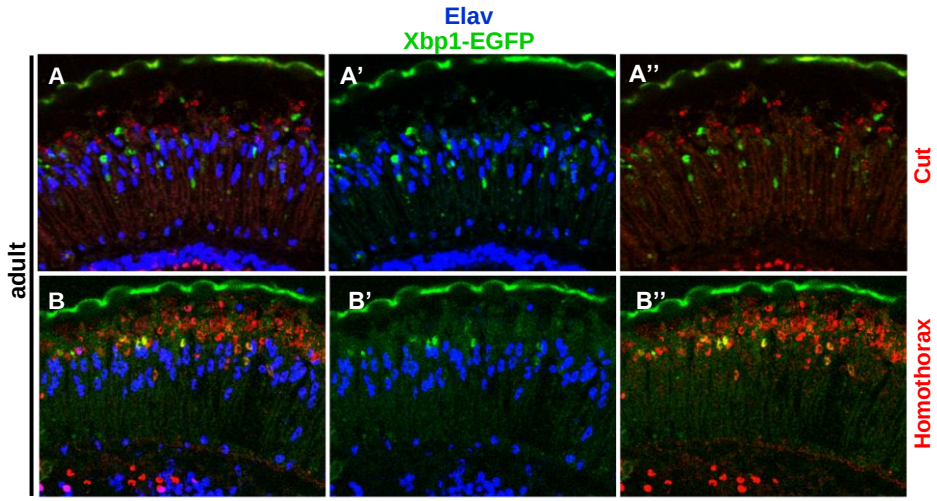

Figure 2.2. Xbp1-EGFP expression persists in pigment cells of the adult eye.

The ER stress reporter UAS-Xbp1-EGFP (green) is expressed under the control of GMR-GAL4.
(A) Xbp1-EGFP positive cells do not correspond to photoreceptors (blue) or cone cells marked by cut (red).
(B) Xbp1-EGFP activation is observed in some Homothorax (red)-positive cells of the lattice.

To ensure that Xbp1-EGFP activation is dependent on Ire1, we designed an assay where activation of the Xbp1-EGFP reporter was tested in mosaic tissue for mutant *PIre1*^{f02170} in the larva and in the pupa. *PIre1*^{f02170} is a loss-of-function allele, caused by the insertion of a 7.234bp PBac(WH) transposon in the coding sequence of Ire1 **(Figure 2.3A)**. Mutant clones were generated by the FRT/FLP technique with the flipase under the control of the *Eyeless* promoter. Xbp1-EGFP fluorescence is not observed in the mutant clones *PIre1*^{f02170} in larval eye imaginal discs treated with DTT and also in mid-pupal eyes **(Figure 2.3B,F)**. In control clones of the precise excision of *PBac(WH)Ire1*^{f02170}, Xbp1-EGFP fluorescence is distributed throughout the mosaic tissue **(Figure 2.3C,G)**. Moreover, Xbp1-EGFP activation in *PIre1*^{f02170} mutant clones is rescued by driving UAS-Ire1 under the control of GMR **(Figure 2.3D,H)** or by introducing an Ire1 genomic construct **(Figure 2.3E,I)**.

Ire1 is not required for photoreceptor specification and maintenance of the apical/basolateral polarity

According to our results, Ire1/Xbp1 signaling is active during the differentiation of photoreceptors in mid and late pupa. To clarify the role of Ire1 during eye development, we analyzed markers of photoreceptor specification and polarization in mutant clones of Ire1. In eye imaginal discs of third instar larva, photoreceptors are recruited into 8-cell clusters behind the morphogenetic furrow. In *PBac{WH}Ire1*^{f02170} mutant clones, older clusters show two cells marked by Runt that correspond to R8 and R7 (the first and the last photoreceptors to be specified), showing that Ire1 is not required for photoreceptor specification **(Figure 2.4A)**.

In early 40hr pupa, photoreceptor already rotated 90º and the apical domain of all eight photoreceptor faces each other at the center of the ommatideal cluster. At this stage of development, the apical domain of photoreceptors is marked by a complex that includes aPKC and its integrity is maintained by the *zonula adherens* (marked by Armadillo). In *PBac{WH}Ire1*^{f02170} mutant clones, the distribution of aPKC and armadillo is normal in 40hr pupa **(Figure 2.4B)**.

By the end of the first half of pupal development, the apical surface of photoreceptors is subdivided into two regions: the most apical, where an accumulation of actin corresponds to the incipient rhabdomere and a sub-apical region, the stalk, where Crumbs now localizes. Immunostaining with an antibody against Crumbs highlights a normal morphology of *PBac{WH}Ire1*^{f02170} mutant photoreceptors at 50hr pupation **(Figure 2.4C)**. In the mid and late pupa (56hr and 70hr pupation), Cadherin is positioning normally in the *zonula adherens* of the *PBac{WH}Ire1*^{f02170} mutant photoreceptors, demonstrating that the establishment and maintenance of apical basal polarity is unaffected by the Ire1 mutantion **(Figure 2.4D,E)**.

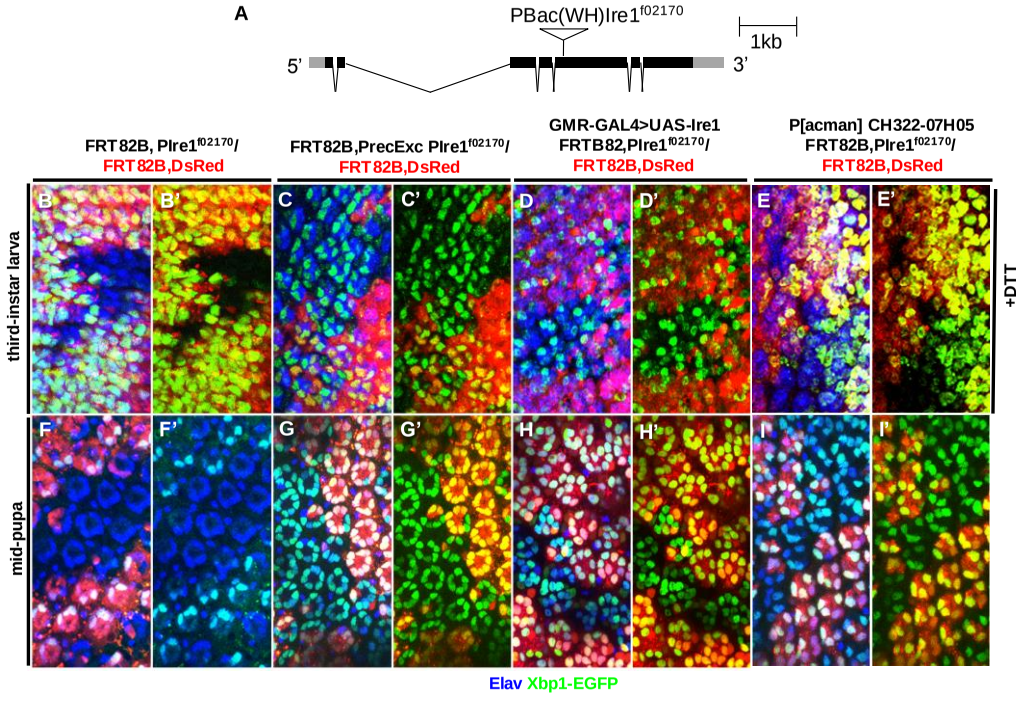

Figure 2.3 Ire1 is required for Xbp1-EGFP activation in the *Drosophila* Eye.
(A) Schematic shows Ire1 genomic region with the PBac(WH)Ire1^{f02170} transposon insertion in the open reading frame of Ire1.
Elav is in blue. (B-E) Third-instar larval stage eyes (posterior to the right) with *eyeless*-Flipase-induced clones of *PBac(WH)Ire1^{f02170}* homozygous cells, labeled by the absence of DsRed, were treated with DTT to activate Xbp1-EGFP (green).
(B) Xbp1-EGFP is not observed in cells homozygous for *PBac(WH)Ire1^{f02170}*.
(C) Xbp1-EGFP is observed in clones of a precise excision of *PBac{WH}^{f02170}* that restores the genomic region.
(D) Expression of UAS-Ire1 under the control of GMR-GAL4 or (E) CH322-07H05 (Pacman) genomic construct covering Ire1 region rescues Xbp1-EGFP activation in *PBac{WH}^{f02170}*homozygous cells.
(F-I) Pupal eyes (48hr) with *eyeless*-Flipase-induced clones of *PBac{WH}^{f02170}* homozygous cells, labeled by the absence of dsRed.
(F) Endogenous Xbp1-EGFP in the photoreceptors is not observed in cells homozygous for *PBac{WH}^{f02170}*.
(G) Xbp1-EGFP is observed in clones of a precise excision of *PBac{WH}^{f02170}*.
(H) Expression of UAS-Ire1 under the control of GMR-GAL4 or from (I) CH322-07H05 (Pacman) genomic construct rescues Xbp1-EGFP activation in *PBac{WH}^{f02170}* homozygous cells.

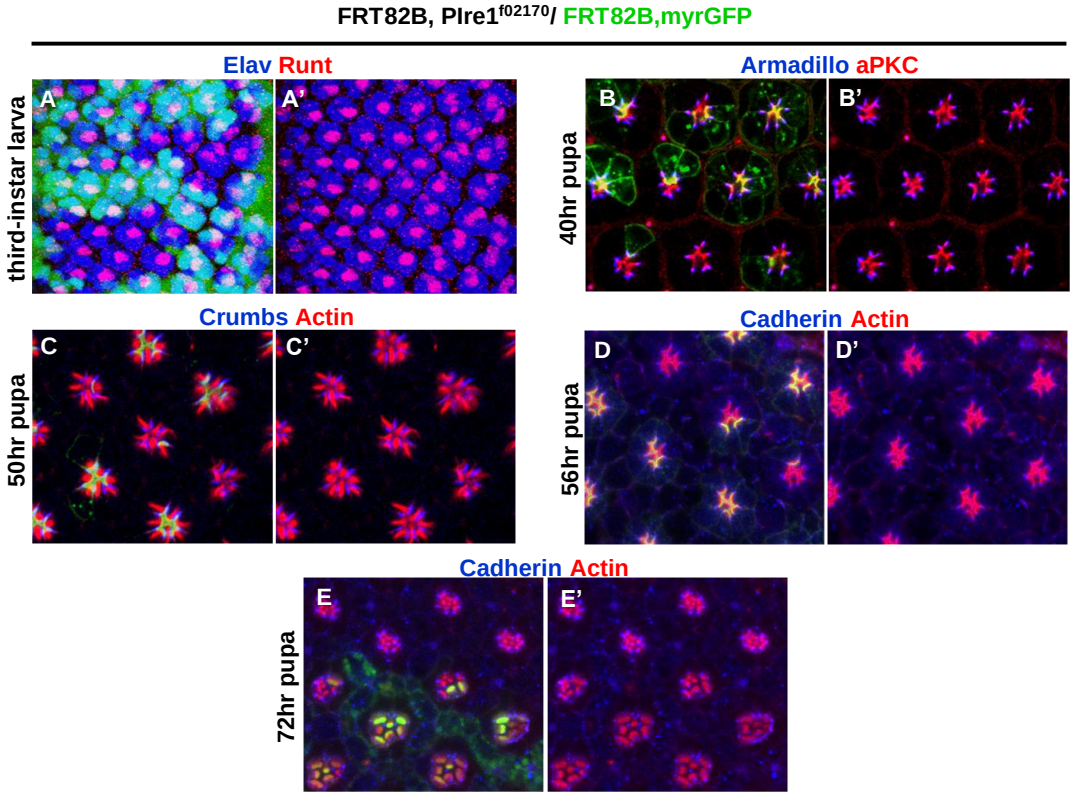

Figure 2.4. Ire1 is not required for photoreceptor specification and maintenance of apical/basolateral polarity.

(A) Third-instar larval stage eyes with *eyeless*-Flipase-induced clones of *PBac(WH)Ire1*^{f02170} homozygous cells, labeled by the absence of GFP (green), show normal expression of the photoreceptor specification markers Elav (blue) and Runt).
(B) 40hr pupal eye with *PBac(WH)Ire1*^{f02170} homozygous cells, labeled by the absence of myrGFP (green), show normal localization of Armadillo (blue) and aPKC (red).
(C) 50hr pupa with *PBac(WH)Ire1*^{f02170} homozygous cells, labeled by the absence of myrGFP (green), show normal localization of Crumbs (blue) and actin (red).
(D) 56hr pupal eye with PBac(WH)Ire1^{f02170} homozygous cells, labeled by the absence of myrGFP (green), show normal localization of Cadherin (blue) and actin (red).
(E) 72hr pupal eye with *PBac(WH)Ire1*^{f02170} homozygous photoreceptors show normal localization of cadherin (blue) and actin (red).

Ire1 is necessary for secretion of Spacemaker into the interrhabdomeral space and Rhodopsin1 localization to the rhabdomere

As development in the pupa continues, Spacemaker (Spam), a large extracellular protein, is secreted towards the apical side of the 8 photoreceptors and forms an extracellular matrix between them, known as the interrhabdomeral space. By 62hr pupation, an interrhabdomeral space marked by the presence of Spacemaker is already formed in wild-type clones of Ire1 **(Figure 2.5A)**. In *PBac{WH}Ire1*^{f02170} mutant ommatidea, Spacemaker is less secreted into the interrhabdomeral space and is found in the cell body of mutant cells **(Figure 2.5A)**. In consequence the interrhabdomeral space is significantly smaller in mutant ommatidea, as quantified by measuring the size of the interrhadomeral space in adjacent wild-type and mutant ommatidea **(Figure 2.5E)**. The size of the interrhadomeral space is not affected in clones of the *PBac{WH}Ire1*^{f02170} precise excision **(Figure 2.5B)**. Interrhabdomeral space in *PBac{WH}Ire1*^{f02170} ommatidia can be rescued by expressing UAS-Ire1 under the control of GMR or by providing in *trans* the CH322-07H05 P[acman] construct carring the genomic region of Ire1 **(Figure 2.5C,D)**. These data indicate that Ire1 is necessary for the efficient delivery of Spacemaker to the apical membrane of photoreceptors and for the formation of the interrhabdomeral space.

Late events of photoreceptors differentiation are compromised in *PBac{WH}Ire1*^{f02170} mutant clones. After 67% of pupal development, rhabdomere morphogenesis takes place depending on an abundant synthesis of Rh1 and its targeted delivery to the apical membrane of photoreceptors. In late 72hr pupa, photoreceptors of wild-type clones present Rh1 co-localizing with the emerging rhabdomere supported by actin microfilaments **(Figure 2.6A)**. In contrast, in *PBac{WH}Ire1*^{f02170} mutant photoreceptors Rh1 is not delivered to the apical membrane and it accumulates in the cell body of the photoreceptor **(Figure 2.6A)**.

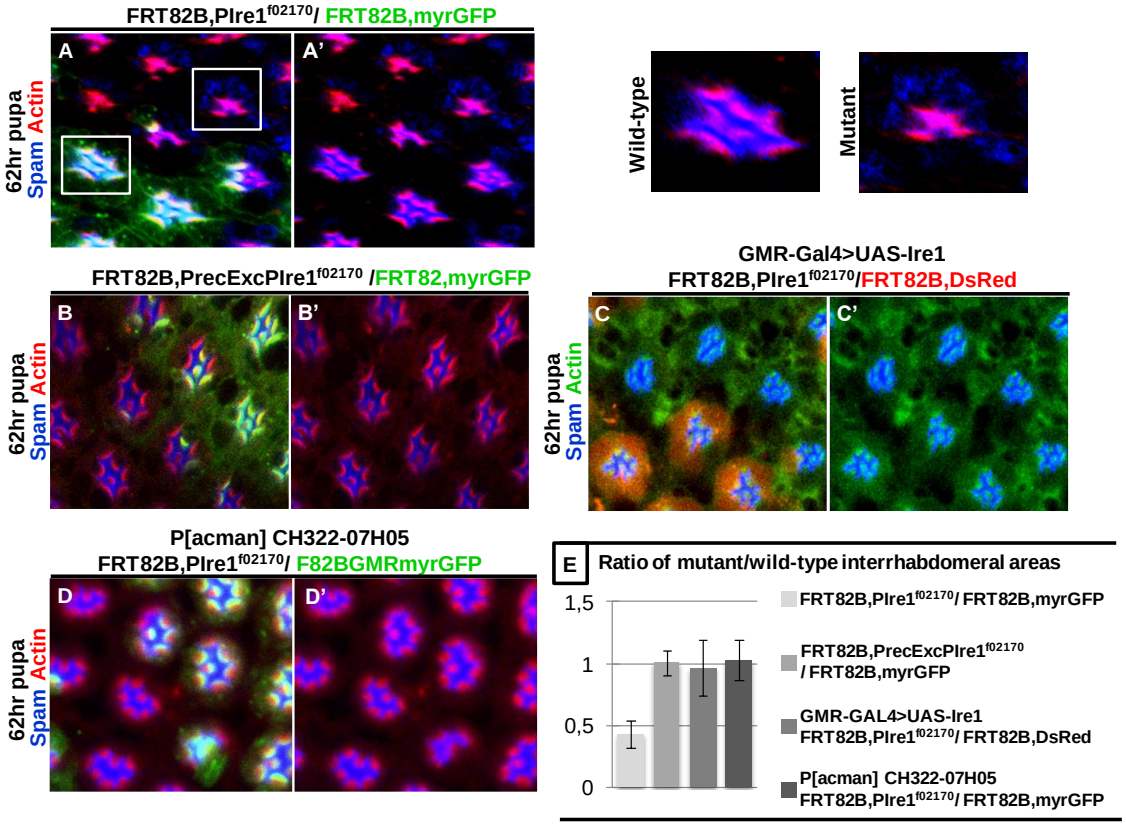

Figure 2.5 Ire1 is required for Spacemaker (Spam) secretion and formation of the interrhabdomeral space.

(A) By 62 hr pupation, *PBac(WH)Ire1*^{f02170} homozygous ommatidia (absence of myrGFP, green) have low levels of Spam (blue) in the interrhabdomeral space and present retention of Spam in the photoreceptor cell body. The rhabdomeres sustained by actin are in red. The magnified mutant and control ommatidia are in the side

(B) Clones of a precise excision of *PBac{WH}Ire1*^{f02170} (absence of myrGFP, green) have normal localization of Spam (blue) in the interrhabdomeral space.

(C) GMR-GAL4>UAS-Ire1 rescues Spam (blue) localization in *PBac(WH)Ire1*^{f02170} homozygous ommatidia (absence of dsRed).

(D) P[acman] CH322-07H05 genomic construct rescues Spam (blue) localization in *PBac(WH)Ire1*^{f02170} homozygous ommatidia (absence myrGFP, green).

(E) Quantification of interrhabdomeral space size is shown. The values are mean ± SD of the ratio of the interrhabdomeral areas of adjacent mutant and wild-type ommatidia. Around 40 pairs of mutant/wild-type ommatidia were quantified for each experimental condition indicated in the figure.

The delivery of Rh1 into the rhabdomere is unaffected in clones of the precise excision *of PBac{WH}Ire1^{f02170}*. Expression of UAS-Ire1 or adding the Ire1 genomic construct CH322-07H05 into the genetic background rescues the delivery of Rh1 to the rhabdomere in *PBac{WH}Ire1^{f02170}* clones **(Figure 2.6C,D)**.

The site of PBac{WH}Ire1^{f02170} insertion in the third chromosome is only 30kb distant from the *ninaE* locus that encodes Rh1. To determine if the transposon insertion in Ire1 is down-regulating the transcription of Rh1 by interfering with any enhancer or other *cis*-acting element in the *ninaE* locus, we evaluated the expression of the reporter Rh1-GAL4>UAS-LacZ in *PBac{WH}Ire1^{f02170}* clones. Expression of β-galactosidase was similar between wild-type and *PBac{WH}Ire1^{f02170}* clones, indicating that the phenotype observed for Rh1 in *PBac{WH}Ire1^{f02170}* clones is not cause by decreased transcription **(Figure 2.6E)**.

The trafficking of proteins along the secretory pathway *en route* to the rhabdomere and the interrhabdomeral space is also affected in the inner photoreceptors, R7 and R8. One example of this is Rh4, a rhodopsin responsible for color vision expressed exclusively in R7. In *PBac{WH}Ire1^{f02170}* mutant clones Rh4 is found in the cell body of the outer photoreceptors (R1-R6). This phenotype is very puzzling because outer photoreceptors only express the major Rh1. We speculate that the strong reduction of Rhodopsin1 in the rhadbomeres initiates a feed-back mechanism that alleviates the repression of Rh4 expression in the outer photoreceptors **(Figure 2.6F)**.

Rhabdomere morphogenesis is drastically impaired in *PBac{WH}Ire1^{f02170}* mutant photoreceptors: the rhabdomere size is drastically reduced and the architecture of this structure is deficient. The morphogenesis of the rhabdomere is not recovered at later stages of development. In opposition, early after eclosion mutant rhabdomeres desintegrate, photoreceptors degenerate and the retina shows severe damages **(Figure 2.7A,C)**. Exposure to constant light accelerates the degeneration process **(Figure 2.7B,D)**.

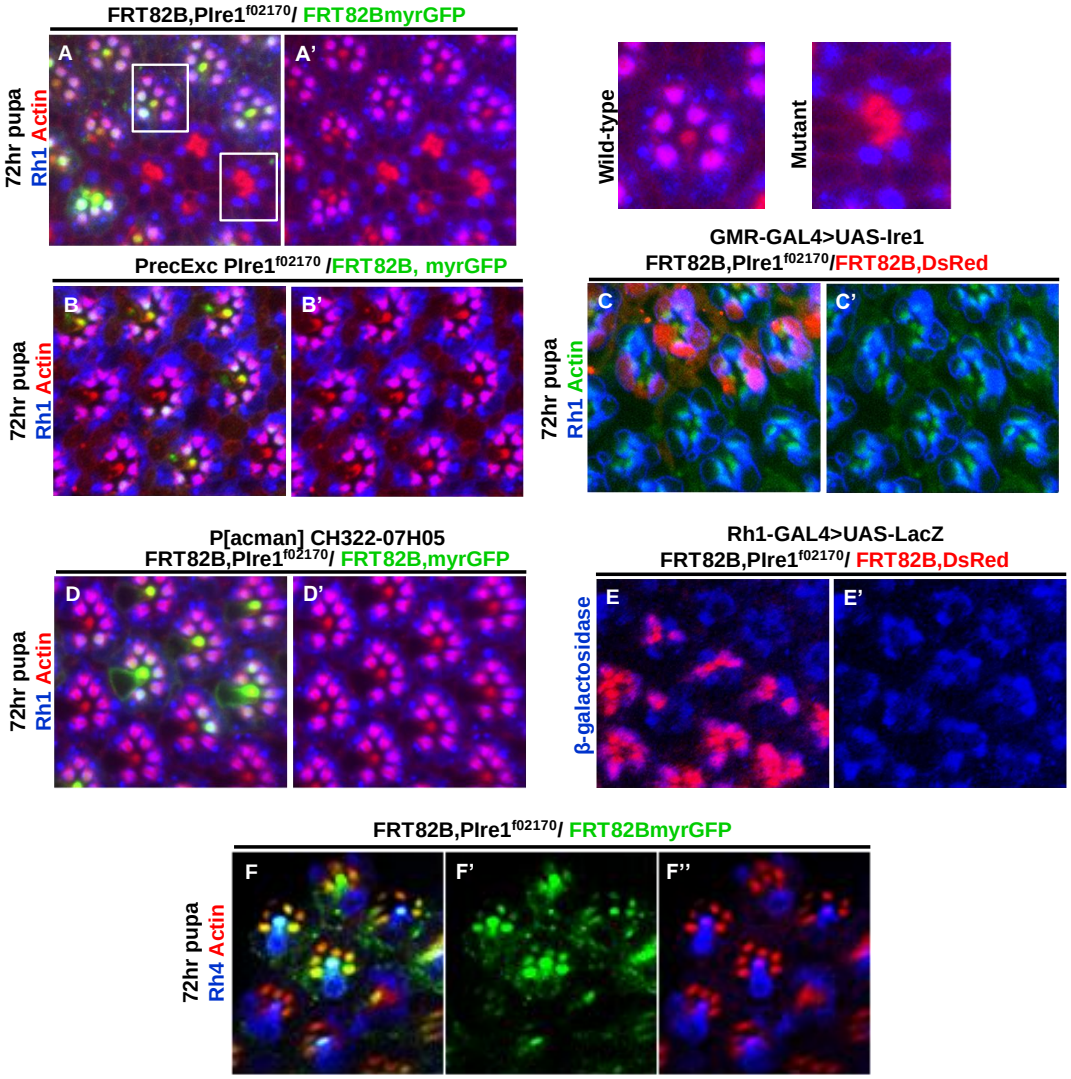

Figure 2.6. Ire1 Is Required for Rh1 Delivery into the Rhabdomere

(A) 72hr pupal eye with *eyeless*-Flipase-induced clones of *PBac{WH}Ire1*^{f02170} homozygous cells, labeled by the absence of myrGFP (green), show defective delivery of Rh1 (blue) into the rhabdomeres (actin, red). The magnified mutant and control ommatidia are indicated with white squares.

(B) Rh1 (blue) delivery into the rhabdomeres is normal in clones of a precise excision of *PBac{WH}Ire1*^{f02170} (labeled by the absence of myrGFP, green).

(C) GMR-GAL4 >UAS-Ire1 expression rescues Rh1 (blue) delivery into the rhabdomeres of *PBac(WH)Ire1*^{f02170} homozygous cells (labeled by the absence of dsRed).

(D) The CH322-07H05 genomic construct rescues Rh1 (blue) delivery into the rhabdomeres of *PBac{WH}Ire1*^{f02170} homozygous cells (absence of myrGFP, green).

(E) Reporter Rh1-GAL4>UAS-LacZ (blue) shows similar transcription levels of the Rh1 promotor between wild-type and *PBac{WH}Ire1*^{f02170} mutant clones (absence of DsRed).

(F) Rh4 (blue) is mislocalizing in the cell body of R1-R6 photoreceptors in clones of *PBac(WH)Ire1*^{f02170} (labeled by the absence of myrGFP, green).

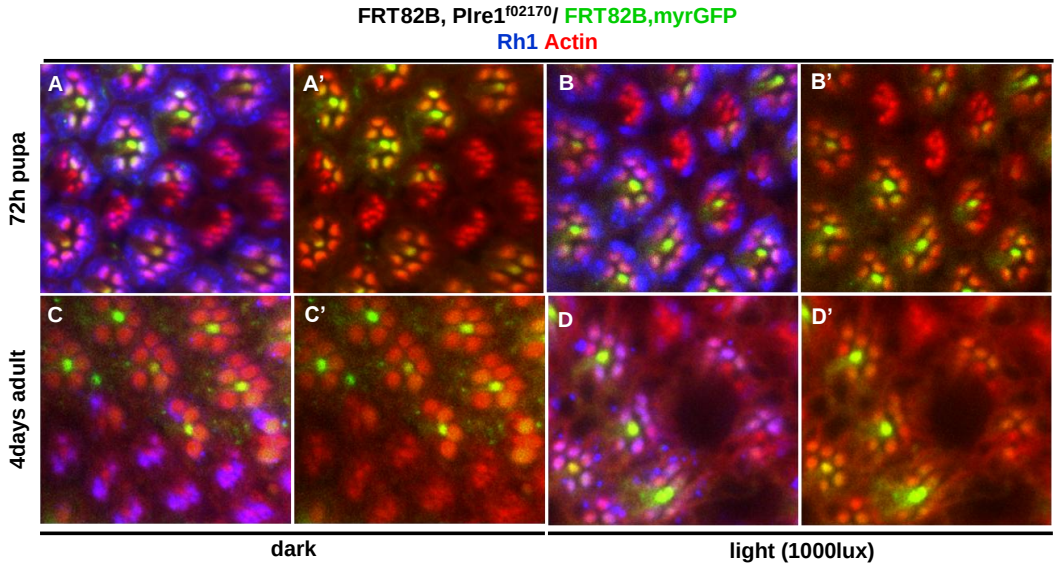

Figure 2.7 PBac(WH)Ire1^{f02170} photoreceptors degenerate early in the adult.

(A, B) Mutant clones of PPac(WH)Ire1^{f02170} (absence of myrGFP) in 72hr pupa show defects in the localization of Rh1 (blue) into the rhabdomere (red).
(C, D) In PBac(WH)Ire1^{f02170} mutant clones (absence of myrGFP) of the adult, rhabdomeres (actin, red) disintegrate and the retina degenerate, phenotype that is aggravated by exposure to light.

ER markers are down-regulated in *PBac{WH}Ire1^{f02170}* mutant photoreceptors

Next, we tested ER folding capacity in *PBac{WH}Ire1^{f02170}* mutant cells by evaluating the levels of ER chaperones/enzymes. We found that the expression of the chaperone Bip/GRP78 is strongly down-regulated in *PBac{WH}Ire1^{f02170}* mutant photoreceptors, mainly at the base of the rhabdomere **(Figure 2.8A)**. Western blot and qRT-PCR data further support immunohistochemistry results **(Figure 2.8B,D)**. In addition, levels of NinaA detected by qRT-PCR and immunohistochemistry are lower in *PBac{WH}Ire1^{f02170}* eyes comparing to control **(Figure 2.8C,D)**. Immunolabeling of the ER quality control machinery component,

Calnexin (Cnx), evidences a reduction of the ER size in *PBac{WH}Ire1*^{f02170} mutant cells **(Figure 2.8E)**.

To address if maturation/biogenesis of Rh1 is affected in *PBac{WH}Ire1*^{f02170} mutants, we performed a western blot to compare Rh1 levels in mutant eyes for *ire1*, *ninaA* and *ninaE*. *NinaE*^{17} is a null mutant of Rh1 and no Rh1 protein is detected. *NinaA*^{E110V} and *NinaA*^{1} are loss-of-function mutations of NinaA that impair Rh1 maturation. In these mutants, Rhodopsin1 accumulates as an immature, glycosilated form in the ER that is mostly degraded **(Figure 2.8F)**. In *PBac{WH}Ire1*^{f02170} mutants, Rhodopsin1 mature levels are strikingly reduced but the immature form of Rh1 is not detected suggesting that the lower levels of ninaA and other ER chaperones mutants are limiting the rate of Rh1 production but are sufficient to ensure its maturation and exit from the ER **(Figure 2.8F)**.

Discussion

Ire1α gene is an essential gene in mammals whose physiological role has been associated with the differentiation of professional secretory cells. Ire1α knock-out mice die during embryonic development from liver hypoplasia, with a deficient expression of several acute phase genes (Zhang et al., 2005). Ire1α also participates in the differentiation of B lymphocytes into antibody secreting plasma cells (Zhang et al., 2005). In *Drosophila* Ire1 is an essential gene, whose physiological function is poorly understood.

In the present work, we characterized for the first time a loss-of-function allele of Ire1 in *Drosophila* and unraveled a novel function for the gene during development. We found that Ire1 is required for differentiation of photoreceptors and the morphogenesis of the rhabdomere in the pupa.

The finding that Ire1 signaling is required for plasma cell development suggested that the high load of antibodies production in these cells cause ER stress and activate the UPR. However, activation of the UPR occurs before large

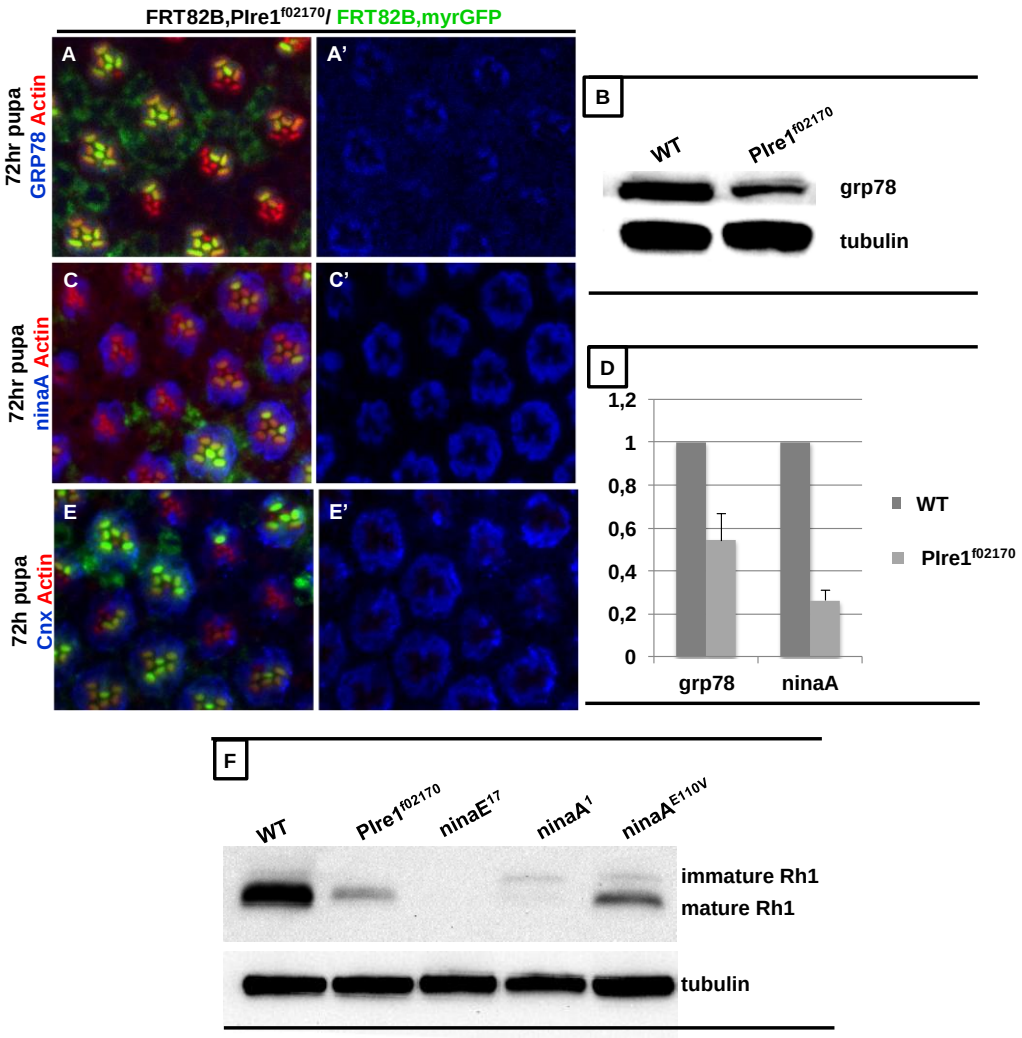

Figure 2.8 ER markers are down-regulated in *PBac{WH}Ire1^{f02170}* mutant photoreceptors.

(A) Levels of BiP/GRP78 (blue) are reduced in mutant clones of PPac(WH)Ire1^{f02170} (absence of myrGFP, green). Actin is in red.
(B) *PBac{WH}Ire1^{f02170}* whole mutant eyes have lower levels of BiP/GRP78 protein than control eyes in western blot.
(C) NinaA (blue) expression is down-regulated in *PBac{WH}Ire1^{f02170}* clones (absence of myrGFP, green) of the eye. Actin is in red.
(D) Transcription levels of GRP78/Bip and NinaA are down-regulated in *PBac{WH}Ire1^{f02170}* whole mutant eyes by quantitative RT-PCR.
(E) Calnexin staining (blue) evidences a small ER in *PBac{WH}Ire1^{f02170}* mutant photoreceptors (absence of myrGFP). Actin is in red.
(F) Western blot analysis shows Rh1 mature (34 kDa) and immature (40 kDa) forms from adult head protein extracts of *yw* (WT, positive control), *FRT82B,PBac{WH}Ire1^{f02170}/FRT82BCL,GMR-hid* (whole eye composed of homozygous Ire1 mutant cells), *ninaE^{17}* (Rh1 protein-null), and two ninaA mutations (*ninaA^{1}* = *ninaA^{P228}* and *ninaA^{E110V}*). Tubulin is used as loading control.

scale production of antibodies and mutant B lymphocytes modified to lack antibody production still activate Xbp1 in response to an antigenic stimulus (van Anken et al., 2003; Hu et al., 2009). These studies suggest that Ire1 activation is part of the developmental program of B lymphocytes and raise the question if this is the case of photoreceptors differentiation. Interestingly, the reporter Xbp1-EGFP is first activated in photoreceptors at 48hr pupa, several hours before the defects in Rh1 and Spacemaker delivery.

Professional secretory cells adapt to the high demand for ER function via UPR, which up-regulates the expression of chaperones and ER enzymes and contributes to the expansion of ER membrane (Sriburi et al., 2004). Our first observation that the Ire1/Xbp1 branch of the UPR is activated in photoreceptors after mid-pupa lead us to hypothesize that the Ire1/Xbp1 signaling is necessary for photoreceptors to increase the synthesis of proteins and membrane in the ER during the morphogenesis of the rhabdomere. As expected, *PBac{WH}Ire1*^{f02170} photoreceptors failed to expanded its ER network and exhibited low levels of ER chaperones and enzymes (GRP78, NinaA, Cnx). In consequence, the production of mature Rh1 was strikingly decreased in *PBac{WH}Ire1*^{f02170} mutants as we attested by western blot. However, we did not detected any glycosylated form of Rh1 corresponding to immature or misfolded forms retained in the ER. This observation supports the idea that the maturation of Rhodopsin1 is not compromised in *PBac{WH}Ire1*^{f02170} photoreceptors and low levels of ER chaperones are still enough to ensure Rh1 exit from the ER. However, the delivery of secretory proteins was severely affected in *PBac{WH}Ire1*^{f02170} mutant photoreceptors, as supported by the deficient transport of Spacemaker into the interrabdomeral space and the accumulation of Rh1 in the cell body of photoreceptors. These observations indicate an additional role of Ire1 signaling during the differentiation of photoreceptors, besides up-regulation of folding machinery of the ER.

Pancreatic β cells deficient in eiF2α phosphorylation are unable to control the influx of proteins, mainly proinsulin, imported into the ER and undergo apoptosis

after dysfunction of the ER (Back et al., 2009). Curiously, in these mutant β cells insulin was confined to the Golgi apparatus and the membrane proteins E-cadherin and GLUT2 had an intracellular localization, a phenotype similar to Spacemaker and Rh1 in *PBac{WH}Ire1*^{f02170} mutant photoreceptors. Taken together, these results corroborate that the UPR effectors, Perk and Ire1, are essential to maintain homeostasis of the secretory pathway by coupling the load of ER client proteins to the ER processing capacity during demanding physiological and development conditions.

PBac{WH}Ire1^{f02170} mutants exhibited a dramatic phenotype: collapse of the interrhabdomeral space, atrophy of the rhabdomeres and early degeneration of photoreceptors after eclosion. We speculate if Xbp1 mutants have such a severe phenotype and if Xbp1 and Ire1 have identical roles on the differentiation of photoreceptors. Recent reports have identified alternative targets for Ire1, growing evidence that Ire1 and Xbp1 are not in a linear pathway in higher eukaryotes, contrary to what happens in yeast. More experiments are necessary to further elucidate which mechanism downstream of Ire1 might be involved in the differentiation of photoreceptors.

Acknowledgments and author contribution

We would like to thank Charles Zuker, Nansi Jo Colley, Tiffany Cook, Andrew, Zelhof, Don Ready, Rui Martinho, Florance Janody, the Bloomington Stock Center, and the Developmental Studies Hybridoma Bank for fly stocks, reagents, and antibodies. Pedro Domingos did the temporal mapping of Xbp1-EGFP expression in the larva and in the pupa.

References

Acosta-Alvear, D., Zhou, Y., Blais, A., Tsikitis, M., Lents, N., Arias, C., Lennon, C., Kluger, Y., and Dynlacht, B.D. (2007). XBP1 controls diverse cell type- and condition-specific transcriptional regulatory networks. Mol. Cell *27*, 53–66.

Van Anken, E., Romijn, E.P., Maggioni, C., Mezghrani, A., Sitia, R., Braakman, I., and Heck, A.J.R. (2003). Sequential waves of functionally related proteins are expressed when B cells prepare for antibody secretion. Immunity *18*, 243–253.

Baker, E.K., Colley, N.J., and Zuker, C.S. (1994). The cyclophilin homolog NinaA functions as a chaperone, forming a stable complex in vivo with its protein target rhodopsin. EMBO J. *13*, 4886–4895.

Back, S.H., Scheuner, D., Han, J., Song, B., Ribick, M., Wang, J., Gildersleeve, R.D., Pennathur, S., and Kaufman, R.J. (2009). Translation Attenuation through eIF2α Phosphorylation Prevents Oxidative Stress and Maintains the Differentiated State in β Cells. Cell Metab. *10*, 13–26.

Beronja, S., Laprise, P., Papoulas, O., Pellikka, M., Sisson, J., and Tepass, U. (2005). Essential function of Drosophila Sec6 in apical exocytosis of epithelial photoreceptor cells. J. Cell Biol. *169*, 635–646.

Calfon, M., Zeng, H., Urano, F., Till, J.H., Hubbard, S.R., Harding, H.P., Clark, S.G., and Ron, D. (2002). IRE1 couples endoplasmic reticulum load to secretory capacity by processing the XBP-1 mRNA. Nature 92–96.

Chang, H., and Ready, D.F. (2000). Rescue of photoreceptor degeneration in rhodopsin null Drsophila mutants by activated Rac1. Science *290*, 1978–1980.

Colley, N.J., Cassill, J.A., Baker, E.K., and Zuker, C.S. (1995). Defective intracellular transport is the molecular basis of rhodopsin-dependent dominant retinal degeneration. Proc. Natl. Acad. Sci. U. S. A. *7*, 3070–3074.

Cox, J.S., and Walter, P. (1996). A novel mechanism for regulating activity of a transcription factor that controls the unfolded protein response. Cell *87*, 391–404.

Credle, J.J., Finer-Moore, J., Papa, F.R., Stroud, R.M., and Walter, P. (2005). On the mechanism of sensing unfolded protein in the endoplasmic reticulum. Proc. Natl. Acad. Sci. *102*, 18773–18784.

Cross, B.C.S., Bond, P.J., Sadowski, P.G., Jha, B.K., Zak, J., Goodman, J.M., Silverman, R.H., Neubert, T.A., Baxendale, I.R., Ron, D., et al. (2012). The molecular basis for selective inhibition of unconventional mRNA splicing by an IRE1-binding small molecule. Proc. Natl. Acad. Sci. U. S. A. *109*, E869–878.

Davidson, F.F., and Steller, H. (1998). Blocking apoptosis prevents blindness in Drosophila retinal degeneration mutants. Nature *391*, 587–591.

Duffy, J.B., Kania, M.A., and Gergen, J.P. (1991). Expression and function of the Drosophila gene runt in early stages of neural development. Development 113, 1223–1230.

Freeman, M. (1996). Reiterative use of the EGF receptor triggers differentiation of all cell types in the Drosophila eye. Cell *87*, 651–660.

Gardner, B.M., and Walter, P. (2011). Unfolded Proteins Are Ire1-Activating Ligands That Directly Induce the Unfolded Protein Response. Science *333*, 1891–1894.

Golic, K.G. (1991). Site-specific recombination between homologous chromosomes in Drosophila. Science *252*, 958–961.

Han, D., Lerner, A.G., Walle, L., Upton, J.-P., Xu, W., Hagen, A., Backes, B.J., Oakes, S.A., and Papa, F.R. (2009). IRE1a Kinase Activation Modes Control Alternate Endoribonuclease Outputs to Determine Divergent Cell Fates. Cell *138*, 562–575.

Hollien, J., and Weissman, J.S. (2006). Decay of Endoplasmic Reticulum-Localized mRNAs During the Unfolded Protein Response. Science *313*, 104–107.

Hu, C.-C.A., Dougan, S.K., McGehee, A.M., Love, J.C., and Ploegh, H.L. (2009). XBP-1 regulates signal transduction, transcription factors and bone marrow colonization in B cells. EMBO J. *28*, 1624–1636.

Husain, N., Pellikka, M., Hong, H., Klimentova, T., Choe, K.-M., Clandinin, T.R., and Tepass, U. (2006). The Agrin/Perlecan-Related Protein Eyes Shut Is Essential for Epithelial Lumen Formation in the Drosophila Retina. Dev. Cell *11*, 483–493.

Kang, M.-J., and Ryoo, H.D. (2009). Suppression of retinal degeneration in Drosophila by stimulation of ER-associated degradation. Proc. Natl. Acad. Sci. U. S. A. *106*, 17043–17048.

Knust, E. (2007). Photoreceptor morphogenesis and retinal degeneration: lessons from Drosophila. Curr. Opin. Neurobiol. *17*, 541–547.

Korennykh, A., and Walter, P. (2012). Structural basis of the unfolded protein response. Annu. Rev. Cell Dev. Biol. *28*.

Kumar, J.P., and Ready, D.F. (1995). Rhodopsin plays an essential structural role in Drosophila photoreceptor development. Development *12*, 4359–4370.

Kumar, J.P., Bowman, J., O'Tousa, J.E., and Ready, D.F. (1997). Rhodopsin Replacement Rescues Photoreceptor Structure during a Critical Developmental Window. Dev. Biol. *188*, 43–47.

Kurada, P., and O'Tousa, J.E. (1995). Retinal degeneration caused by dominant rhodopsin mutations in Drosophila. Neuron *14*, 571–579.

Li, B.X., Satoh, A.K., and Ready, D.F. (2007). Myosin V, Rab11 and dRip11 direct apical secretion and cellular morphogenesis in Drosophila photoreceptor cells. J. Cell Biol. *177*, 659–669.

Lin, J.H., Walter, P., and Yen, T.S.B. (2008). Endoplasmic Reticulum Stress in Disease Pathogenesis. Annu. Rev. Pathol. Mech. Dis. Is 399–425.

Liu, C.Y. (2002). The Protein Kinase/Endoribonuclease IRE1alpha That Signals the Unfolded Protein Response Has a Luminal N-terminal Ligand-independent Dimerization Domain. J. Biol. Chem. *277*, 18346–18356.

Mori, K., Kawahara, T., Yoshida, H., Yanagi, H., and Yura, T. (1996). Signalling from endoplasmic reticulum to nucleus: transcription factor with a basic-leucine zipper motif is required for the unfolded protein-response pathway. Genes Cells *9*, 803–817.

Newsome, T.P., Asling, B., and Dickson, B.J. (2000). Analysis of Drosophila photoreceptor axon guidance in eye-specific mosaics. Dev. Camb. Engl. *127*, 851–860.

Ondek, B., Hardy, R.W., Baker, E.K., Stamnes, M.A., Shieh, B.H., and Zuker, C.S. (1992). Genetic dissection of cyclophilin function. Saturation mutagenesis of the Drosophila cyclophilin homolog ninaA. J. Biol. Chem. *267*, 16460–16466.

Pichaud, F., and Desplan, C. (2002). A new view oh photoreceptors. Nature *416*, 139–140.

Rasheva, V.I., and Domingos, P.M. (2009). Cellular responses to endoplasmic reticulum stress and apoptosis. Apoptosis *14*.

Ready, D.F., Hanson, T.E., and Benzeur, S. (1976). Development of the Drosophila retina, a neurocrystalline lattice. Dev. Biol. *2*, 217–240.

Ron, D., and Walter, P. (2007). Signal integration in the endoplasmic reticulum unfolded protein response. Nat. Rev. Mol. Cell Biol. *8*.

Rosenbaum, E.E., Hardie, R.C., and Colley, N.J. (2006). Calnexin is essential for rhodopsin maturation, Ca2+ regulation, and photoreceptor cell survival. Neuron *49*, 229–241.

Ryoo, H.D., Domingos, P.M., Kang, M.-J., and Steller, H. (2007). Unfolded protein response in a Drosophila model for retinal degeneration. EMBO J. *1*, 242–252.

Satoh, A.K., O'Tousa, J.E., Ozaki, K., and Ready, D.F. (2005). Rab11 mediates post-Golgi trafficking of rhodopsin to the photosensitive apical membrane of Drosophila photoreceptors. Development *132*, 1487–1497.

Shamu, C.E., and Walter, P. (1996). Oligomerization and phosphorylation of the Ire1p kinase during intracellular signaling from the endoplasmic reticulum to the nucleus. EMBO J. *15*, 3028–3039.

Sidrauski, C., and Walter, P. (1997). The transmembrane kinase Ire1p is a site-specific endonuclease that initiates mRNA splicing in the unfolded protein response. Cell *90*, 1031–1039.

Sik Lee, Y. (2003). Making a better RNAi vector for Drosophila: use of intron spacers. Methods *30*, 322–329.

Sriburi, R., Jachowski, S., Mori, K., and Brewer, J.W. (2004). XBP1: a link between the unfolded protein response, lipid biosynthesis, and biogenesis of the endoplasmic reticulum. J. Cell Biol. *167*, 35–41.

Tirasophon, W., Welihinda, A.A., and Kaufman, R.J. (1998). A stress response pathway from the endoplasmic reticulum to the nucleus requires a novel bifunctional protein kinase/endoribonuclease (Ire1p) in mammalian cells. Genes Dev. *12*, 1812–1824.

Tomlinson, A., and Ready, D.F. (1987). Neuronal differentiation in Drosophila ommatidium. Dev. Biol. *2*, 366–376.

Urano, F., Bertolotti, A., Zhang, Y., Chung, P., Harding, H.P., and Ron, D. (2000). Coupling of stress in the ER to activation of JNK protein kinases by transmembrane protein kinase IRE1. Science *287*, 664–666.

Walter, P., and Ron, D. (2011). The unfolded protein response: from stress pathway to homeostatic regulation. Science *334*.

Wildonger, J., Sosinsky, A., Honig, B., and Mann, R.S. (2005). Lozenge directly activates argos and klumpfuss to regulate programmed cell death. Genes Dev. 19, 1034–1039.

Yang, L., and Baker, N.E. (2001). Role of the EGFR/Ras/Raf pathway in specification of photoreceptor cells in the Drosophila retina. Dev. Camb. Engl. *128*, 1183–1191.

Yoneda, T., Imaizumi, K., Oono, K., Yui, D., Gomi, F., Katayama, T., and Tohyama, M. (2001). Activation of Caspase-12, an Endoplastic Reticulum (ER) Resident Caspase, through Tumor Necrosis Factor Receptor-associated Factor 2-dependent Mechanism in Response to the ER Stress. J. Biol. Chem. *276*, 13935–13940.

Yoshida, H., Matsui, T., Yamamoto, A., Okada, T., and Mori, K. (2001). XBP1 mRNA Is Induced by ATF6 and Spliced by IRE1 in Response to ER Stress to Produce a Highly Active Transcription Factor. Cell *107*, 881–891.

Zelhof, A., Hardy, R.W., Becker, A., and Zuker, C.S. (2006). Transforming the architecture of compound eyes. *443*, 696–699.

Zhang, K., Wong, H.N., Song, B., Miller, C.N., Scheuner, D., and Kaufman, R.J. (2005). The unfolded protein response sensor IRE1α is required at 2 distinct steps in B cell lymphopoiesis. J. Clin. Invest. *115*, 268–281.

Generation and characterization of Xbp1 deficiencies

CHAPTER III

Summary

Xbp1 is a major player of the Unfolded Protein Response (UPR) in metazoans that up-regulates the folding capacity of the endoplasmic reticulum (ER) in professional secretory cells. Xbp1 is activated by Ire1, an ER localized bifunctional enzyme, in response to ER stress and accumulation of misfolded proteins in the lumen of the ER.

In spite of being an essential gene in *Drosophila*, no Xbp1 null mutant was available until date. Using fruit fly genetics, we generated Xbp1 deficiencies and characterized them at a molecular level. Using these deficiencies, we investigated a hypothetic role for Xbp1 during photoreceptor differentiation. We found that Xbp1 up-regulates the expression of Rhodopsin1 (Rh1) chaperone NinaA, but is not necessary for NinaA transcription or Rhodopsin1 biogenesis.

Xbp1 mutants have a very mild phenotype during differentiation of photoreceptors in the pupa, which consists of a slight delay in Rh1 delivery to the rhabdomere. The morphogenesis of the light gathering organelle, the rhabdomere, is not impaired in Xbp1 mutants in contrast to Ire1 mutants that show a dramatic defect in rhabdomere architecture. We conclude that Ire1 has a role during the development of the eye in the pupa, which is not mediated by its canonical target, Xbp1.

Introduction

During differentiation, cells must undergo dramatic morphological transformations. In particular, cells specialized to secrete large amounts of proteins must remodel their secretory apparatus and increase their ER folding capacity. B lymphocytes and pancreatic exocrine cells adapt to such dramatic morphological changes by activation of the transcription factor Xbp1 (Iwakoshi et al., 2003; Lee et al., 2005). Containing a bZIP DNA binding motif, Xbp1 was first described as a transcription factor that binds to the x-box sequence in the

promoter region of genes of the major human histocompatibility complex class II (Liou et al., 1990).

Xbp1 is a main player of the Unfolded Protein Response, an adaptive response of the cell to the over-accumulation of misfolded proteins in ER caused by environmental stresses or physiological conditions. During ER stress, a transmembrane ER stress sensor, Ire1 is activated and removes a small intron from Xbp1 mRNA (with 26 nucleotides in vertebrates, or 23 nucleotides in *C. elegans* and *Drosophila*) (Calfon et al., 2002; Ryoo et al., 2007; Shen et al., 2001; Yoshida et al., 1998). This unconventional splicing causes a frameshift during translation of Xbp1 mRNA that introduces a new C-terminus in the protein with a potent trans-activation domain and generates an effective transcription factor (Calfon et al., 2002). Xbp1 spliced enhances the expression of genes encoding ER chaperones and enzymes, lipid synthetic enzymes or ER protein degradation machinery (Lee et al., 2003, 2008; Yamamoto et al., 2007).

Xbp1 has homologues in yeast, mammals, worms and flies but its physiologic role remains poorly described (Moore and Hollien, 2012). Xbp1 deficient mouse are embryonic lethal and loss-of-function analyses revealed multiples functions for Xbp1 during development namely in liver and pancreas development, skeleton formation and differentiation of epithelial Paneth cells (Reimold et al., 2000; Lee et al., 2005; Tohmonda et al., 2011; Kaser et al., 2008). Deletion of Xbp1 impaired secretion of digestive granules by the exocrine pancreas, consequence of a disorganized and reduced ER network and increased apoptosis. Xbp1 seems to coordinate synthesis of the ER resident protein machinery with membrane biogenesis in secretory cells. In fact, transfection of Xbp1spliced was sufficient to induce expansion of endomembranar system in plasma B cells and increase phospholipid biosynthesis in fibroblasts (Shaffer et al., 2004; Sriburi, 2004).

In *Drosophila*, Xbp1spliced expression was first detected in salivary glands of third instar larva and in male reproductive system of the adult (Souid et al., 2007). A more recent report identified other organs where Xbp1 is activated: Malpighian

tubules, trachea, gut, brain (glial cells) and thraquea of the third instar larva (Sone et al., 2012). Xbp1 was also described as a protector factor in photoreceptor cells against degeneration in *Drosophila* models of *Retinitis Pigmentosa* caused by misfolding and mislocalization of the photosensitive protein, Rhodopsin1, in the ER (Colley et al., 1995; Ryoo et al., 2007).

Rhodopsin is a G-protein coupled receptor that initiates the phototransduction cascade in photoreceptor cells by conformational changes upon light absorption (Hardie, 2012). The major rhodopsin in the *Drosophila* eye, Rhodopsin 1 (Rh1), shares 22% of the amino acids with human Rhodopsin (O'Tousa et al., 1985; Zuker et al., 1985). Rhodopsins are synthesized and core-glycosilated in the ER, and travel along the secretory pathway to be inserted in a specialized comportment of the apical domain of photoreceptors, the rhabdomere in *Drosophila* or the outer segment, in vertebrates (Murray et al., 2009; Xiong and Bellen, 2013). Along its transport, Rh1 is escorted in a complex with NinaA, a resident chaperone of the secretory pathway. The cyclophilin homology domain of NinaA has *cis-trans* isomerase activity that is necessary for proline isomerization and proper folding of Rh1 (Baker et al., 1994; Colley et al., 1991; Stamnes et al., 1991).

In spite of being an essential gene in *Drosophila*, no Xbp1 null mutant was yet available. Using fruit fly genetics, we generated Xbp1 deficiencies and characterized them at a molecular level. We then used these deficiencies to investigate a hypothetic role for Xbp1 during photoreceptor differentiation. We found that Xbp1 up-regulates NinaA expression, but is not necessary for Rhodopsin1 biogenesis.

Materials and Methods

Drosophila stocks and crosses

Flies and crosses were raised with standard cornmeal, at 25ºC. Xbp1 genomic deficiencies were generated by crossing lines carrying the transposons, *P{lacW}Xbp1*^{k13803} or *P{SUPor-P}CG9418*^{KG05183}, with a *Δ23* transposase line.

Males with mosaic orange eyes were selected and crossed with double balancer females. White eyed male progeny were tested for complementary with *P{lacW}xbp1*^{k13803} virgins.

Excisions were balanced on the second chromosome over CyO-GFP to collect homozygous mutant larvae. Cages to collect larvae were set on apple juice plates and maintained at 25ºC. Larvae were collected 3 days after females have started laying eggs.

To generate mosaic clones using the FRT/FLP system, excisions were recombined into a *P{neoFRT}42D* chromosome. Crosses were flipped daily on food with 1mg/ml geneticin (G418 sulfate) and heat shocked for 1hr at 37ºC. Neomycin survivors were collected and tested for recombination.

To recover clones of ExcisionF211 in the pupa, the following transgenes were introduced into the genetic background: CH322-150001 genomic construct from P[acman] library, UAS-p35 rescue construct (a gift from Don Ryoo) and Xpd^{wt} transgene (obtained from Beat Sutter). P[acman] transgenic lines were generated by PhiC31 integrase-mediated transgenesis (BestGene Strain #9752, attP acceptor site in 76A2). The injection of DNA into embryos to establish *Drosophila* transgenic lines was performed by BestGene.

Immunostaining and imaging

White pre-pupa (0hr) were collected and aged at 25ºC until the appropriate stage. Using these conditions flies eclode at around 86hr of pupal development, stage that corresponds to 100% pupation.

Pupa and adult eyes were dissected in PBS, fixed in 1X PBS + 4%formaldehyde for 30min at room temperature and washed 3X in PBT (1X PBS+ 0,3% Triton X-100), 10 min each. Primary antibody was diluted in BBT (1xPBS, 1% BSA, 0.1% Tween 20, 250 mM NaCl) and incubated overnight at 4ºC under gentle agitation. Primary antibodies used in immunohistochemistry were: rat anti-ELAV (7E8A10, Developmental Studies Hybridoma Bank - DSHB), mouse anti-spam (21A6, DSHB), mouse anti-Rh1 (4C5, DSHB), rabbit anti-

Bip/GRP78 (StressMarq 18 Biosciences, SPC-180), mouse anti-Pdi (ab2792, abcam), rabbit anti-calnexin (Rosenbaum et al., 2006), rabbit anti-ninaA (Baker et al., 1994), rabbit anti-β galactosidase (MP Biomedicals), mouse anti-VCP (Léon et al., 1999). Samples were washed 3X for 10min in PBT and incubated with appropriate secondary antibodies (Jackson ImmunoResearch) in BBT for 2hr at room temperature. Phalloidin-TRITC or Phalloidin-FITC (Sigma) was incubated together with secondary antibodies. Samples were mounted in glycerol 70% and analyzed in a Zeiss LSM 510 Meta or Zeiss 710 confocal microscopes. Images were acquired with Zeiss SP 2 version 4.0 and processed with Adobe Photoshop.

Measure of the mean Rh1 fluorescence was performed using ImageJ. For each pair of adjacent wild-type and Xbp1 mutant ommatidia was calculated a ratio of the mean fluorescence and a mean value for the ratio was obtained.

Analysis of Xbp1 mRNA splicing by PstI digestion

Splicing of Xbp1 mRNA was accessed by restriction analysis with PstI of a fragment containing Ire1 splice site as described in Casas-Tinto et al., 2011. Heterozygous larvae were dissected in PBS and brains and eye imaginal discs were cultured in Schneider *medium* supplemented with 5mM DTT for 4hr. Total RNA was extracted with *High Pure RNA Tissue* kit (Roche) and used to synthesize cDNA with random hexamers (RevertAid First Strand kit - Thermo/Fermentas). Fragments flanking Ire1 splice site were amplified using specific primers for CyO chromosome or Excision101 (xbp1n+xbp1k for CyO and Xbp1_n + Exc101_new3' for Exc101). PCR amplification fragments were digested with PstI overnight. Primers sequence: Exc101_new3': 5'ATC AAC TAC AAG GTA ATT CCT TG3'; xbp1n: 5'CAT CAA CGA GTC ACT GCT GGC CAAG3'; xbp1k:5'GT CTG CTG TGA TAT CTG CGA GCA GAC3'.

Analysis of Xbp1 mRNA splicing by sequencing

Total RNA was extracted from heterozygous larva with *High Pure RNA Tissue* kit (Roche). Tissue from Excision101 was incubated in Schneider *medium*

with 5mM DTT for 4hr. cDNA was synthesized with (RevertAid First Strand kit - Thermo/Fermentas), cloned in pJet (Thermo/Fermentas) and sequenced to detect the presence of the xbp1 unconventional intron. Primers used in cDNA synthesis were: for Excision30, xbp1a (5'ATG GCA CCC ACA GCA AAC ACA GTG3') and Exc30_newC (5'CAG TCT AGA TGA TCA CGG CAG GAG CAC GT A3'); and for Excision101, primers xbp1n (5'CAT CAA CGA GTC ACT GCT GGC CAAG3') and Exc101_miniW (5'C TGG TTA ATG CAG CTC TGC GAA GCC3').

Molecular biology

Genomic DNA was isolated from larvae or flies using the High Pure PCR Template Preparation kit (Roche). Samples were snap frozen in liquid nitrogen and macerated with a motorized pestle in lysis buffer.

The limits of excisions generated with *P{lacW}Xbp1*^{k13803}, *{SUPor-P}CG9418*^{KG05183} *and P{GSV3}GS*^{6093} *were* determined with the primers: xbp1_m 5'AT CAC GTT GAG ATA GAC CTG TGA CGG3'; xbp1_L 5'C TGT GAT TGT GGC TGT TCT CGA GGC3'; GSV3_Z 5'C GTC GAA AGC CGA AGC TTA CCG AAG3'; GSV3_Y 5'CA GAT TAT TCT GGT AGC TGT GCT CGC3'; GSV3_X 5'G GAG AAA GGA AGC GTC TGG CAT TCG3'; GSV3_W 5'AT TTA GGT GTT CAC CTC AGA GCT GCC3'; GSV3_U 5'TT CGT AGT TGC TCT TTC GCT GTC TCC3'; SOX_C 5'CAT GGG CAT GAC TGT GGA CAT ACA CC3'; SOX_B 5'CCA CAT TAT GCG GAG ATA GAG TTG CC3'; PUNCH_J 5' CCT CCG CCT GGT TCT GCT GC3'; PUNCH_I 5'ATC CTG GCC GCG CAA TAC GC3'; PUNCH_H 5'TCG ACG TTA TCG GCG CCG TG3'; PUNCH_G 5'ACC AGC CTG TGC TAT TCC CAA CTG3'; PUNCH_F 5'TCC ACC GCT GCT TAG GGT CGA3'; PUNCH_E 5'GCA AAC CAC ACG CAG TGC CG3'; PUNCH_D 5'AGC CCA GTC AGT GCC ACA GCT3'; PUNCH_C 5'AAA TTC GGA GCG AGC GCG CC3'; PUNCH_B 5'TTG GGG CTC TGA ACG CGT GG3'; PUNCH_A 5'AAG CGC AGC GCG AGT TTT GC3'; SOX102F_A 5'GT ATG TCC ACA GTC ATG CCC ATG AGC3'; GLYCOGENIN_B 5'AG CAA CAT TTC CTG GCG TTT GCT TGC3'; GLYCOGENIN_A 5'ATA GAA TTC GCT TGG GTG ACG CTG AC3';

CG15658_B 5’TA TCC GAC TGT CGA CCA ACG GAT TGC3’; CG15658_A 5’AAG AGT CTC CAC GAC AGC ATA ATG CG3’; TUD_B 5’CA TAG CTC AGT GAC ACG TTG TTA GCC3’; TUD_A 5’AGT GGA CCT GTA CAT CAC TCA TGT GG3’; CG30389_Y 5’GA CAA CAG TAC GAG CGA GAG TGC A3’; CG30389_ Z 5’AGG ATA AGG AGA AGT CAG ACT GGG3’; CG30389_L 5’GTC ACT CAG CCA AGC AAC GTC ACT3’; CG30389_K 5’C CGA AGT GAT GGC CAT GAT CTT GG3’; CG30389_J 5’CC AAG ATC ATG GCC ATC ACT TCG G3’; CG30389_I 5’GG CTC AAC GCT GGA TCC CAA TGC3’; CG30389_H 5’GCA TTG GGA TCC AGC GTT GAG CC3’; CG30389_G 5’GG AGT GCA GTT CCC AGT GCA AGC3’; CG30389_F 5’GCT TGC ACT GGG AAC TGC ACT CC3’; CG30389_E 5’CC CTC ACC CTG AGT GCG ACC3’; CG30389_D 5’GC ACG GTG GTT CCG TAG TAT CCC3’; XPD_G 5’TGT GTG CTA GTG TAC TTC ACG ATC GC3’; XPD_F 5’GAT CCA AGA GCA TCT GGT GGA CAG C3’; XPD_E 5’CAT GCA TGT GCA ACC AGT CTC ACC G3’; XPD_D 5’CAA CGA CCA GGT GAC CAT TTC GTC C3’; XPD_C 5’CAC GCT TGA GAT CAG TGA TTT GAC GG3’; XPD_B 5’CCT GTG TGG TCT TTG ATG AGG CGC3’; XPD_A 5’TGC TCA GCT CTA GGA AGA ACA TGT GC3’; CG30389_C 5’CGC AAG AAG AGG GTT CTT AAC TCC3’; CG30389_B 5’GGA TAC TAC GGA ACC ACC GTG C3’; CG30389_A 5’GGT CGC ACT CAG GGT GAG GG3’; XBP1_D 5’TCA GAT CAA ACT GGG AAA CAG CTC G3’; XBP1_A 5’ATG GCA CCC ACA GCA AAC ACA GTG3’; GSV3_3P 5’CGT ATT GAG TCT GAG TGA GAC AGC3’; PROBE7_REV 5’CCG TAA CAT TTA CCG TCC ACG GCC3’; PROBE7_FORW 5’GCA CAG GGA ATT GTG AAT TAT CCC GG3’; PROBE6_REV 5’GCC ATG CAG TTT AAG TTG CGG G3’; PROBE6_FORW 5’GGC ACT AGC GCT ATT TGG CTC C3’; PROBE5_REV 5’CTG GGC GCT GCC AAG CGC C3’; PROBE5_FORW 5’GCA GCG GCA TTT GCT GCA GCC3’; PROBE4_FORWB 5’CTC GAA AAC GAG TGT TAA GCG AGG3’; LM5PV3_PX 5’CCT GGT ACA TCA AAT ACC CTT GGA TCG3’; XBP1_UTR 5’GGT TTA TAT TTT GAA TAT TTT TTA G3’; PROBE4_REV 5’ATT TGT TTT CGA TAT TCC GTG3’; PRY1 5’TTA GCA TGT CCG TGG GGT TTG AAT3’; PLAC4 5’ACT GTG CGT TAG

GTC CTG TTC ATT3'; PLAC1 5'ACC CAA GGC TCT GCT CCC A3'; SP1 5'ACA CAA CCT TTC CTC TCA ACA A3'; PRY2 5'TTG CCG ACG GGA CCA CCT TAT3'; PRY4 5'CAA TCA TAT CGC TGT CTC ACT C3'; XBP1_G 5'TCA GCC AAT CCA ACG CCA GC3'; XBP1_B 5'TGT ATA CCC TGC GGC AGA TCC AAG GTT GG3'; XBP1_C 5'AAC CTT GGA TCT GCC GCA GGG TAT ACA AC3'; XBP1e 5'GCA GCA CAA CACCAG ATG C3'; 3R 5'TAA CTG GTT CGG GGC TAA ATG ATA3'; XBP1F 5'CGC TGA CGA CTG TGT GTC C3'; XBP1J 5'ATG AGA AAA TTG CGT GAG ACG3'; Probe 3F 5'TCC CTC ATT ACC CCA ACT CTT CTA3'; Probe 1F 5'CAC AAT CGC AGC ACG GAG AAT GAG3'; Probe 1R 5'AGT GAC GTT GCT TGG CTG AGT GAC3'; Probe 2R 5'TGC CTA CCA CCA ACT TCC ATC3'; Probe 2F 5'AAA CAC GAA ACG AAA AAC AAA ACA3'; SPL_FORM 5'ACC AAC CTT GGA TCT GCC GC3'.

To clone ninaA open reading frame, total RNA was extracted from adult flies using High Pure RNA Tissue kit (Roche) and 200ng were used as a template in Revertaid H Minus First Strand cDNA Synthesis kit (Fermentas/Thermo). 2 µl of total cDNA was used in a PCR reaction performed with Phusion polymerase with specific primers for ninaA coding sequence (ninaAstart: 5'GCC AGA TCT ATG AAG TCA TTG CTC AAT CG G AT3' and ninaAstop: 5'CGA GGT ACC TCA GCA GTA CAT GTT GAG CT G3'). Ire1 open reading frame was then cloned into *Drosophila* expression vector pUAST using BglII and Acc65I restriction sites.

Quantitative RT-PCR

For reverse transcription-PCR (RT-PCR), total RNA was extracted from second instar larvae with *High Pure RNA Tissue* kit (Roche). Quality of RNA was controlled by gel electrophoresis. cDNA was synthesized with 500ng of total RNA using RevertAid First Strand kit (Thermo/Fermentas) and random hexamers. 2µl of each cDNA was used in a quantitative RT-PCR with 25 cycles. A probe for rp49 was used as a loading control for cDNA levels. Primers used in qRT-PCR were xbp1e (sequence above) and xbp1k (sequence above), ninaA forward

(5'CGT GGC CAG TGG TCT GAG CTT CAC3') and ninaA reverse (5'CTC CAC CGC CAG AGC CTT ATC CTC3'),

Plasmid rescue

The site of *P{GSV3}GS*^{6093} re-insertion was determined by plasmid rescue according to O. Masuda and T. Matsuo, 2001. Genomic DNA extracted from flies carrying the insertion *P{GSV3}GS*^{6093} was digested with Sau3AI and digestion fragments were re-ligated with T4 ligase. PCR reaction was performed with the digestion fragments and using primers for *P{GSV3}GS*^{6093} borders (3pOut:TAA TTC AAA CCC CAC GGA CAT GCT AAG and 3pIn:GCA AAG CTT GGC TGC AGG TCG AGC). Resulting amplification bands were sequenced.

Results

***P{lacW}Xbp1*^{k13803} does not have a phenotype for photoreceptor morphology**

Ire1 is required for the differentiation of photoreceptors during late pupa and *PBac{WH}Ire1*^{f02170} mutants show a severe phenotype with early degeneration of the retina (Chapter II of this thesis). To determine if the canonical target of Ire1, Xbp1, is also required for the morphogenesis of the rhabdomere, we generated clones of *P{lacW}Xbp1*^{k13808} in the eye and analyzed markers of photoreceptor differentiation. *P{lacW}Xbp1*^{k13808} mutant photoreceptors show a normal localization of Rh1 to the rhabdomere and have a normal morphology with rhabdomeres organized in a trapezoidal pattern in the adult eye (**Figure 3.1**).

P{lacW}Xbp1^{k13803} is an homozygous lethal mutation, caused by the insertion of a *P[lacW]* transposon with 10.691bp in the 5'UTR of Xbp1, 156bp downstream of the transcription start site (**Figure 3.3A**). This allele is a hypomorph that maintains residual expression of the Xbp1 transcript, which may be sufficient to ensure normal differentiation of photoreceptors (Ryoo *et al*, 2007).

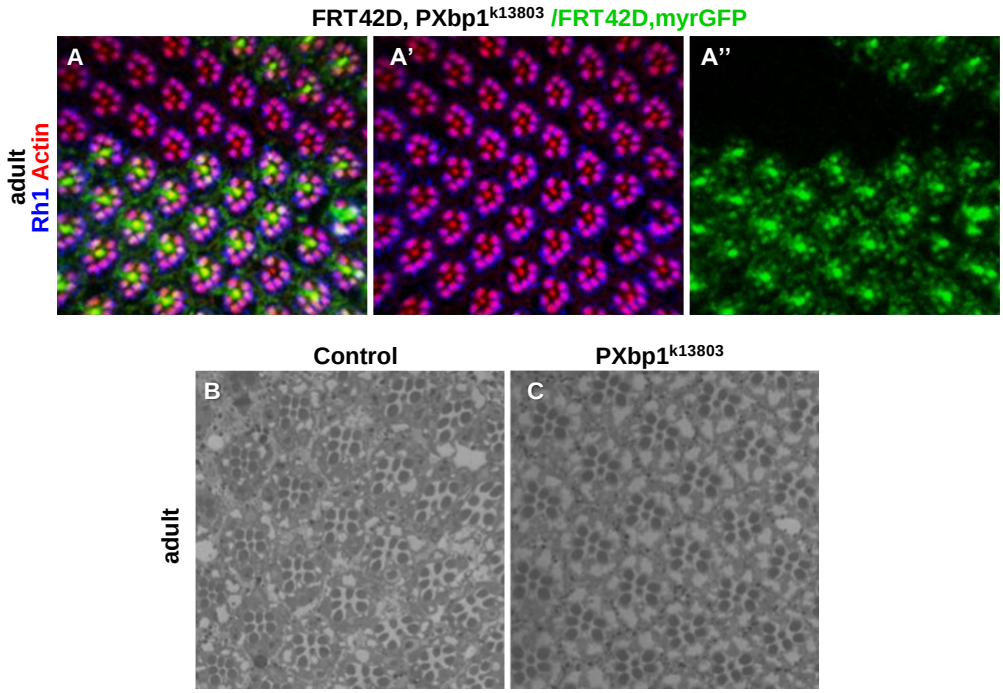

Figure 3.1 *P{lacW}Xbp1^{k13803}* eye clones show a normal morphology of the photoreceptors in the adult.
(A) Rh1 (in blue) is co-localizing with the rhabdomere (in red) in *P(lacW)Xbp1^{k13803}* mutant clones (absence of myrGFP) of the adult eye.
(B,C) Thin section of adult eyes. (C) Whole *P(lacW)Xbp1^{k13803}* mutant eyes show a normal morphology of the photoreceptors with a trapezoidal arrangement of the rhabdomeres, comparing to (B) control eyes.

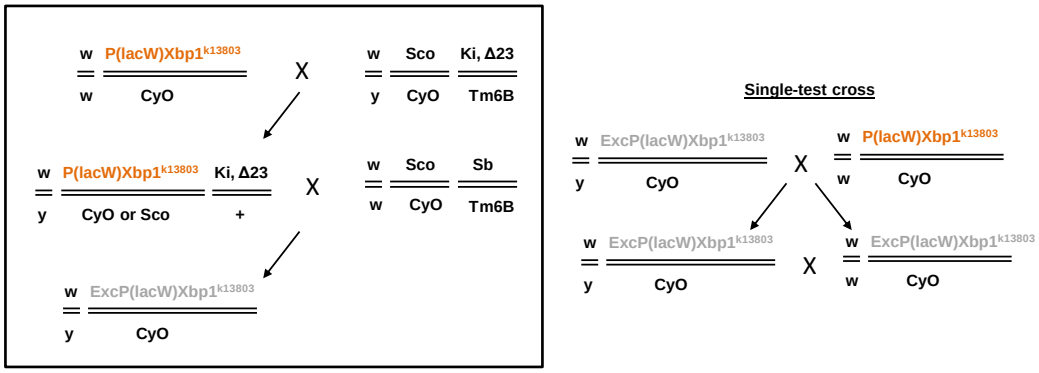

Figure 3.2 Genetic scheme followed to generate *P(lacW)Xbp1^{k13803}* excisions.

P(lacW)Xbp1^{k13803} carries a mini-white gene. *Δ23* transposase promotes the mobilization of P(lacW) elements.

Characterization of *P{lacW}Xbp1*^{k13803} excisions

In spite of being an essential gene in *Drosophila*, no null mutant was available for Xbp1. In order to generate a Xbp1 null allele, we induce the excision of *P{lacW}Xbp1*^{k13803} and selected imprecise excisions where Xbp1 coding sequence might be deleted (**Figure 3.2**). Concerning the genetic scheme, the original line *P{lacW}Xbp1*^{k13803} was crossed to a line carrying a Δ23 transposase to cause the mobilization of the P element (Mlodzik, 1990). Progeny carrying an excision was recognized by white eyes due to the loss of the mini-white gene in P{lacW}*Xbp1*^{k13803}. Using this strategy, 130 excisions were collected. From this total, 5 excisions failed to complement the original *P{lacW}Xbp1*^{k13803} insertion in single test-crosses and were selected as candidates for Xbp1 deletion (**Figure 3.3B**).

The 5 lethal lines over *P{lacW}Xbp1*^{k13803} were characterized at a genomic level by PCR. Using different combinations of primers that hybridize with Xbp1 genomic region and P{lacW}Xbp1^{k13803} ends, we concluded that the 5 lethal lines selected are partial excisions where a part of the original P{lacW} element remained inserted in the same position and a part encoding the mini-white gene was lost. For example, the band amplified by primer Plac4 and Probe3F has an intermediate size between the wild-type allele and the *P{lacW}Xbp1*^{k13803} allele in all 5 excisions selected (**Figure 3.3C**).

The genetic scheme used to generate Xbp1 deficiencies favored partial excisions of *P{lacW}Xbp1*^{k13803}, where the open reading frame of Xbp1 is not affected. So we performed another round of *P{lacW}Xbp1*^{k13803} excisions but not discarding any of them. After establishing stable lines of the new excisions, we tested the lethality over the *P{lacW}Xbp1*^{k13803} insertion and characterized them by PCR. All non-lethal excisions collected in the second round correspond to precise excisions, where Xbp1 genomic region reverted to wild-type. A PCR of Xbp1 genomic region with primers 2F + 1R in these precise excisions amplifies a band with the wild-type size (wt ≈5 kb) (**Figure 3.3D**).

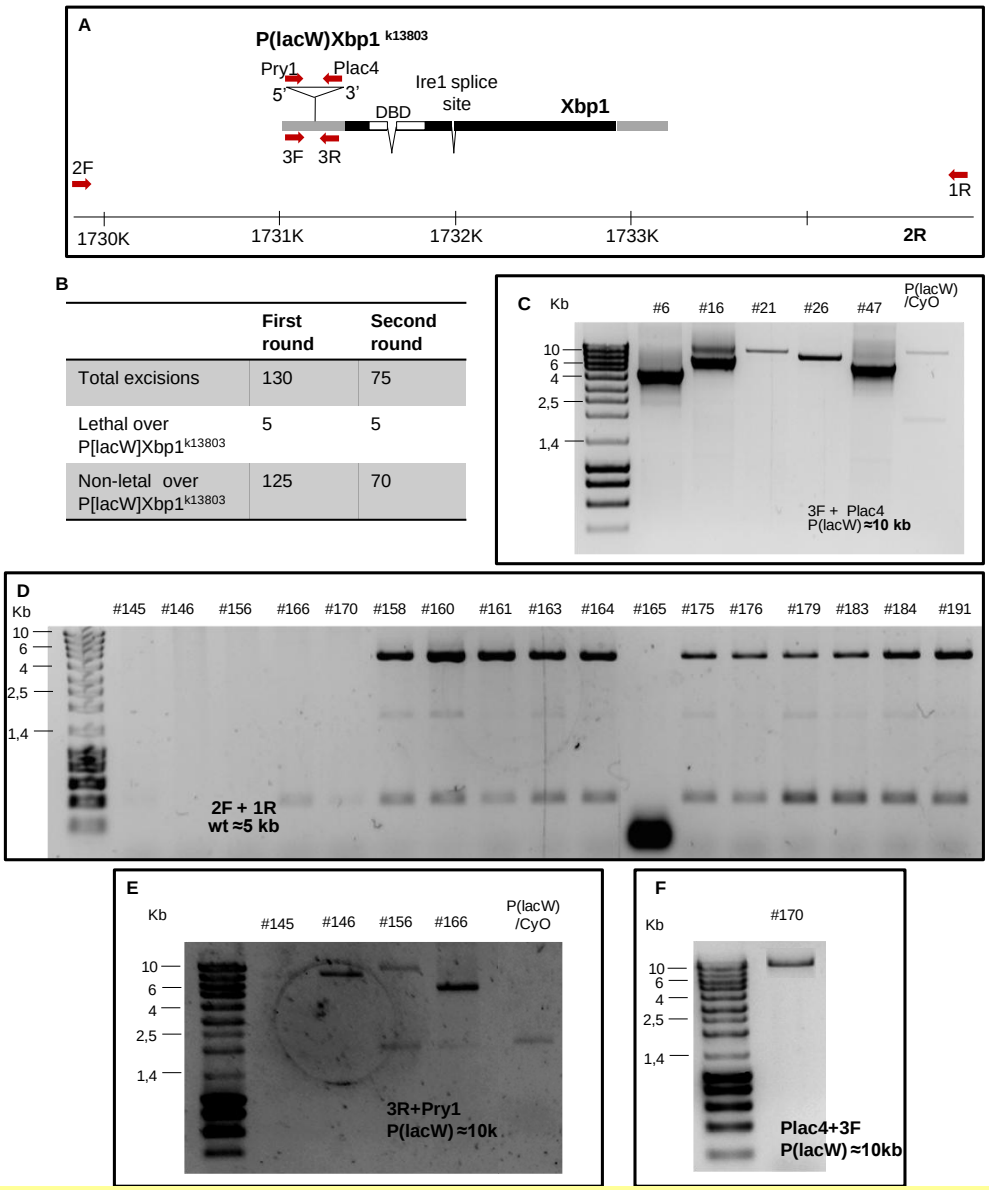

	First round	Second round
Total excisions	130	75
Lethal over P[lacW]Xbp1^{k13803}	5	5
Non-letal over P[lacW]Xbp1^{k13803}	125	70

Figure 3.3 Characterization of P(lacW)Xbp1^{k13803} excisions by PCR.

(A) Schematic representing Xbp1 genomic region, including the insertion site of P(lacW)Xbp1^{k13803} and the localization of primers used in the characterization of the excisions. DBD: DNA binding domain.

(B) Number of total excisions generated by *P(lacW)Xbp1^{k13803}* jump and number of excisions which were lethal over *P(lacW)Xbp1^{k13803}*

(C) Lethal excisions #6, #16, #21, #26 and #47 maintain an insertion of *P(lacW)Xbp1^{k13803}* amplified by primers Plac4 and 3F with smaller size than the original *P(lacW)Xbp1^{k13803}* allele (10kb).

(D) In non-lethal excisions Xbp1 genomic region amplified by primers 2F and 1R reverted to the wild-type size (5kb).

(E) Lethal excisions #145, #146, #156, #166 maintain an insertion of *P(lacW)Xbp1^{k13803}* amplified by primers 3R and Pry1.

(F) Lethal excision #170 has an insertion of *P(lacW)Xbp1^{k13803}* amplified by primers Plac4 and 3F.

The lethal excisions collected in the second round are again imprecise excisions that maintain a large portion of the P{lacW} element inserted in Xbp1 5' UTR (**Figure 3.3E,F**). The PCR band amplified by primers 3R and Pry1 has an intermediate size between the wild-type allele and the *P{lacW}Xbp1*^{k13803} allele in the 5 lethal excisions selected.

Characterization of *P{SUPor-P}CG9418*^{KG05183} excisions

We could not obtain a null allele of Xbp1 by excision of *P(lacW)Xbp1*^{K13803}. Therefore we tried to generate a null allele of Xbp1 by imprecise excision of another transposable element, *P{SUPor-P}CG9418*^{KG05183}. Placed in the 5'UTR of the gene downstream of Xbp1 (*cg9418*), *P{SUPor-P}CG9418*^{KG05183} is a non lethal insertion with 11.467Kb, that can be mobilized by the same Δ23 transposase (**Figure 3.4A**). *P{SUPor-P}CG9418*^{KG05183} complements *P{lacW}Xbp1*^{k13803} and flies carring both insertions *in trans* are viable. Following the same genetic crossing scheme as before, we selected 318 white eyed-males that were then crossed with *P{lacW}Xbp1*^{k13808} virgins to test for complementation. Excision30, Excision101 and Excision250 were lethal over *P{lacW}*Xbp1^{k13808} and were then characterized by PCR and sequencing.

Excision30 is a 2.4kb deficiency that deletes CG9418, the 3' UTR of Xbp1, and 183 nucleotides of the Xbp1spliced coding sequence (**Figure 3.4B**). Excision101 is a partial excision, where 6.5kb of the original *P{SUPor-P}CG9418*^{KG05183} transposon were lost and 5kb remained in the same insertion point (**Figure 3.4C**). During the excision event, 1.7kb of Xbp1 gene were deleted. Excision250 is a 4.7kb deficiency in the second chromosome missing 3 genes: *xbp1*, *cg9418* and *cg15657* (**Figure 3.4D**). In Excision250, the coding sequence of Xbp1 was completely eliminated with exception for the first two codons, thus turning Excision250 a null mutant of Xbp1.

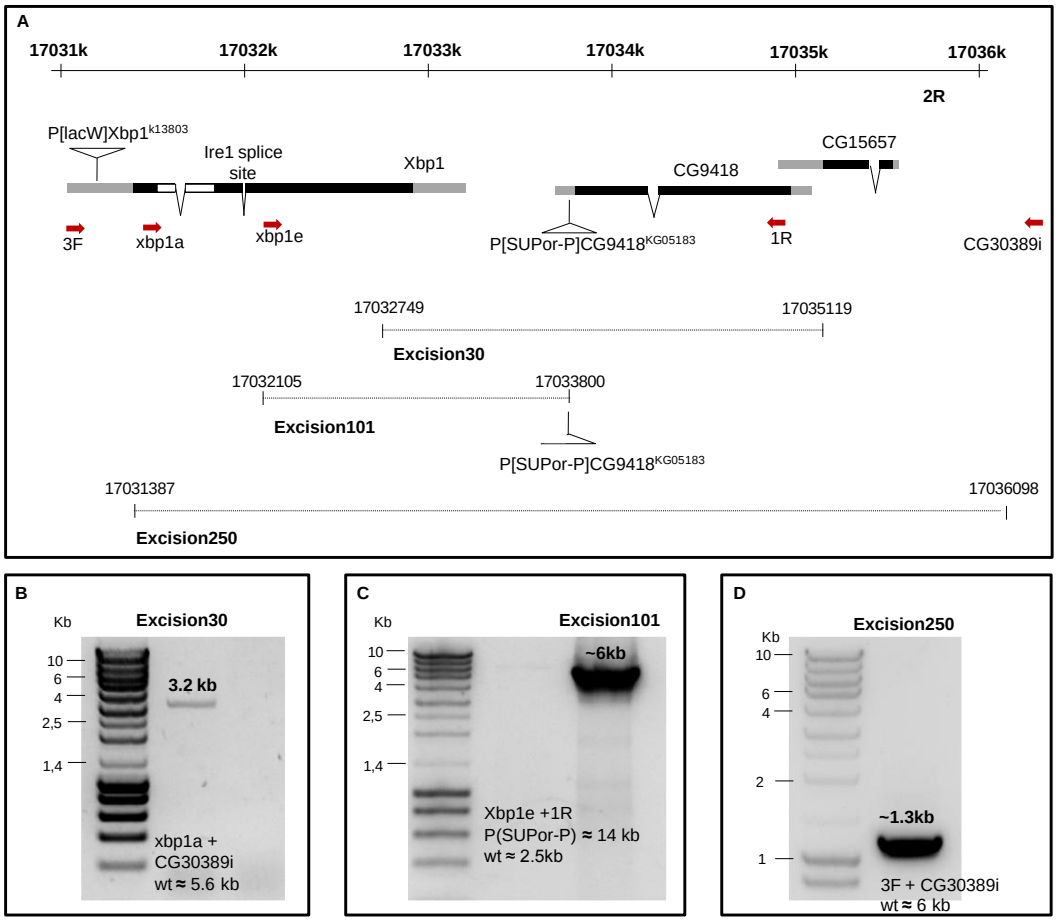

Figure 3.4. Characterization of *P{SUPor-P}CG9418*^{KG05183} excisions by PCR.

(A) Schematic shows Xbp1 genomic region with the localization of *P{SUPor-P}CG9418*^{KG05183} and primers used in PCR to characterize excisions. *P[SUPor-P]CG9418*^{KG05183} is inserted in the 5' UTR of *CG9418*.
(B) In Excision30, primers xbp1a and CG30389i amplify a band with 3.2kb, while the wild-type locus has 5.6kb.
(C) The genomic region amplified by primers xbp1e and 1R in Excision101 has an intermediate size between the wild-type allele and *P[SUPor-P]CG9418*^{KG05183} alelle.
(D) Excision250 is an extensive deletion with 4.7kb whose limits are amplified by primers 3F and CG30389i.

We predict that in Excision30 a chimera protein is produced, with the last 61 C-terminal amino acids of Xbp1spliced replaced by 71 ectopic amino acids derived from a fusion with *cg15657* open reading frame (**Figure 3.5A**). We verified by RT-PCR that the chimera transcript of Excision30 is synthesized at equivalent levels of the endogenous Xbp1 transcript (**Figure 3.5B**).

Excision101 originates theoretically a Xbp1 protein with a truncated C-terminal region (**Figure 3.5A**). In the spliced form, the last 278 codons (at the 3' region of the coding sequence) were deleted and 4 new codons (GITL) were added before the introduction of a STOP codon. In the unspliced form, the last 87codons (at the 3' region of the coding sequence) were deleted and introduced 5 new codons (ELPCS) followed by a nonsense codon.

The unspliced Xbp1 mRNA has elements and motifs in the 3' region which are important for recruitment to Ire1 and increase the efficiency of splicing. In yeast a bipartite element (BE) at 3'UTR of Xbp1 homolog mRNA helps in the localization of the transcript to clusters of Ire1 (Aragón et al., 2009). In mammals, the hydrophobic region2 (HR2) in the C-terminal region of the Xbp1 unspliced protein facilitates the recruitment of the Xbp1 mRNA-ribosome-nascent chain complex to the ER membrane (Yanagitani et al., 2009). Taking into account that Excision30 lacks the 3' UTR of Xbp1 unspliced mRNA and Excision101 predicted encoded protein does not have HR2, we checked if the mRNA of each excision is still spliced by Ire1 using two types of assays.

In a first approach, we synthesized by RT-PCR cDNA for Xbp1 with RNA extracted from Excision30 or Excision101 heterozygous mutant larva and determined by sequencing the presence of the 23-nucleotide intron. The cDNA encoding Xbp1 was then cloned in pJET and sequenced. For Excision30, 25% of the clones did not present the unconventional intron, even in the absence of DTT (**Figure 3.5C**). For Excision101, approximately 23% of the clones encoded the spliced form after treatment with DTT for 4hr (**Figure 3.5C,D**).

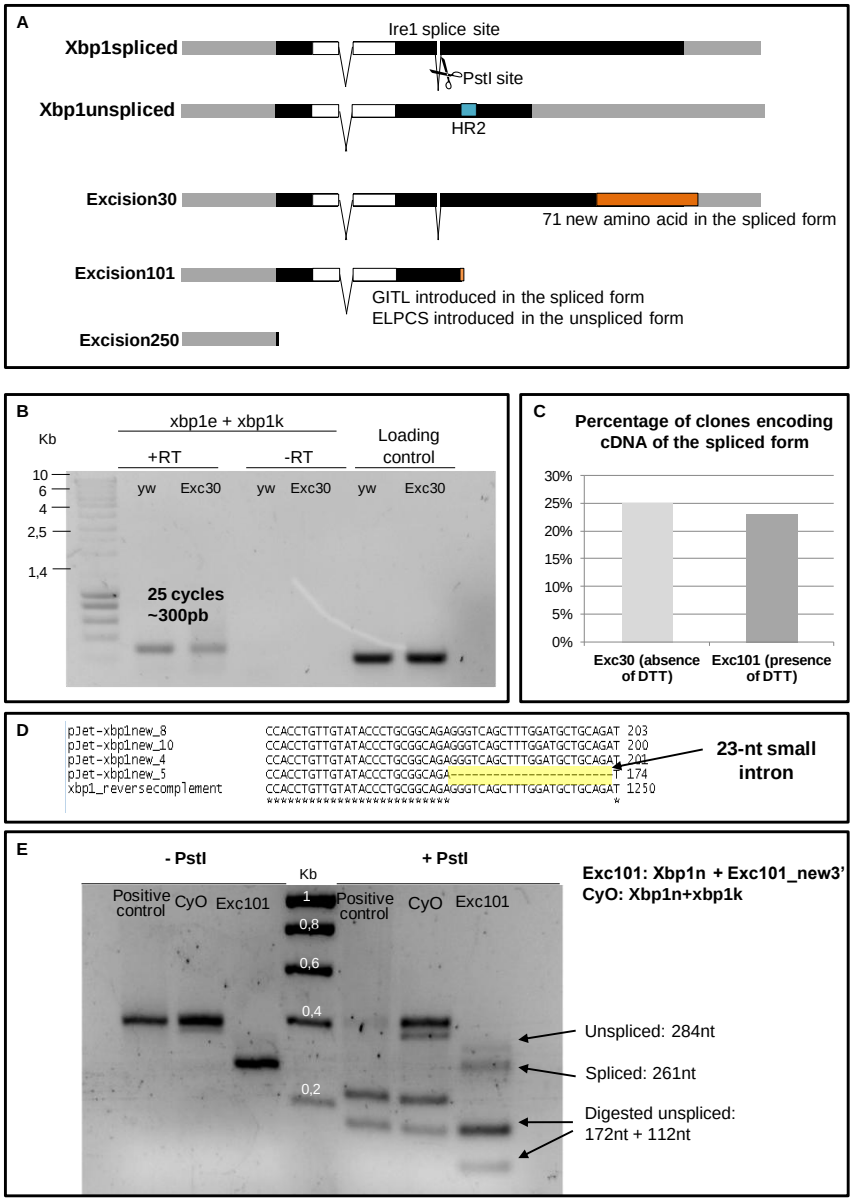

Figure 3.5 Excision30 and Excision101 originate truncated Xbp1 mRNAs that are spliced by Ire1.

(A) Schematic of truncated Xbp1 proteins originated by Excision30, Excision101 and Excision250. PstI has a clivage site in the unconventional intron spliced by Ire1. HR2: hydrophobic region 2.
(B) Excision30 generates an Xbp1-CG15657 chimeric transcript that is expressed at equilalent levels as endogenous Xbp1 transcript.
(C) Percentage of clones encoding cDNA without the unconventional intron spliced by Ire1.
(D) Sequencing of the region containig Ire1 splice site in clones encoding cDNA of Excision101.
(E) Digestion with PstI of cDNA containg the Ire1 splice site from Excision101/CyO larva treated with DTT. cDNA of the flanking Ire1 splice site region was synthesized and specific primers were used for the Excision101 or CyO chromosome. A lower weight band resistent to PstI digestion corresponds to a spliced form of the transcript. The positive control is a PCR product derived from a plasmid encoding Xbp1spliced.

In the second assay, we distinguished the spliced form from the unspliced form by restriction analysis of a fragment containing Ire1 splice site. The enzyme PstI has a restriction site in the unconventional intron of Xbp1 and consequently cuts only the fragment corresponding to the unspliced form. Larvae were treated with DTT for 4hr and a fragment containing Ire1 splice site was amplified from cDNA and digested with PstI to distinguish the spliced form from the unspliced form. PstI digestion of Xbp1 cDNA from Excision101 originates a band resistant to digestion and with 261nt (lower size than the unspliced form) that corresponds to the spliced form (**Figure3.5E**). These results suggest that in spite of the elements missing in the 3'region of Xbp1 transcript, the unconventional splicing mediated by Ire1 still occurs in Excision101 and Excision30.

Characterization of *P{GSV3}GS^{6093}* excisions

We also characterized ExcisionF211 originated by mobilization of *P{GSV3}GS^{6093}*, a gift from Alexander Djiane. *P{GSV3}GS^{6093}* has 4.828bp and is originally inserted in *magi*, a gene in the neighborhood of Xbp1 (**Figure 3.6A**). ExcisionF211 failed to complement *P{lacW}Xbp1^{k13803}* and was a good candidate for a *xbp1* deficiency.

PCR characterization of ExcisionF211 confirmed that the coding sequence of *xbp1* is not present (**Figure 3.6B**). The genomic region upstream of *P{GSV3}GS^{6093}* insertion site including Magi gene is intact (**Figure 3.6C**). The genomic region downstream of *P{GSV3}GS^{6093}* insertion site was eliminated and by walking PCR we found that all genes between *magi* and *punch* were deleted, representing an extensive deficiency with 35kb (**Figure 3.6D-G**). Using a primer in Xbp1 genomic region and primers at different points in the *P{GSV3}^{GS6093}*, we found that the complete transposon in still present in the original insertion site in ExcisionF211 (**Figure 3.7A-D**). Plasmid rescue revealed that a copy of the *P{GSV3}^{GS6093}* is re-inserted in the *sox102f* gene on the 4th chromosome (**Figure 3.7A,E**).

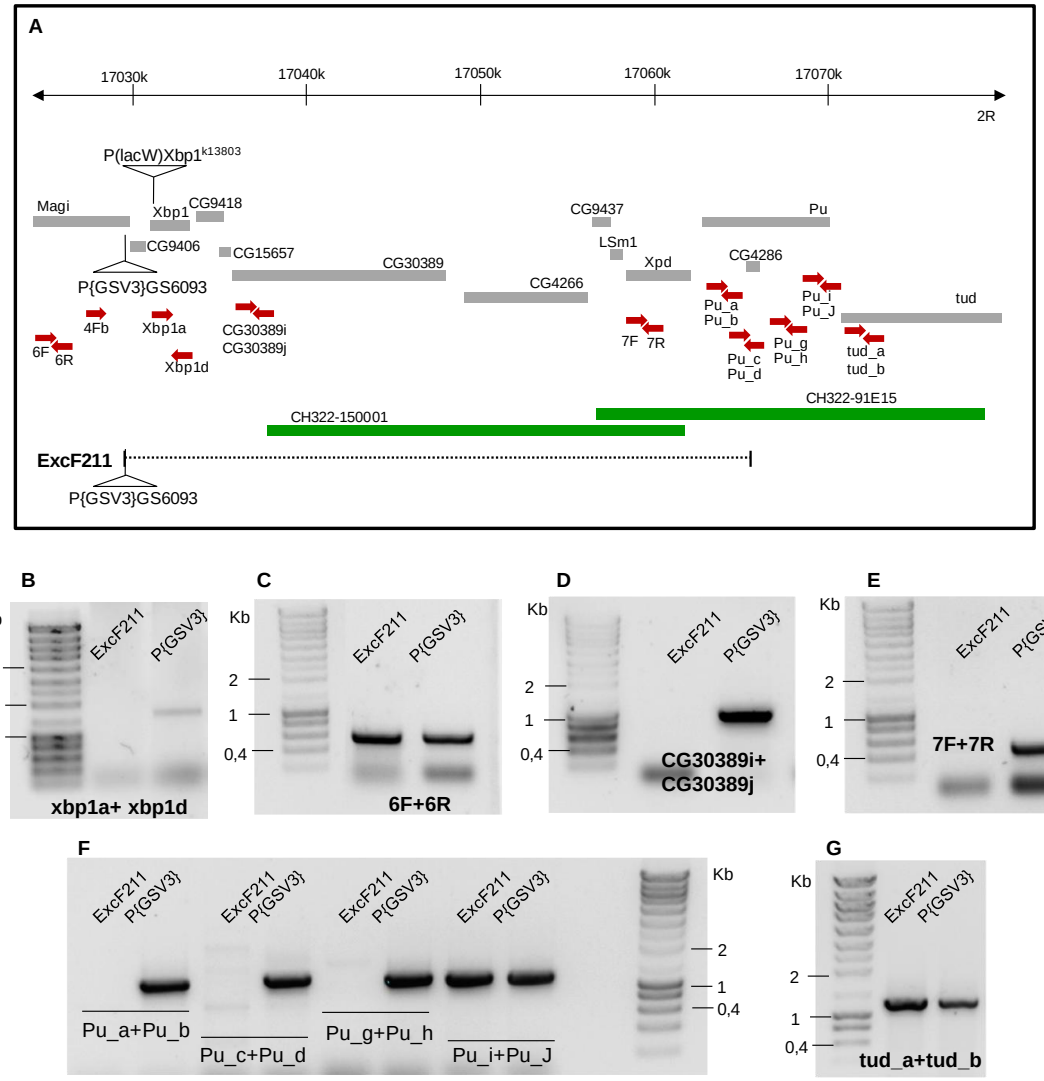

Figure 3.6. Determination of ExcisionF211 genomic limits by PCR.

(A) Schematic shows extended Xbp1 genomic region with the localization of *P{GSV3}*^{GS6093} and primers used in PCR. Excision F211 is a 35kb deficiency that deletes genes between *cg9406* and *punch*. The coverage of CH322-150001 genomic construct is also represented.
(B) The coding sequence of *xbp1* amplified by primers xbp1a and xbp1d is absent in ExcisionF211.
(C) The genomic region upstream of *P{GSV3}*^{GS6093} insertion amplified by primers 6F and 6R is present in ExcisionF211.
(D) ExcisionF211 lacks the sequence of *cg30389* gene amplified by primers CG30389i and CG30389j.
(E) *Xpd* gene sequence amplified by primers 7R and 7R is not present in ExcisionF211.
(F) Punch gene was partially deleted in ExcisionF211.
(G) The genomic sequence downstream of *punch* gene and amplified by tud_a and tud_b is present in ExcisionF211.

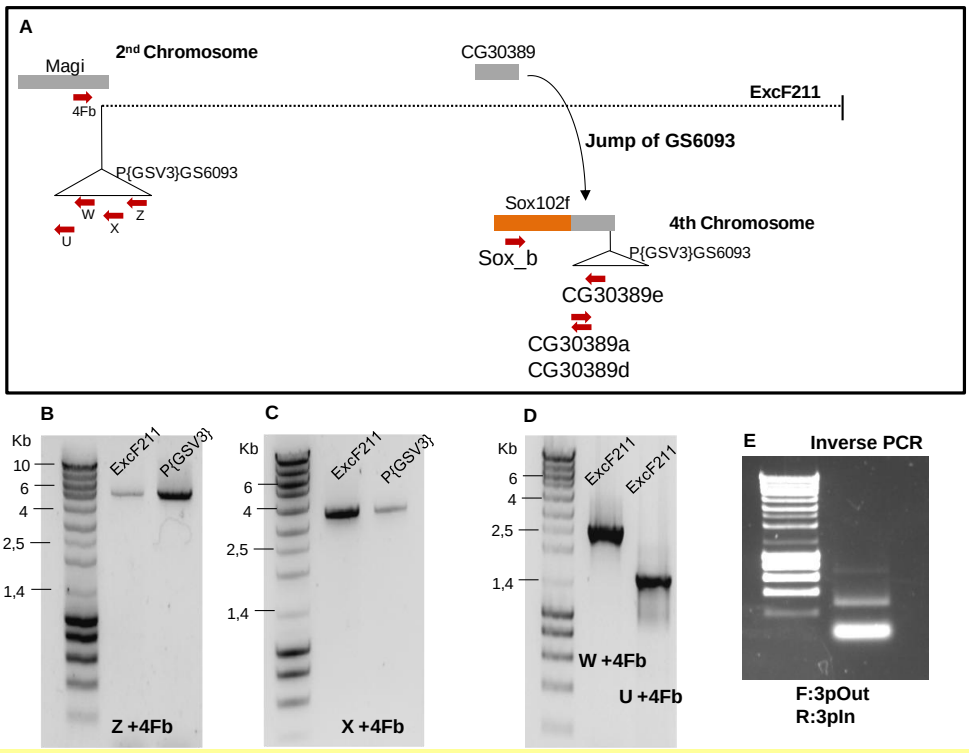

Figure 3.7 *P{GSV3}*^{GS6093} transposon continues inserted in the origal site in ExcisionF211.

(A-D) *P{GSV3}*^{GS6093} and ExcisionF211 chromosomes generates bands in PCR with the same size using a combination of primers that hybridize with the magi gene region and the P{GSV3} transposion.
(E) Result of the plasmid rescue PCR.

After recombination of ExcisionF211 into FRT chromosomes to generate mitotic clones in the eye, we could not observe any mutant cells neither in larval eye discs nor in pupal eyes. We identified some patches of cells with different intensity of myrGFP, so we believe that ExcisionF211 is cell lethal and that mutant clones are dying (**Figure 3.8A**). We tried to rescue ExcisionF211 clones to then analyze its phenotype in three different manners: 1) suppression of cell death by expression of the inhibitor of caspases p35, 2) introducing Xpd^{wt} transgene in the genetic background and 3) replacement of missing genes with CH322-150001 P[acman] genomic construct (**Figure 3.6A**). The first strategy

was successful to recover mutant clones in the larva but not in the pupa (**Figure 3.8B**). The second strategy gave an incomplete rescue because we could only detect very small mutant clones in pupa (**Figure 3.8C**). The third strategy was able to rescue the viability of the mutant clones, but ommatidia showed a very strong rough phenotype and thus are not useful to analyze the phenotype (**Figure 3.8D**).

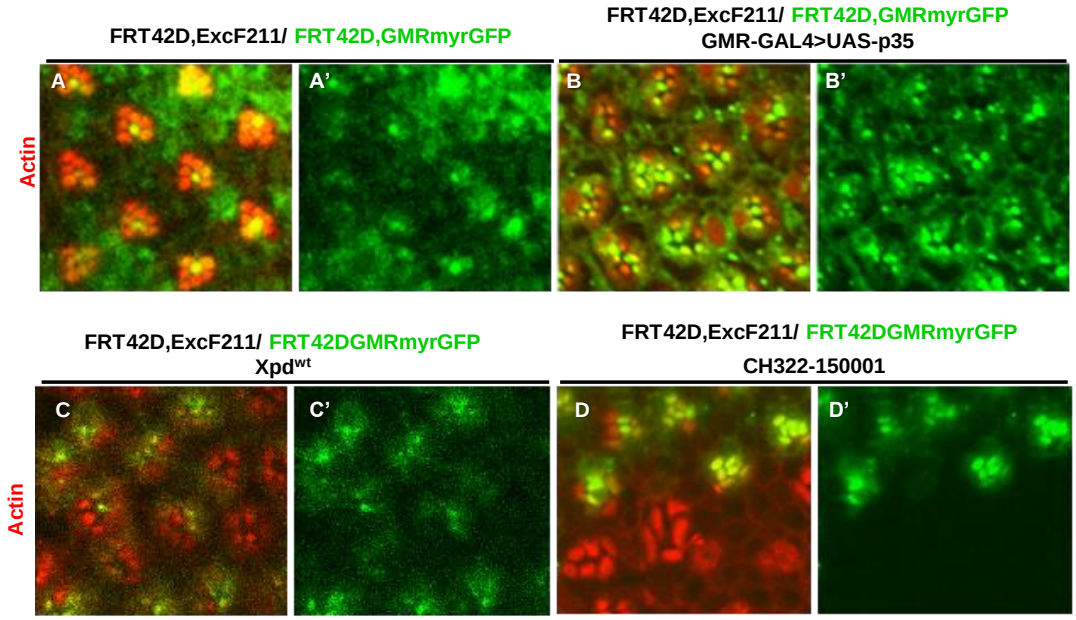

Figure 3.8. Rescue of ExcisionF211 clones viability.

(A) ExcisionF211 is cell lethal and clones of homozygous mutant cells (absence of myrGFP) are not visible in the pupa.
(B) Expression of GMR-GAL4>UAS-p35 in the pupal eye does not rescue viability of homozygous cells for ExcisionF211.
(C) Introduction of Xpd^{wt} gene partially recoveres clones of ExcisionF211 (absence of myrGFP.)
(D) P[acman] CH322-150001 genomic construct fully rescues Excision F211 clones (absence of myrGFP) but mutant photoreceptors show a strong rough phenotype.

***P{SUPor-P}CG9418^{KG05183}* excisions present photoreceptors with a normal morphology**

Next we checked the differentiation of photoreceptors in the *P[SUPor-P]CG9418^{KG05183}* excisions generated previously. In Excision30 and Excision101, Rh1 subcellular localization is similar between mutant and wild-type clones and photoreceptors have a normal morphology (**Figure 3.9B,C**). In Excision250, which corresponds to an Xbp1 null mutant, the differentiation of photoreceptors is not affected, except in some mutant clones where a slight down-regulation of Rh1 expression is observed (**Figure 3.9D**).

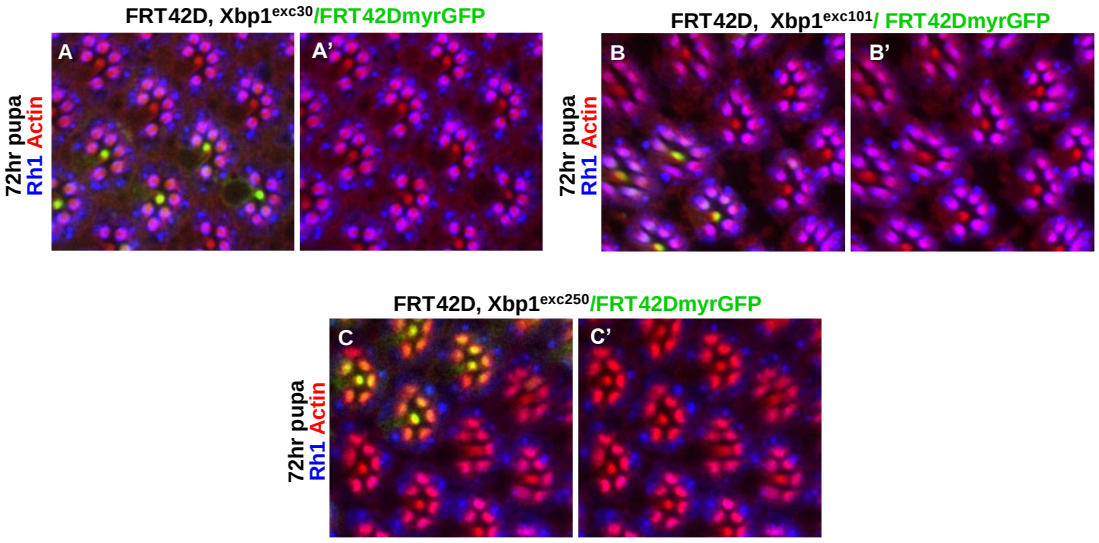

Figure 3.9 Xbp1^{exc30}, Xbp1^{exc101} and Xbp1^{250} show a normal morphology of the photoreceptors in 72hr pupa.

(A-C) In mutant clones of (A) Excision30 (Xbp1^{exc30}), (B) Excisio101 (Xbp1^{exc101}) or (C) Excision250 (Xbp1^{250}) (marked by the absence of myrGFP), Rh1 (blue) is normally localizing to the rhabdomere (in red) at 72hr pupation.

***P[PTT-GB]Xbp1^{CB02061}* excisions show a normal morphogenesis of the rhabdomere**

Our collaborator Hyung Don Ryoo kindly provided us two Xbp1 null mutants, Excision81 and Excision79, which delete partially the coding sequence of Xbp1 (including DNA binding domain) These deficiencies in the Xbp1 genomic region were generated by imprecise excision of transposon P[PTT-GB]Xbp1^{CB02061} (**Figure 3.10A**). At 62hr pupation, Spacemaker localizes at the interrhadomeral space and is not retained in the cytoplasm of Excision81 or Excision79 mutant photoreceptors (**Figure 3.10B,C**).

Analysis of Rh1 distribution at different stages of pupal development reveals a delay in the transport of Rh1 to the rhabdomere in Excision81 and Excision79 mutant photoreceptors (**Figure 3.11**). Rhodopsin1 is strongly detected in the cell body of photoreceptors after the beginning of its synthesis in late pupa (Kumar and Ready, 1995a). Hours later, Rhodopsin1 fills evenly the total rhabdomere area and just before eclosion forms a typical crescent-shaped gradient of concentration with higher levels at the rhabdomere base (Kumar and Ready, 1995).

In Excision79 mutant photoreceptors, distribution of Rhodopsin1 resumes all these stages but with a time lapse comparing with wild-type clones of the same eye (**Figure 3.11A-C**). In Excision81 transport of Rhodopsin1 to the rhabdomere is normal with a little retention in the cell body of photoreceptors of the mutant clones and the architecture of the rhabdomere is regular (**Figure 3.11D,E**).

We also accessed levels of ER markers in Excision79 and Excision81 clones. There was a significant reduction in the expression of the folding enzyme Pdi and the chaperone GRP78 in Excision79 mutant photoreceptors (**Figure 3.12A,B**). Excision81 presents reduced expression of GRP78 but unaffected expression of VCP/p97 in mutant clones (**Figure 3.12D,E**). VCP (valosin-containing protein) is an ATPase involved in the dislocation of misfolded proteins from the ER lumen to the degradation machinery in the cytoplasm. Furthermore,

Calnexin immunelabeling highlights a smaller ER size in Excision81 or Excision79 mutant photoreceptors (**Figure 3.12C,F**).

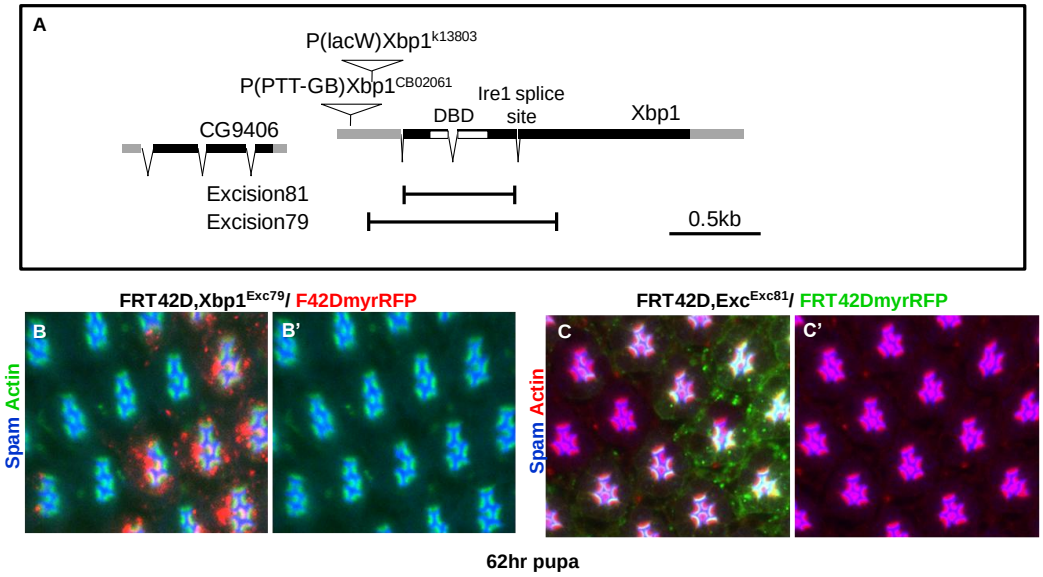

Figure 3.10 Xbp1^{exc79} and Xbp1^{exc81} have a normal morphology of photoreceptors at 62hr pupation.

(A) Schematic shows Xbp1 genomic region with the localization of *P[PTT-GB]Xbp1*^{CB02061} and the extension of Excisions 81 and 79. In Excision81, the sequence from 4 to 622bp downstream from Xbp1 start codon (ATG) is deleted. In excision79, the sequence between 260bp upstream and 748bp downstream from Xbp1 start codon (ATG) is deleted.
(B) By 62hr pupation,*eyeless*-Flipase-induced clones of cells homozygous for Excision79 (Xbp1^{exc79}), labeled by the absence of myrRFP (red), have normal levels of Spacemaker (Spam - blue) in the interrhabdomeral space. The rhabdomeres supported by actin are in green.
(C) Spacemaker (blue) is secreted normally into the interrhabdomeral space in clones of cells homozygous for Excision 81 (Xbp1^{exc81}), labeled by the absence of myrGFP (green), of 62hr pupal eyes. Microfilaments of the rhabdomeres are in red.

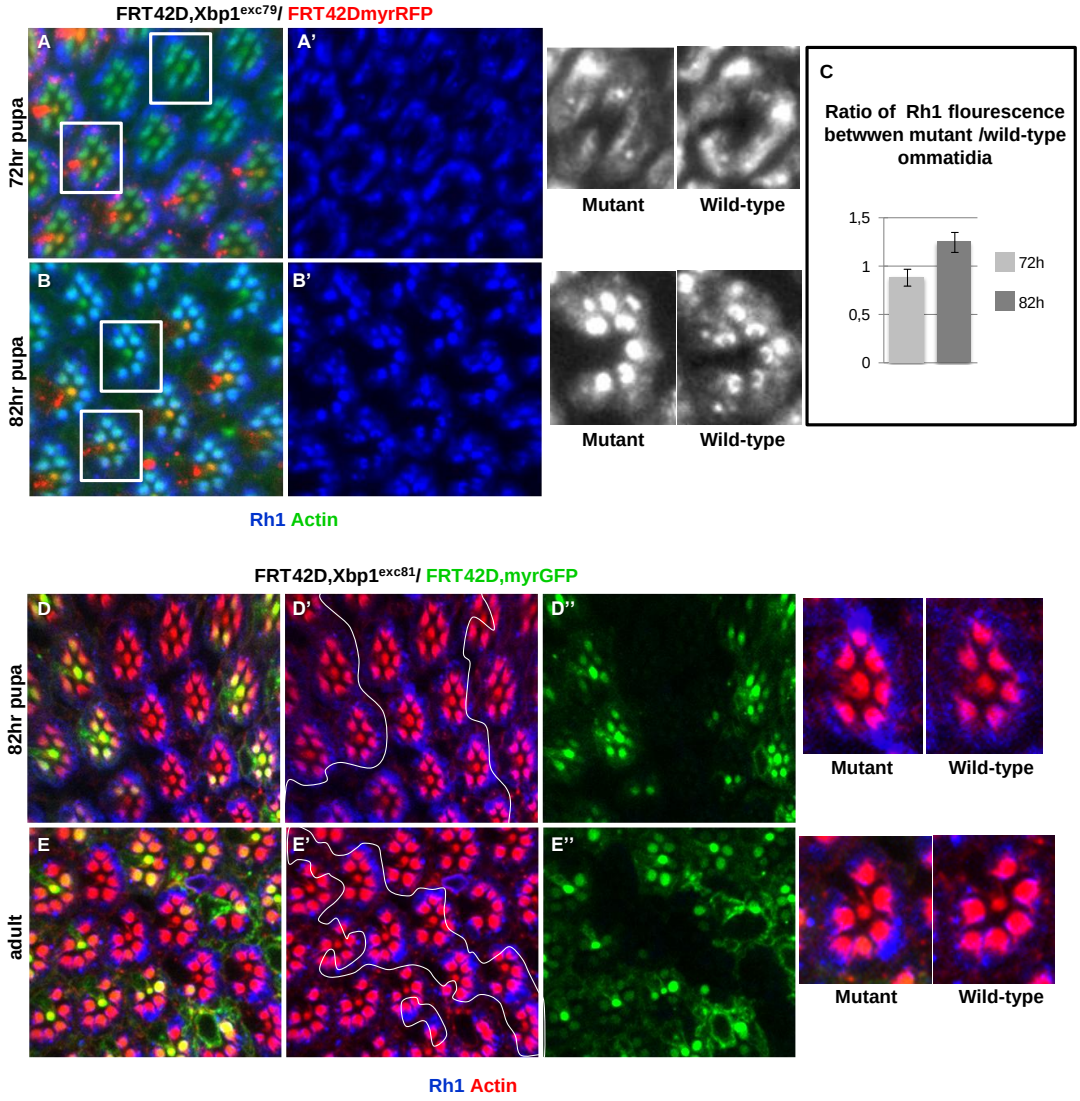

Figure 3.11. Xbp1^{exc79} and Xbp1^{exc81} photoreceptors present mild defects in the delivery of Rh1 to the rhabdomere.

(A) In 72hr pupa, Xbp1^{exc79} homozygous photoreceptors, labeled by the absence of myrRFP (red), have lower levels of Rh1 (blue) in the rhabdomere than in wild-type (monochrome magnifications with wild-type and mutant ommatidia).

(B) At 82hr pupa, Xbp1^{exc79} homozygous photoreceptors (non myrRFP cells) present higher levels of Rh1 in the rhabdomere than in wild-type. Xbp1^{exc79} homozygous photoreceptors show even distribution of Rh1 in the rhabdomere, whereas wild-type photoreceptors show the typical crescent-shaped gradient of concentration with higher levels at the rhabdomere base (monochrome magnifications).

(C) Quantification of Rh1 intensity is shown. The values are mean ± SD of the ratio of Rh1 fluorescence intensity divided by respective area between pairs of adjacent Xbp1^{exc79} homozygous and wild-type ommatidia, at 72hr and 82hr of pupal development (FluoEx79/AreaEx79/FluoWT/AreaWT).

(D) At 82hr pupation, Xbp1^{exc81} clones (marked by the absence of myrGFP) present localization of Rh1 to the rhabdomere (red) with a mild retention of Rh1 in the cell body of photoreceptors. Magnifications of wild-type and Xbp1^{exc81} mutant ommatidea.

(E) In the adult, retention of Rh1 (blue) in the cell body of Xbp1^{exc81} mutant phtoreceptors is not recovered. Clones of Excision 81 are marked by the absence of myrGFP and the rhabdomeres are in red. Magnifications of wild-type and Xbp1^{exc81} mutant ommatidea.

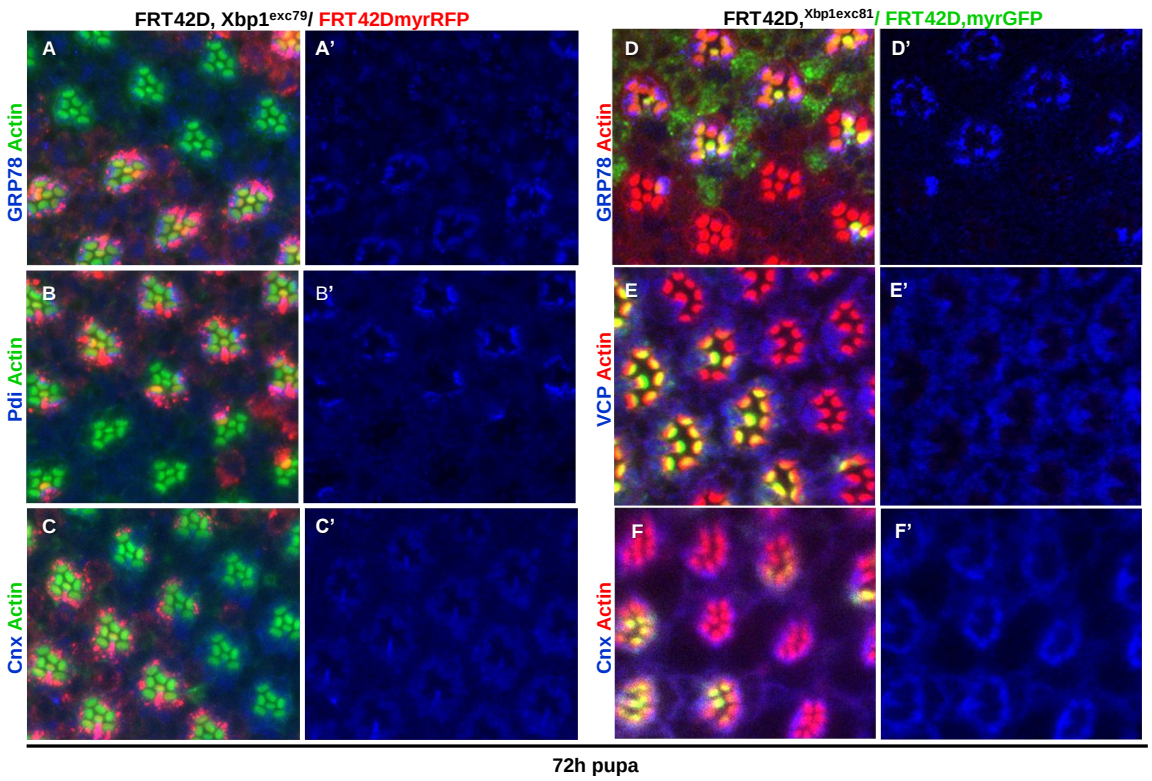

Figure 3.12 ER markers are down-regulated in Xbp1^{exc79} and Xbp1^{exc81} mutant photoreceptors.

(A–C) At 72hr pupa, Xbp1^{exc79} homozygous photoreceptors (absence of myrRFP) have reduced levels of (A) BiP/GRP78 (blue) and (B) Pdi (blue), and show a smaller ER network marked by (C) Calnexin (blue).
(D–F) At 72hr pupa, Xbp1^{exc81} homozygous photoreceptors (absence of myrGFP) have reduced levels of (A) BiP/GRP78 (blue), but not (E) VCP (blue) or (F) Cnx (blue).

Photoreceptors mutant for Xbp1 show a regular architecture in pupa and adult and do not present early degeneration, in opposition to Ire1 mutants, indicating that Xbp1 is not necessary for the differentiation of photoreceptors and morphogenesis of the rhabdomere.

Xbp1spliced is sufficient but not necessary for ninaA expression

In a microarray to unravel targets of Xbp1spliced, we found that the mRNA of NinaA is up-regulated 17.7-fold by GMR>Xbp1spliced in eye imaginal discs of the larva comparing to the control. These results were then validated by qRT-PCR for NinaA transcript in eye imaginal discs with ectopic expression of GMR>Xbp1spliced (**Figure 3.13A**).

We tested the endogenous expression of NinaA under physiological conditions by immunohistochemistry in Excision79 mutant clones for Xbp1. We detected similar levels of NinaA protein between Excision79 mutant clones and wild-type clones. (**Figure 3.13B**). The reporter of NinaA transcription nina-LacZ (Stamnes et al., 1991) further supported the similar expression of NinaA in mutant and wild-type clones (**Figure 3.13C**). Altogether the results above suggest that NinaA is a target of Xbp1spliced, but other transcription factors might activate its expression.

NinaA expression in the retina starts around 48hr of pupal development

To address NinaA role during the differentiation of photoreceptors, we mapped the temporal expression of NinaA in the retina using a *ninaA-LacZ* reporter (gene of β-galactosidase under the control of ninaA endogenous promoter - data not shown). NinaA expression starts around 48hr of pupal development and is stronger at 72hr of pupal development. NinaA expression precedes several hours the beginning of Rh1 production, which starts around 68hr of pupal development (under our experimental conditions). This time lapse may allow an increase in the steady state levels of NinaA protein, for the chaperone to be immediately available to escort Rh1 along the secretory pathway.

Ectopic expression of NinaA does not rescue Rhodopsin1 localization in *PBac{WH}Ire1^{f02170}* clones

PBac{WH}Ire1^{f02170} photoreceptors have a severe phenotype with Rh1

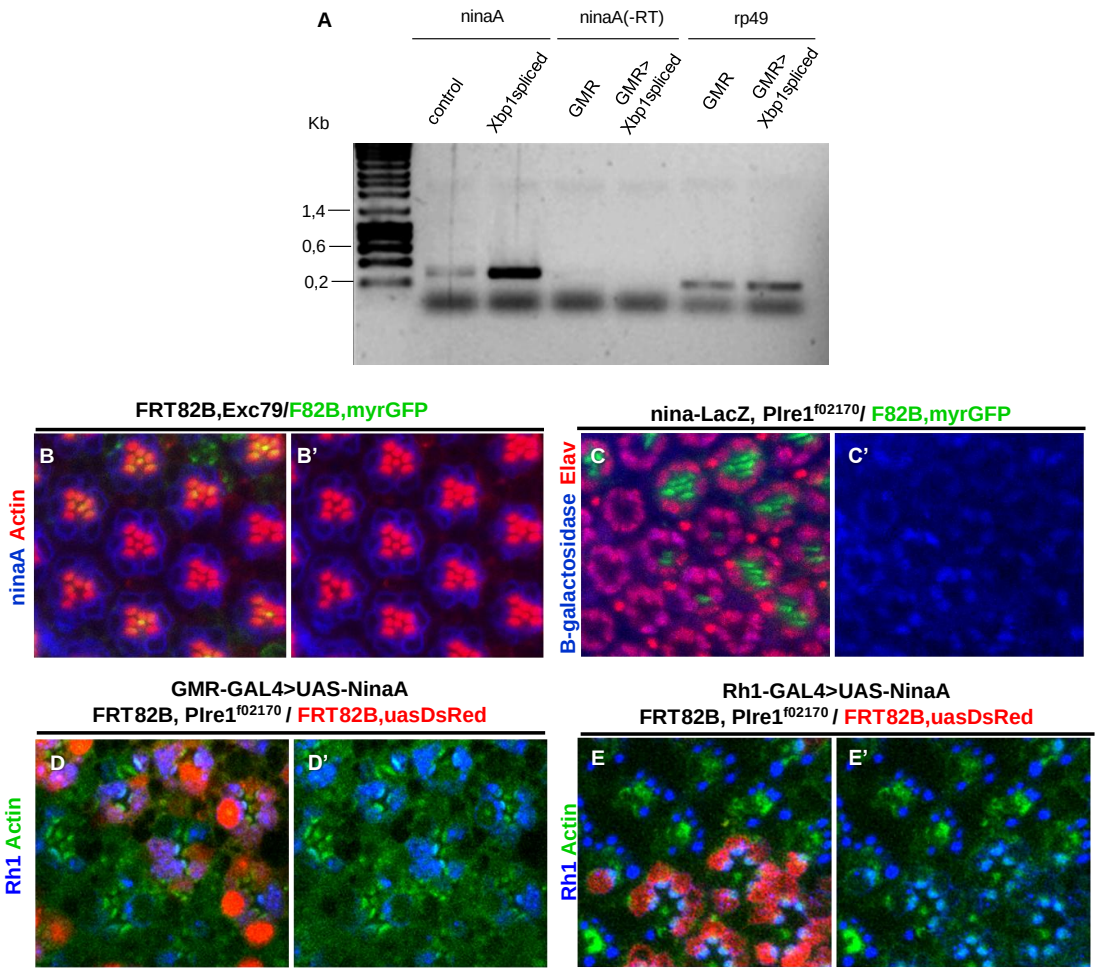

Figure 3.13. Xbp1spliced induces NinaA expression.

(A) Quantitative RT-PCR showing NinaA transcript levels up-regulated by expression of GMR-GAL4>UAS-Xbp1spliced comparing to control (GMR-GAL4) in eye imaginal discs of third instar larva.
(B) Xbp1^{exc79} mutant clones (absence of myrGFP) and wild-type clones have similar levels of NinaA in photoreceptors in 72hr pupal eye.
(C) The transcriptional reporter *nina-LacZ* is expressed at similar levels in wild-type and mutant *PBac(WH)Ire1*^{f02170} (absence of myrGFP) photoreceptors of mid-pupal eye.
(D,E) Expression of NinaA under the control of (D) the GMR promotor or (E) the Rh1 promotor does not rescue Rh1 (blue) localization to the rhabdomere (actin, in green) or formation of the interrhabdomeral space in *PBac(WH)Ire1*^{f02170} clones (labeled by DsRed).

mislocalizing in the photoreceptor cell body and an atrophy of the rhabdomere. We wondered if increasing the expression of the ER chaperone NinaA in *PBac{WH}Ire1*^{f02170} mutant photoreceptors would improve the delivery of Rh1 to the apical membrane and thus ameliorate the phenotype. Either early or late expression of a UAS-ninaA construct under control of the GMR promoter or the Rh1 promoter, respectively, failed completely to rescue the mutant phenotype (**Figure 3.13D,E**). We conclude that low levels of ninaA do not explain the severe defects of rhabdomere morphogenesis in *PBac{WH}Ire1*^{f02170} photoreceptors.

Discussion

Xbp1 is an essential gene in *Drosophila* whose functions during development are still poorly described. We generated for the first time Xbp1 null mutants in *Drosophila* and analyzed its phenotype in mosaic clones of the eye. Xbp1 is not required for differentiation of photoreceptors and morphogenesis of the rhabdomere. Deletion of Xbp1 in photoreceptors causes a very mild phenotype, with a slight delay of Rh1 delivery to the rhabdomere.

Most surprisingly Xbp1 and Ire1 mutations have distinct consequences on the differentiation of photoreceptors. While Xbp1 mutation has no effect on rhabdomere morphogenesis, Ire mutants exhibited a dramatic phenotype with collapse of the interrhabdomeral space, atrophy of the rhabdomeres and early degeneration of photoreceptors after eclosion. Recent reports have identified other targets and interactors of Ire1 cytoplasmic domain, growing evidence that Ire1 and Xbp1 are not in a linear pathway in higher eukaryotes, contrary to what happens in the budding yeast. In *Drosophila S2* cells and mammalian cell cultures, Ire1 promotes the degradation of mRNA targeted to the ER by a mechanism independent of Xbp1 and known as RIDD (Regulated Ire1-Dependent Decay) to reduce the ER client protein (Hollien and Weissman, 2006; Han et al., 2009; Cross et al., 2012). The cytoplasmic domain of activated Ire1 interact physically with Traf2 (tumour necrosis factor receptor-associated factor 2), triggering the activation of the apoptosis signal-regulating kinase 1 (ASK1)

and the initiation of the c-Jun N-terminal Kinase (JNK) apoptotic pathway (Urano et al., 2000; Yoneda et al., 2001). More experiments are necessary to further elucidate which mechanism dependent on Ire1 and independent on Xbp1 might be involved in the differentiation of photoreceptors.

The expression of ER chaperones and enzymes including GRP78 and Pdi was down-regulated in Xbp1 mutant clones and the size of the ER network marked by calnexin was slightly smaller in Xbp1 mutant photoreceptors. GRP78 and Pdi are direct targets of Xbp1spliced and therefore the impairment of ER size and capacity was expected. The delay of Rh1 delivery to the rhabdomere in Xbp1 mutants is a consequence of the lower capacity of the secretory pathway to process Rh1.

We were expecting a stronger impact on rhabdomere morphogenesis in null mutants of Xbp1 because our preliminary data indicated Xbp1 as an effective activator of NinaA transcription and ninaA is a known exclusive chaperone of Rh1. Literature describes *ninaA*^{P269}, a null mutation of NinaA with a premature stop codon, to cause dramatic decreases of mature Rh1 levels and defects in the ER architecture (Baker et al., 1994; Webel, 2000). We found that Xbp1spliced is sufficient but is not necessary to induce NinaA expression. We speculate that other UPR components, namely ATF6 may bind to the NinaA promoter to activate its transcription. Xbp1 and AT6 bind the same *cis*-acting elements in the promoter of mammalian UPR targets (Wang et al., 2000; Yoshida et al., 1998, 2003). Moreover, genes encoding ER degradation machinery depend both on ATF6 and Ire1 for maximum expression, supporting the possibility that ATF6 and Xbp1 form heterodimers with stronger affinity for UPR-regulated elements (Yamamoto et al., 2007; Yoshida et al., 2003) It would be interesting to determine if ATF6 binds NinaA promoter.

Xbp1 excisions 30, 101 and 250 die during 2nd instar larva and show hatching defects. We still do not know what is causing lethality during development in these mutants. In mouse, Xbp1 is essential for viability to ensure differentiation and survival of professional secretory cells. In *Drosophila* Xbp1

must have essential and exclusive functions during larval development and we speculate that Xbp1 mutant larva are dying from defects in secretory tissue, possibly the fat body that secretes hormones required for growth.

It has been extensively proposed that the component of the UPR, Xbp1, is necessary mostly for increasing processing capacity of the ER rather than combating acute ER stress (Cross et al., 2012). According to this model, late activation of Xbp1 permits the cell committed with secretion to adapt to chronic ER stress. In *Drosophila* this may not be the case as Xbp1 is not necessary for differentiation of photoreceptors during normal development.

Acknowledgments and author contribution

We would like to thank Charles Zuker, Nansi Jo Colley, Andrew Zelhof, the Bloomington Stock Center, Pacmanfly and the Developmental Studies Hybridoma Bank for fly stocks, reagents, and antibodies. Pedro M. Domingos performed the microarray with Xbp1 spliced. Fátima Cairrão did the qRT-PCR for ninaA in the eye imaginal discs of larva. Gonçalo Poças did the temporal mapping of ninaA expression. Xiaomei Zeng and Hyung Don Ryoo generate Excision79 and Excision81. Alexander Djiane made ExcisionF211.

References

Aragón, T., van Anken, E., Pincus, D., Serafimova, I.M., Korennykh, A.V., Rubio, C.A., and Walter, P. (2009). Messenger RNA targeting to endoplasmic reticulum stress signalling sites. Nature *457*, 736–740.

Baker, E.K., Colley, N.J., and Zuker, C.S. (1994). The cyclophilin homolog NinaA functions as a chaperone, forming a stable complex in vivo with its protein target rhodopsin. EMBO J. *13*, 4886–4895.

Calfon, M., Zeng, H., Urano, F., Till, J.H., Hubbard, S.R., Harding, H.P., Clark, S.G., and Ron, D. (2002). IRE1 couples endoplasmic reticulum load to secretory capacity by processing the XBP-1 mRNA. Nature *415*, 92–96.

Casas-Tinto, S., Zhang, Y., Sanchez-Garcia, J., Gomez-Velazquez, M., Rincon-Limas, D.E., and Fernandez-Funez, P. (2011). The ER stress factor XBP1s prevents amyloid-neurotoxicity. Hum. Mol. Genet. *20*, 2144–2160.

Colley, N.J., Baker, E.K., Stamnes, M.A., and Zuker, C.S. (1991). The cyclophilin homolog ninaA is required in the secretory pathway. Cell *67*, 255–263.

Colley, N.J., Cassill, J.A., Baker, E.K., and Zuker, C.S. (1995). Defective intracellular transport is the molecular basis of rhodopsin-dependent dominant retinal degeneration. Proc. Natl. Acad. Sci. U. S. A. *92*, 3070–3074.

Cross, B.C.S., Bond, P.J., Sadowski, P.G., Jha, B.K., Zak, J., Goodman, J.M., Silverman, R.H., Neubert, T.A., Baxendale, I.R., Ron, D., et al. (2012a). The molecular basis for selective inhibition of unconventional mRNA splicing by an IRE1-binding small molecule. Proc. Natl. Acad. Sci. U. S. A. *109*, E869–878.

Han, D., Lerner, A.G., Walle, L., Upton, J.-P., Xu, W., Hagen, A., Backes, B.J., Oakes, S.A., and Papa, F.R. (2009). IRE1a Kinase Activation Modes Control Alternate Endoribonuclease Outputs to Determine Divergent Cell Fates. Cell *138*, 562–575.

Hardie, R.C. (2012). Phototransduction mechanisms in Drosophila microvillar photoreceptors. Wiley Interdiscip. Rev. Membr. Transp. Signal. *1*, 162–187.

Hollien, J., and Weissman, J.S. (2006). Decay of Endoplasmic Reticulum-Localized mRNAs During the Unfolded Protein Response. Science *313*, 104–107.

Iwakoshi, N.N., Lee, A.-H., and Glimcher, L.H. (2003a). The X-box binding protein-1 transcription factor is required for plasma cell differentiation and the unfolded protein response. Immunol. Rev. *194*, 29–38.

Iwakoshi, N.N., Lee, A.-H., Vallabhajosyula, P., Otipoby, K.L., Rajewsky, K., and Glimcher, L.H. (2003b). Plasma cell differentiation and the unfolded protein response intersect at the transcription factor XBP-1. Nat. Immunol. *4*, 321–329.

Kaser, A., Lee, A.-H., Franke, A., Glickman, J.N., Zeissig, S., Tilg, H., Nieuwenhuis, E.E.S., Higgins, D.E., Schreiber, S., Glimcher, L.H., et al. (2008). XBP1 links ER stress to intestinal inflammation and confers genetic risk for human inflammatory bowel disease. Cell *134*, 743–756.

Kumar, J.P., and Ready, D.F. (1995). Rhodopsin plays an essential structural role in Drosophila photoreceptor development. Dev. Camb. Engl. *121*, 4359–4370.

Lee, A.-H., Iwakoshi, N.N., and Glimcher, L.H. (2003). XBP-1 regulates a subset of endoplasmic reticulum resident chaperone genes in the unfolded protein response. Mol. Cell. Biol. *23*, 7448–7459.

Lee, A.-H., Chu, G.C., Iwakoshi, N.N., and Glimcher, L.H. (2005). XBP-1 is required for biogenesis of cellular secretory machinery of exocrine glands. EMBO J. *24*, 4368–4380.

Lee, A.-H., Scapa, E.F., Cohen, D.E., and Glimcher, L.H. (2008). Regulation of hepatic lipogenesis by the transcription factor XBP1. Science *320*, 1492–1496.

León, A., and McKearin, D. (1999). Identification of TER94, an AAA ATPase protein, as a Bam-dependent component of the Drosophila fusome. Mol. Biol. Cell *10*, 3825–3834.

Liou, H.C., Boothby, M.R., Finn, P.W., Davidon, R., Nabavi, N., Zeleznik-Le, N.J., Ting, J.P., and Glimcher, L.H. (1990). A new member of the leucine zipper class of proteins that binds to the HLA DR alpha promoter. Science *247*, 1581–1584.

Moore, K.A., and Hollien, J. (2012). The Unfolded Protein Response in Secretory Cell Function. Annu. Rev. Genet. *46*, 165–183.

Murray, A.R., Fliesler, S.J., and Al-Ubaidi, M.R. (2009). Rhodopsin: The Functional Significance of Asn-Linked Glycosylation and Other Post-Translational Modifications. Ophthalmic Genet. *30*, 109–120.

O'Tousa, J.E., Baehr, W., Martin, R.L., Hirsh, J., Pak, W.L., and Applebury, M.L. (1985). The Drosophila ninaE gene encodes an opsin. Cell *40*, 839–850.

Reimold, A.M., Etkin, A., Clauss, I., Perkins, A., Friend, D.S., Zhang, J., Horton, H.F., Scott, A., Orkin, S.H., Byrne, M.C., et al. (2000). An essential role in liver development for transcription factor XBP-1. Genes Dev. *14*, 152–157.

Rosenbaum, E.E., Hardie, R.C., and Colley, N.J. (2006). Calnexin is essential for rhodopsin maturation, Ca2+ regulation, and photoreceptor cell survival. Neuron *49*, 229–241.

Ryoo, H.D., Domingos, P.M., Kang, M.-J., and Steller, H. (2007). Unfolded protein response in a Drosophila model for retinal degeneration. EMBO J. *26*, 242–252.

Shaffer, A.L., Shapiro-Shelef, M., Iwakoshi, N.N., Lee, A.-H., Qian, S.-B., Zhao, H., Yu, X., Yang, L., Tan, B.K., Rosenwald, A., et al. (2004). XBP1, downstream of Blimp-1, expands the secretory apparatus and other organelles, and increases protein synthesis in plasma cell differentiation. Immunity *21*, 81–93.

Shen, X., Ellis, R.E., Lee, K., Liu, C.-Y., Yang, K., Solomon, A., Yoshida, H., Morimoto, R., Kurnit, D.M., Mori, K., et al. (2001). Complementary Signaling Pathways Regulate the Unfolded Protein Response and Are Required for C. elegans Development. Cell *107*, 893–903.

Sone, M., Zeng, X., Larese, J., and Ryoo, H.D. (2012). A modified UPR stress sensing system reveals a novel tissue distribution of IRE1/XBP1 activity during normal Drosophila development. Cell Stress Chaperones *18*, 307–319.

Souid, S., Lepesant, J.-A., and Yanicostas, C. (2007). The xbp-1 gene is essential for development in Drosophila. Dev. Genes Evol. *217*, 159–167.

Sriburi, R. (2004). XBP1: a link between the unfolded protein response, lipid biosynthesis, and biogenesis of the endoplasmic reticulum. J. Cell Biol. *167*, 35–41.

Stamnes, M.A., Shieh, B.H., Chuman, L., Harris, G.L., and Zuker, C.S. (1991). The cyclophilin homolog ninaA is a tissue-specific integral membrane protein required for the proper synthesis of a subset of Drosophila rhodopsins. Cell *65*, 219–227.

Tohmonda, T., Miyauchi, Y., Ghosh, R., Yoda, M., Uchikawa, S., Takito, J., Morioka, H., Nakamura, M., Iwawaki, T., Chiba, K., et al. (2011). The IRE1α-XBP1 pathway is essential for osteoblast differentiation through promoting transcription of Osterix. EMBO Rep. *12*, 451–457.

Urano, F., Bertolotti, A., Zhang, Y., Chung, P., Harding, H.P., and Ron, D. (2000). Coupling of stress in the ER to activation of JNK protein kinases by transmembrane protein kinase IRE1. Science *287*, 664–666.

Wang, Y., Shen, J., Arenzana, N., Tirasophon, W., Kaufman, R.J., and Prywes, R. (2000). Activation of ATF6 and an ATF6 DNA binding site by the endoplasmic reticulum stress response. J. Biol. Chem. *275*, 27013–27020.

Webel, R. (2000). Role of Asparagine-linked Oligosaccharides in Rhodopsin Maturation and Association with Its Molecular Chaperone, NinaA. J. Biol. Chem. *275*, 24752–24759.

Xiong, B., and Bellen, H.J. (2013). Rhodopsin homeostasis and retinal degeneration: lessons from the fly. Trends Neurosci.

Yamamoto, K., Sato, T., Matsui, T., Sato, M., Okada, T., Yoshida, H., Harada, A., and Mori, K. (2007). Transcriptional induction of mammalian ER quality control proteins is mediated by single or combined action of ATF6alpha and XBP1. Dev. Cell *13*, 365–376.

Yanagitani, K., Imagawa, Y., Iwawaki, T., Hosoda, A., Saito, M., Kimata, Y., and Kohno, K. (2009). Cotranslational targeting of XBP1 protein to the membrane promotes cytoplasmic splicing of its own mRNA. Mol. Cell *34*, 191–200.

Yoneda, T., Imaizumi, K., Oono, K., Yui, D., Gomi, F., Katayama, T., and Tohyama, M. (2001). Activation of Caspase-12, an Endoplastic Reticulum (ER) Resident Caspase, through Tumor Necrosis Factor Receptor-associated Factor 2-dependent Mechanism in Response to the ER Stress. J. Biol. Chem. *276*, 13935–13940.

Yoshida, H., Haze, K., Yanagi, H., Yura, T., and Mori, K. (1998). Identification of the cis-acting endoplasmic reticulum stress response element responsible for transcriptional induction of mammalian glucose-regulated proteins. Involvement of basic leucine zipper transcription factors. J. Biol. Chem. *273*, 33741–33749.

Yoshida, H., Matsui, T., Hosokawa, N., Kaufman, R.J., Nagata, K., and Mori, K. (2003). A time-dependent phase shift in the mammalian unfolded protein response. Dev. Cell *4*, 265–271.

Zuker, C.S., Cowman, A.F., and Rubin, G.M. (1985). Isolation and structure of a rhodopsin gene from D. melanogaster. Cell *40*, 851–858.

Regulation of Fatp by RIDD is critical for rhabdomere morphogenesis

CHAPTER IV

Summary

Ire1 is an important transducer of the Unfolded Protein Response (UPR) that signals primarily via the activation of the transcription factor Xbp1. Several recent studies have highlighted roles of Ire1 independent of Xbp1, as for example Regulated Ire1 Dependent Decay (RIDD). Here, we describe that RIDD has an important role during the development of the *Drosophila* eye in the pupa.

During the differentiation of photoreceptors in the pupa a light gathering structure, the rhabdomere, takes shape at the apical domain of the photoreceptors. Morphogenesis of the rhabdomere relies on the ER to synthesize a large amount of proteins like Rhodopsin1 (Rh1) and other components of the light transduction cascade, imposing a huge stress to the photoreceptor. We have previously demonstrated that Ire1 is required independently of Xbp1 for the morphogenesis of the rhabdomere and differentiation of the photoreceptors. However the mechanism underlying the requirement for Ire1 in photoreceptors was still missing.

We now found that RIDD is activated in the *Drosophila* eye and promotes the degradation of several mRNA substrates. One of them, Fatp, facilitates the cellular uptake of fatty acids which are the precursors of the signaling phospholipid phosphatidic acid. We discovered that Ire1 mutant eyes have elevated levels of phosphatidic acid, which is known to disrupt vesicular trafficking of Rh1 to the rhabdomere, causing early retinal degeneration. The regulation of Fatp levels by Ire1 turned out to be critical for the control of phosphatidic acid levels during rhabdomere morphogenesis.

Introduction

Perturbations of the folding environment in the endoplasmic reticulum (ER) lead to accumulation of misfolded proteins in the lumen of the ER and activation the Unfolded Protein Response (UPR), a collection of adaptative signaling

pathways. The UPR is essential for cell survival during external environmental insults and for cell adaptation to physiological conditions or differentiation states in various tissues and organisms.

The UPR increases the ER folding capacity, and the cell secretory capacity in general, by the up-regulation of genes involved in protein translocation into the ER, protein folding, glycosylation, vesicular trafficking and membrane biogenesis (Lee et al., 2003; Travers et al., 2000). The UPR was first described in the budding yeast in the 1990s, where a single transducer, Ire1, initiates the response to ER stress (Cox et al., 1993; Mori et al., 1993). Ire1 is a conserved ER-resident transmembrane protein containing two enzymatic activities, kinase and endoribonuclease (RNase), which are activated by ER stress (Credle et al., 2005; Shamu and Walter, 1996; Welihinda and Kaufman, 1996). Ire1 mediates the site-specific cleavage of Hac1 mRNA (in yeast) and splices out a 252 base intron that blocks translation in unstressed conditions (Cox and Walter, 1996; Kawahara et al., 1997; Gonzalez et al., 1999; Rüegsegger et al., 2001; Sidrauski and Walter, 1997). Re- ligation of the 5' and 3' fragments by tRNA ligase 1 (Trl1) generates a spliced mRNA encoding a potent transcription factor (Sidrauski et al., 1996; Mori et al., 2000).

Although the sole substrate of Ire1 in budding yeast is Hac1, several studies in metazoans show that Ire1 has additional functions in cell signaling besides splicing Hac1 homolog (Xbp1) (Calfon et al., 2002; Yoshida et al., 2001). The cytosolic domain of activated Ire1 binds to the adaptor protein TNFR-associated factor 2 (TRAF2), triggering the activation of the apoptosis signal-regulating kinase 1 (ASK1) and cJun-N terminal kinase (JNK) pathway (Urano et al., 2000; Nishitoh et al., 2002). Ire1/TRAF2 interaction has been proposed to mediate in part apoptosis under irreversible ER stress.

In addition, both in mammalian and insect cells Ire1 promotes the cleavage and degradation of ER associated mRNAs (Hollien, 2006; Hollien et al., 2009; Cross et al., 2012; Han et al., 2009). This process, known as RIDD (regulated Ire1-dependent decay), represents an Xbp1-independent post-transcriptional

mechanism for Ire1 to selectively relieve the burden on the ER and alleviate stress. The two functions of Ire1 RNase activity seem to be activated in different modes. Ire1 shows high specificity for Xbp1 mRNA and the splicing reaction can be induced by artificial dimerization and activation of Ire1 in the absence of ER stress. Ire1-dependent mRNA decay requires ER stress that elicits formation of Ire1 high-order oligomers, where Ire1 RNase attains a loose conformation with low specificity for alternative substrates (Han et al., 2009; Hollien et al., 2009). Under severe ER stress conditions, the promiscuous degradation of ER associated mRNAs, including mRNAs encoding ER chaperones and proteins of the plasma membrane, might cause severe damages to the cell and induce apoptosis.

The sequential steps of Ire1 activation - oligomerization, autophosphorylation and RNase activitation - have been known for some time. The recent crystal structure models for Ire1 provided important clues about the molecular mechanisms of Ire1 activation and catalysis, in particularly about the coupling of the kinase and RNase activity. Accumulation of misfolded proteins in the ER promotes homodimerization of Ire1 luminal domains and initiates Ire1 activation (Bertolotti et al., 2000; Credle et al., 2005; Kimata et al., 2007). Assembly of dimers juxtaposes Ire1 kinase domains at the cytoplasmic side of ER membrane and favors trans-autophosphorylation (Shamu and Walter, 1996; Ali et al., 2011). Phosphorylation and nucleotide binding at the kinase active site stabilize a back-to-back dimer and generates the RNase active site (Lee et al., 2008; Korennykh et al., 2011). Ire1 dimers can form higher order oligomers with a reinforced active conformation (Korennykh et al., 2008; Li et al., 2010). Ligands that modulate Ire1 enzymatic activity might be used as therapeutic drugs to treat conditions characterized by a chronic ER stress as cancer, viral infections and inflammation.

Ire1 is widely conserved in eukaryotes. Mammals possess two Ire1 isoforms: Ire1α, which is an essential gene expressed ubiquitously, and Ire1β, that is expressed mainly in intestinal epithelial cells (Tirasophon et al., 1998; Bertolotti et al., 2001). Ire1α is necessary during two different steps of B

lymphocytes differentiation into plasma cells (Zhang et al., 2005). Ire1β is not essential during development but deletion of Ire1β increases the susceptibility of mice to colitis (Bertolotti et al., 2001). Although both Ire1 isoforms can activate the RIDD pathway in mammals, Ire1β appears to be more specialized in RIDD, displaying a broader RNase specificity and higher activity in the cleavage an alternative substrate (Imagawa et al., 2008).

Materials and Methods

Fly stocks and crosses

All *Drosophila* stocks were raised with standard cornmeal medium, at 25°C, in a 12hr light/dark cycle. Somatic mosaic clones in the eye were generated by the Flp/FRT system with Flipase under the control of the *eyeless* promoter (Golic, 1991; Newsome et al., 2000). UAS-Fatp and UAS-Fatp RNAi were a gift from B. Mollereau and were described in Dourlen et al., 2012. UAS-lazaro was a gift from P. Raghu and was described in Raghu et al., 2009. Ectopic expression was driven by GMR-GAL4 or Rh1-GAL4 lines. To reduce the fluorescence background from the red pigment a RNAi against the white gene carried on the transgenic construct pWIZ was used (Sik Lee, 2003). Hyung Don Ryoo contributed with the $Ire1^{H890A}$ and $Ire1^{K576A}$ transgenic flies.

Quantitative RT-PCR

For quantitative reverse transcription-PCR (RT-PCR) analysis, total RNA was extracted from adult heads with Trizol and Direct-zol RNA mini-prep (Zymo Research). 0,5mg of total RNA was retro-transcribed using RevertAid First Strand (Thermo/Fermentas). Each PCR reaction was performed on 1/40 of the cDNA obtained using SSoFast EvaGreen Supermix (Bio-Rad) according to the manufacturer's instructions and using a Bio-Rad Cfx-96 detection system. All samples were analyzed in triplicates and from 3 independent RNA extractions. For each sample, the levels of mRNAs were normalized using rp49 as a loading

control. PCR primers were: sparc (F: AGC TCC ATC TGC ATG TAG TGC TCG, R: ATC TGC CAG ATG CAC GAC GAG AAG), indy (F:GCT TGC GGG TGA AGT ACA TCA CAA CC, R:TAC CTT CAA GGG CAT CTA CGA GGC), lamp1 (F: CTT ATT GGC TTG CCG AGA GTC GGT, R: TGG ATG GTT GCG GAT ATG GTT GCG , fatp (F: CCT TGG AAG TCT GGT AGT ACA GCG, R: AGA ATG TTT CCA CCA GCG AGG TGG), CG5888 (F: ACT CGG TTG GCA CAT TAT CAC CGC, R: GGA AGC AGT GAT TTG CCC GGT AAC), mys (F: AGC AGG TGA GCT TCA CAG CTC AGA, R: TCG ATG TTA GAT CCG TTG CCG AGC), CG11562 (F:TGA GAC TGC ACG ATG GTG TCC TGA, R: CCA TCG TGA TTA GTC GTT CCA CCC), CG6805 (F: ACC ACT TGT CCG GAT AAC CAG CTG, R:GCG AAA GTC GAA TGC TTA CGG CAC), Pld (F:ACG GAC TCA GCT TTC GGA TCA CGT, R: GTC TCA GTA GCT GTT AGA CGG TGC), dgk (F: CTT CTG TTG CTG CTC GAA CTG GAG, R:ATC ACT AGC TGT CGA GGA AGC TGC), Lpp (lazaro) (F:CTC GTT GTC GTC CTC ATT CTC TGC, R: TAC GTG GAG CAG TTC CAC TGC ACT), cds (F:GAA GTT CCT GGT GAC CTA TCA CCG, R:GTC TTC TTG GGG CTG AGC TTG ATG) and rp49 (F:AGA TCG TGA AGA AGC GCA CCA AGC, R: GCA CCA GGA ACT TCT TGA ATC CGG).

In vitro Ire1 mRNA cleavage assay

The *in vitro* Ire1 mRNA cleavage assay was performed as in Cross et al., 2012. *Drosophila* Xbp1 mRNA was produced in vitro with T7 RNA polymerase (Promega Ribomax Express RNA) from pOT2-Xbp1 after linearization with NotI. *Drosophila* Fatp mRNA was produced from a PCR product obtained with Forward: 5'TAA TAC GAC TCA CTA TAG GGA GAC CGG3' and Reverse: 5'CGG TGT GGT ACA AAG GCA AGG3'. Fatp Mut1 was done by changing GTGGCCAATGTGctgcagGCTCAGGGCTAC into GTGGCCAATGTGctccacGCTCAGGGCTAC and Fatp Mut. 2 by changing TCCCTCCCTGctgcacAGCATCAC into TCCCTCCCTGctccaaAGCATCAC. The mRNAs (1µM) were incubated at 29°C with purified human Ire 1 (5 µM) and with

or without the Ire1 inhibitor 4μ8C (10μM). Cleavage products were resolved by electrophoresis on a 1% denaturing agarose gel stained with ethidium bromide.

Analysis of retinal phosphatidic acid

The analysis of retinal phosphatidic acid by LC-MS was performed following the protocol described in Raghu et al., 2009. For each genotype 150 retinas were separated from the head after being frozen in liquid nitrogen and dehydrated in acetone. The retinas were homogenized using a glass piston in 1mL methanol containing 500ng of a 12:0/12:0 PA standard (Avanti Polar Lipids). The lipids were extracted with addition of 2mL of chloroform and 1ml of 0.88% (w/v) KCl to split the phases. The lower organic phase was dried in a speedvac during 30min and stored at -20ºC until further analysis. Phospholipids extracts were profiled using the LC-MS in order to identify and quantify the PA species present. The analysis was performed using a Surveyor HPLC system (Thermo Scientific) interfaced to an externally calibrated LTQ-Ion trap mass spectrometer (Thermo Scientific) with an electrospray ionization (ESI) source in negative mode. The capillary was operated at 5kV and source temperature was set to 300ºC, the sheath gas and auxiliary gas setting was 20 (arbitrary units). For normal-phase chromatographic analysis, a 10μL aliquot of phospholipid extract dissolved in 30μL of chloroform was injected into a Luna, Phenomenex silica column (150 mm x 1.0mm, 3um particle size). PA phospholipids species originating from fly extracts were separated using chloroform/methanol/water (90:9.5:0.5) containing 7.5mM ethylamine changing to acetonitrile/chloroform/methanol/water (30:30:35:5) containing 10mM ethylamine at flow rate of 50 μL/min. The column temperature was maintained at 25ºC. The relative amount of each PA species was determined dividing the area of the corresponding m/z peak by that of the internal standard.

Immunohistochemistry and electron microscopy

Pupa and adult eyes were dissected in PBS, fixed in 1X PBS + 4%formaldehyde for 30min at room temperature and washed 3X in PBT (1X PBS+ 0,3% Triton X-100) 10 min each. Primary antibody was diluted in BBT (1xPBS, 1% BSA, 0.1% Tween 20, 250 mM NaCl) and incubated overnight at 4ºC under gentle agitation. Primary antibodies used in immunohistochemistry were: rabbit anti-fatp (Dourlen et al., 2012) mouse anti-Sparc (Portela et al., 2010), mouse anti-Rh1 (4C5, Developmental studies hybridoma bank), rabbit anti-Rab11 (Satoh, 2005), rabbit anti-Pld (provided by P. Raghu), guinea pig anti-ATF4 (Kang et al., 2012). Samples were washed 3X for 10 min in PBT and incubated with appropriate secondary antibodies (Jackson ImmunoResearch) in BBT for 2hr at room temperature. Phalloidin-TRITC or Phalloidin-FITC (Sigma) was incubated together with secondary antibodies. For Sparc staining, secondary antibody used was anti-mouse conjugated-HRP followed by Cy5-tyramide incubation to enhance antibody signal. Samples were mounted in glycerol 70% and analyzed in a Zeiss LSM 710 microscope. Images were processed with Adobe Photoshop.

For electron microscopy, adult eyes were fixed in 2.5% glutaraldehyde in 0.1M cacodylate buffer (pH 7.4) and postfixed with 1% osmium tetroxide. After dehydration in ethanol and propylene oxide, the eyes were infiltrated with resin and mounted in silicone molds. Ultrathin sections (60nm) were cut and examined with an electron transmission microscope (JEOL; JEM).

Results

Regulation of Fatp by RIDD is critical for rhabdomere morphogenesis

We demonstrated on previous Chapters that Ire1, but not Xbp1, is required for photoreceptors morphogenesis. *In vitro* studies, both in insect and mammallian cells, demonstrated that Ire1 has a Xbp1-independent role in promoting the degradation of ER associated-mRNAs, which are predicted to

encode hydrophobic domains difficult to fold (Han et al., 2009; Hollien et al., 2009). Next, we tested if regulated Ire1 dependent decay (RIDD) of ER-targeted mRNAs also occurs in the *Drosophila* eye. By qRT-PCR, we observed that specific targets of RIDD (Indy Fatp, Sparc, CG5888, Mys and Smt3) are 1.5 to 2.5-fold up-regulated in *PBac{WH}Ire1*^{f02170} whole mutant retinas comparing to controls (**Figure 4.1A**). We validated these results by immunohistochemistry and observed that Sparc and Fatp protein expression is strongly up-regulated in *PBac{WH}Ire1*^{f02170} mutant clones in the eye (**Figure 4.1B,C**). This observation raises the possibility that the role of Ire1 during photoreceptors differentiation relies on RIDD.

We confirmed that Ire1 specifically cleaves Fatp mRNA in a cell-free system (**Figure 4.2**). Purified human Ire1 incubated with *in vitro* transcribed Fatp mRNA, degrades it into smaller fragments (940bp, 530bp, 140bp). Addition of the drug 4μ8C (an inhibitor of Ire1 RNase) to the cleavage reaction prevents the degradation of Fatp mRNA. The Ire1 cleavage sites in the Fatp transcript are similar to previous consensus sites recognized by Ire1 in the insulin mRNA (Han et al., 2009). Mutagenesis of one or two cleavage sites abrogated the degradation of Fatp mRNA by Ire1.

One target of RIDD, Fatp (Fatty acid transport protein), was recently described to be a major regulator of Rhodopsin1 (Rh1) metabolism in the *Drosophila* eye (Dourlen et al., 2012). Fatp facilitates the uptake of fatty acids into the cell and is expressed in both accessory and photoreceptor cells of the adult. Fatp null mutant photoreceptors have increased levels of Rh1 that lead to an abnormal visual response and progressive retinal degeneration (Dourlen et al., 2012). To determine the impact on photoreceptor differentiation of increased levels of Fatp, as present in *PBac{WH}Ire1*^{f02170} eyes, we over-expressed UAS-Fatp under the control of the GMR driver. In GMR-GAL4>UAS-Fatp eyes, we observed a phenotype very alike with the *PBac{WH}Ire1*^{f02170} phenotype: rhabdomeres with an irregular and smaller section and massive accumulation of Rh1 in the cell body of photoreceptors (**Figure 4.3A,B**).

These results support the idea that higher levels of Fatp may contribute to the rhadomere defects observed in *PBac{WH}Ire1*^{f02170} photoreceptors. Moreover, we could rescue Rh1 localization to the rhabdomere and restore normal architecture of the rhabdomere by down-regulating Fatp levels through RNA interference in *PBac{WH}Ire1*^{f02170} mutant clones (**Figure 4.3C**).

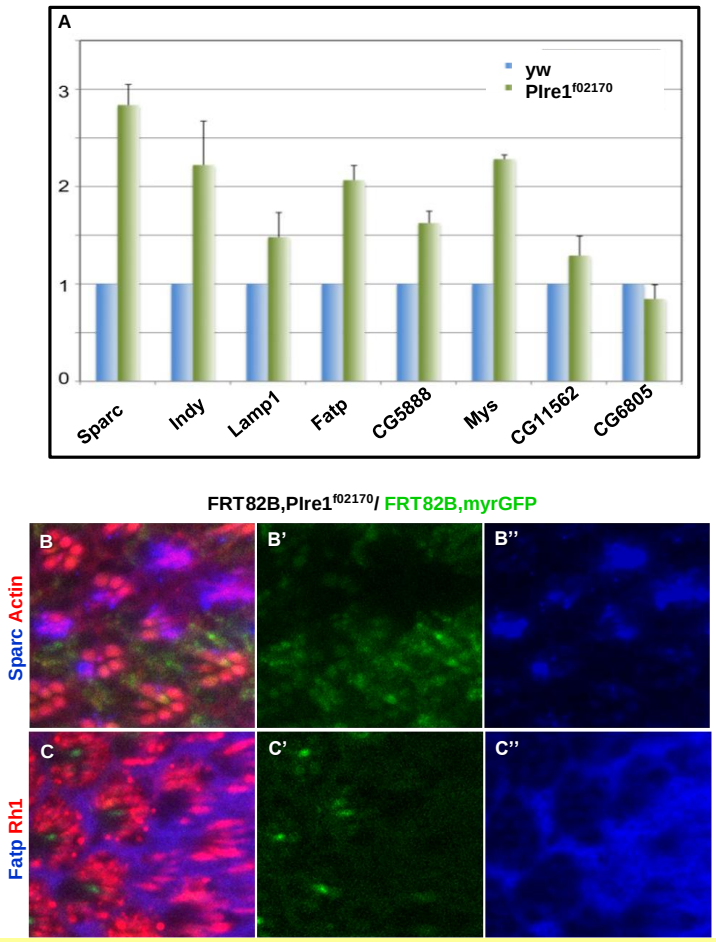

Figure 4.1. Ire1 regulates mRNA decay of Fatp in *Drosophila* eye.

(A) Quantitative RT-PCR comparing the mRNA levels (y axis) of RIDD targets (x axis) in control (blue bars,*yw*) and Ire1 mutant eyes (green bars, *eyFlp;FRT82B,PBac(WH)Ire1*^{0217f0}*/FRT82B,CL,GMR-hid*). The mRNA levels are presented as mean ± SD of arbitrary units (fold change) relative to control (*yw*). (B,C) Clones of *PBac{WH}Ire1*^{f02170} homozygous ommatidia (absence of myrGFP) have higher levels of (B) Sparc (blue) and (C) Fatp (blue) than surrounding control tissue.
(C) Fatp is increased both in the lattice cells and in the photoreceptors (marked by Rh1, in red).

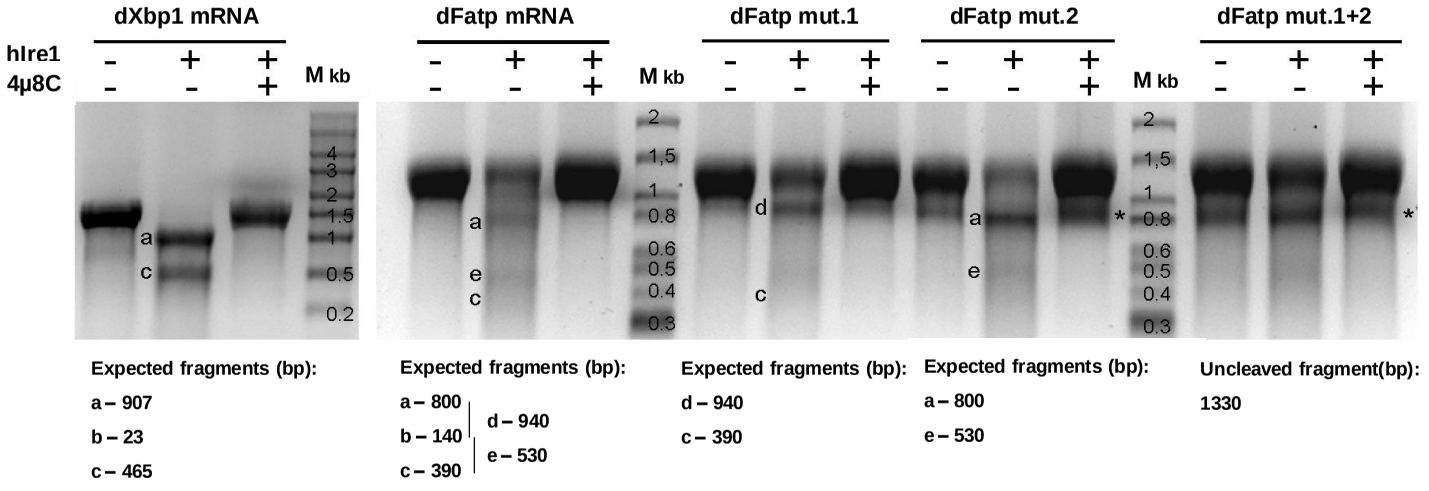

Figure 4.2. *Drosophila* Xbp1 and Fatp mRNAs are cleaved by purified human Ire1.

Addition of the selective Ire1 RNase inhibitor 4μ8C prevents the cleavage of Xbp1 and Fatp mRNAs. Mutagenesis of Ire1 recognition sites in Fatp mRNA (mut1 or mut2), prevents the cleavage of mRNA by Ire1. The size (in base pairs, bp) of the expected fragments is indicated below each panel. An unexpected band (*) in the Fatp Mut2 panels probably results from an mRNA conformation that was resistant to the denaturing conditions used.

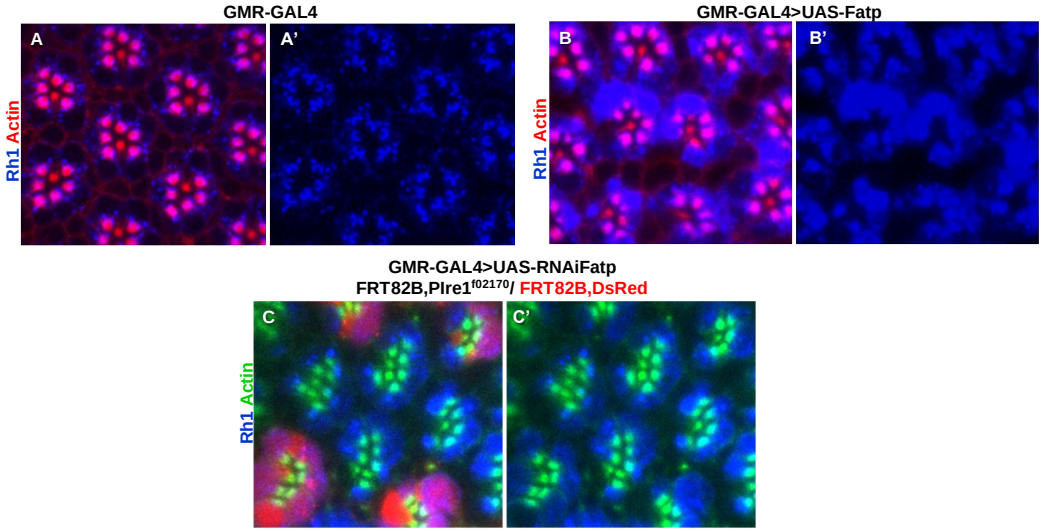

Figure 4.3 Increased levels of Fatp deregulate the delivery of Rh1 to the rhabdomere.

(A) Adult control eyes (GMR-GAL4) have normal localization of Rh1 (blue) in the rhabdomere (actin, in red).
(B) Adult GMR-GAL4> UAS-Fatp eyes have defective delivery of Rh1 (blue) to the rhabdomere (actin, in red).
(C)Knock-down of Fatp by expression of GMR-GAL4>UAS-RNAiFatp rescues Rh1 (blue) localization to the rhabdomere (actin, in green) in *PBac{WH}Ire1*^{f02170} mutant clones (marked by the absence of DsRed).

Rab11 positive vesicles accumulate in the cytoplasm of *PBac{WH}Ire1*^{f02170} mutant photoreceptors

Rhagu and collaborators showed that high levels of a minor specie of phosphatidic acid interferes with the homeostasis of the endomembrane system in photoreceptors during late pupation and compromises the morphogenesis of the rhabdomere (Raghu et al., 2009). In fact, mutants of the biosynthetic pathway of the phosphatidic acid exhibit accumulation of vesicles and membranes in the cell body of the rhabdomere, atrophy of the rhabdomere and down-regulation of rhabdomere markers, as Rh1 and TRP, a phenotype (Raghu et al., 2009) that resembles *PBac{WH}Ire1*^{f02170} mutant phenotype observed in EM (**Figure 4.4A,B**).

The levels of phosphatidic are critical for secretory traffic dependent on Arf1 (ADP-ribosylation factor 1) activity during a small window of time before rhabdomere morphogenesis (Raghu et al., 2009). To analyze the trafficking of secretory vesicles to the rhabdomere in *PBac{WH}Ire1*^{f02170} mutant photoreceptors, we immunolabeled the small GTPase Rab11. Rab11 mediates the post-Golgi transport of vesicles containing Rh1 and other phototransduction proteins to the rhabdomere (Satoh, 2005; Li et al., 2007). A reduction of Rab11 activity results in the accumulation of vesicles in the cytoplasm of photoreceptors and degeneration of rhabdomeres, a phenotype similar to mutants that accumulate phosphatidic acid (Satoh, 2005; Li et al., 2007). We observed a strong accumulation of Rab11 in the cytoplasm of *PBac{WH}Ire1*^{f02170} photoreceptors, supporting the idea that the trafficking of Rh1 is perturbed and Rab11-positive vesicles are accumulating in the cytoplasm (**Figure 4.4C**).

Increased levels of fatty acids in *PBac{WH}Ire1*^{f02170} retinas disrupt rhabdomere morphogenesis

Fatty acids are precursors of phosphatidic acid biosynthesis. We hypothesized that Fatp up-regulation in *PBac{WH}Ire1*^{f02170} photoreceptors increases the levels of phosphatidic acid species, which are known to disrupt Rh1 trafficking to the apical membrane and impair rhabdomere biogenesis. By liquid chromatography followed by mass spectroscopy, we confirmed that *PBac{WH}Ire1*^{f02170} whole mutant retinas have increased levels of phosphatidic acid comparing to control retinas (**Figure 4.5A**). The minor specie of phosphatidic acid (16:0/18:2) found to mediate the phenotype described in Rhagu et al, 2009 is also up-regulated in *PBac{WH}Ire1*^{f02170} retinas (**Figure 4.5B**).

To further clarify the source of elevated phosphatidic acid in *PBac{WH}Ire1*^{f02170} retinas, we evaluated the expression of enzymes of the biosynthetic pathway of phosphatidic acid by qRT-PCR and immunohistochemistry. The levels of *pld*, *dgk* and *lazaro* transcripts are not significantly different between *PBac{WH}Ire1*^{f02170} and control eyes (**Figure 4.5C**).

In addition, expression of Pld (phosphatidylcholine-hydrolyzing phospholipase D), an enzyme that converts phosphatidylcholine into phosphatidic acid, is similar between *PBac{WH}Ire1*^{f02170} and wild-type clones in the eye (**Figure 4.5D**).

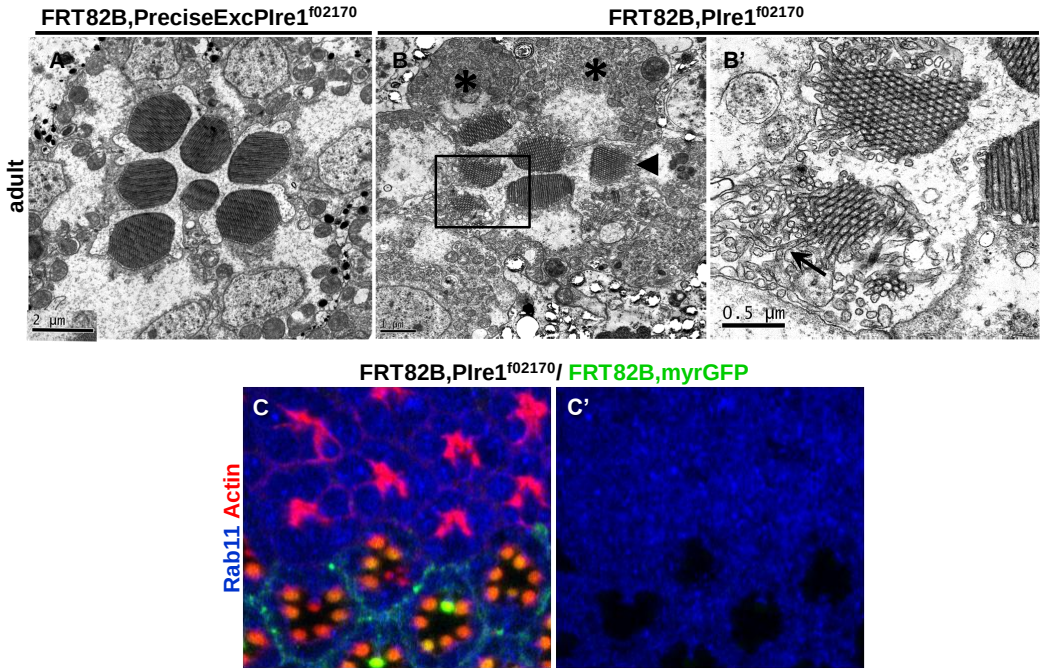

Figure 4.4. The vesicular transport is affected in *PBac{WH}Ire1*^{f02170} *eyes*.

(A,B) Electron microscopy micrographs of adult ommatidia.
(A) Photoreceptors of a precise excision of *PBac{WH}Ire1*^{f02170} (*FRT82B,PreciseExcisionPBac{WH}Ire1*^{f02170}) show a trapezoidal arranjement of the rhabdomeres, which have a regular section and an eletron dense structure formed by closely packed microvilli.
(B) Photoreceptors of *PBac{WH}Ire1*^{f02170} whole mutant eye (EGUF;;FRT82B,*PBac{WH}Ire1*^{f02170}*/FRT82B,GMR-hid,CL)* show small and irregular rhabdomeres with a loose organization of the microvilli (arrowhead). The rhabdomere base is disorganized and electron dense material (endomembranes and vesicles - asterix) is accumulating in the cell body of the rhabdomeres. (B') In the inset, the rhabdomere is degenerating and shealths of rhabdomere membrane are invading the cytoplasm (arrow).
(C) Mutant photoreceptors of *PBac{WH}Ire1*^{f02170} *clones* (absence of myrGFP) in the adult eye show increased levels of Rab11 (blue) in the cytoplasm. Actin is in red.

These data excludes the possibility that higher levels of phosphatidic acid in *PBac{WH}Ire1*^{f02170} retinas are due to differences in the expression of enzymes of the metabolic pathway of phosphatidic acid.

We then tried to rescue the phenotype in *PBac{WH}Ire1*^{f02170} by down-regulating the levels of phosphatidic acid. Lazaro is a lipid phosphatase phosphohydrolase (LPP) enriched in the eye that converts phosphatidic acid into diacylglycerol and whose over-expression in the eye rescues the rhabdomere defects caused by higher levels of phosphatidic acid (Garcia-Murillas et al., 2006; Raghu et al., 2009). Over-expression of UAS-Lazaro under the control of GMR rescued the delivery of Rh1 to the rhabdomere and the morphology of photoreceptors in *PBac{WH}Ire1*^{f02170} eye clones (**Figure 4.5E**). These results support the idea that higher levels of phosphatidic acid are disturbing the morphogenesis of the rhabdomere in *PBac{WH}Ire1*^{f02170} photoreceptors.

RNase activity of Ire1 is essential for rhabdomere morphogenesis

To further elucidate the function of Ire1 required for rhabdomere morphogenesis we tried to rescue *PBac{WH}Ire1*^{f02170} phenotype by expressing different mutants of Ire1. Ire1^{H890A} is an RNase defective mutant and Ire1^{K576A} is a kinase defective mutant. Taking into account that Ire1 trans-autophosphorylation precedes and is necessary for the engagement of RNase active conformation, the Ire1^{H890A} RNase mutant should still maintain the kinase activity, but the Ire1^{K576A} kinase mutant is not predicted to have RNase activity. First, both constructs failed to splice Xbp1-EGFP in photoreceptors of the mid-pupa (**Figure 4.6A,B**). Second, both constructs failed to rescue Rh1 localization to the rhabdomere in *PBac{WH}Ire1*^{f02170} clones (**Figure 4.6C,D**).

These findings support the idea that Ire1 mediated phosphorylation of downstream targets is not sufficient to ensure a normal rhabdomere morphogenesis and Ire1 RNase activity is necessary for the normal differentiation of photoreceptors.

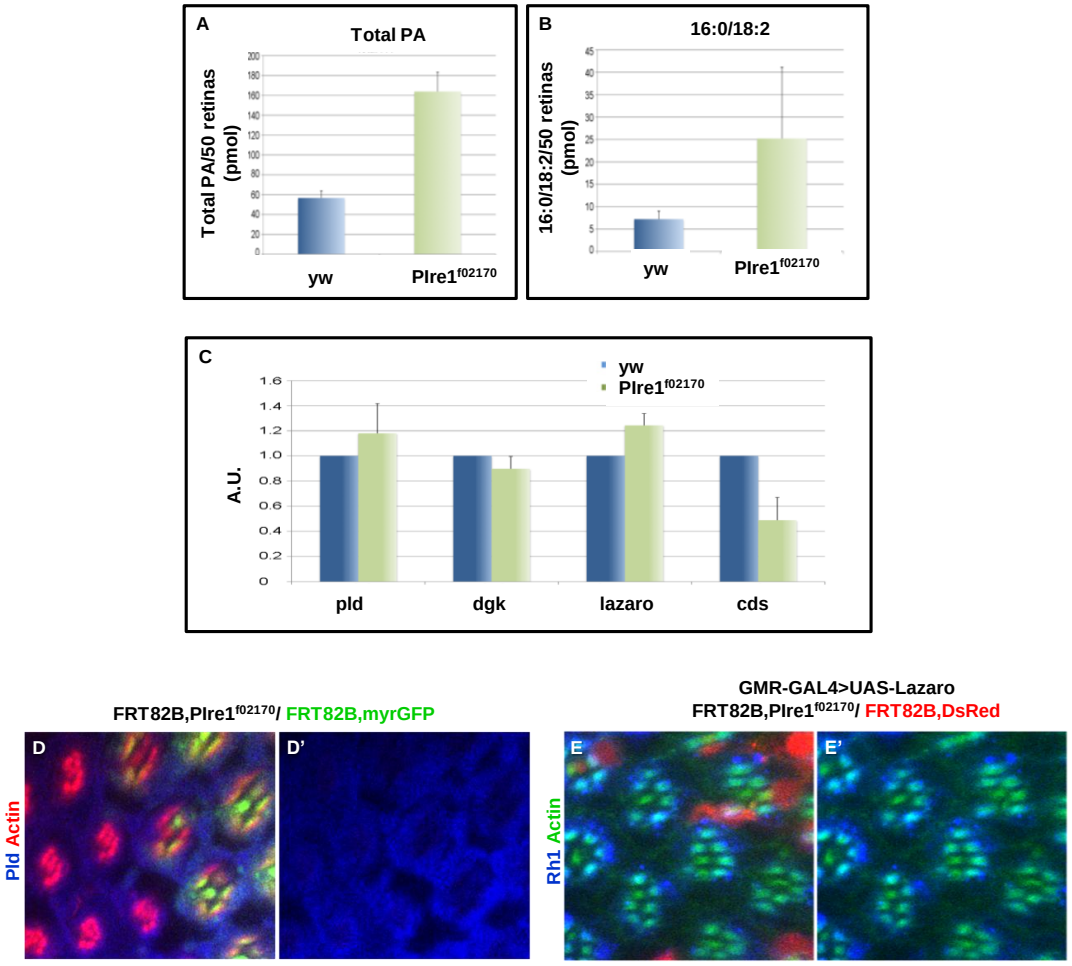

Figure 4.5 Levels of phosphatidic acid are increased in *PBac{WH}Ire1^{f02170}* retinas.
(A) Quantification of phosphatidic acid (PA) species in *yw* (control) and *PBac{WH}Ire1^{f02170}* homozygous adult eyes by LC-MS. Total PA includes the quantification of 16:0/16:1, 16:0/18:0, 16:0/18:2, 16:1/18:2, 18:1/18:2 and 16:0/20:4 species. The values are presented as mean ± SD of at least 3 independent experiments.
(B) Quantification of the 16:0/18:2 PA specie in *yw* (control) and *PBac{WH}Ire1^{f02170}* homozygous adult eyes by LC-MS.
(C) qRT-PCR analysis of *pld*, *dgk*, *lazaro* and *cds* in *yw* (control) and *PBac{WH}Ire1^{f02170}* homozygous adult eyes. The mRNA levels are presented as mean ± SD of arbitrary units (fold change) relative to control (yw).
(D) Pld (blue) is detected at similar levels between photoreceptors of *PBac{WH}Ire1^{f02170}* clones (absence of myrGFP) and wild-type clones in pupal eye.
(E) GMR-GAL4 > UAS-lazaro rescues the delivery of Rh1 (blue) to the rhabdomere in clones of *PBac{WH}Ire1^{f02170}* homozygous ommatidia (absence of DsRed). Rhabdomeres are in green.

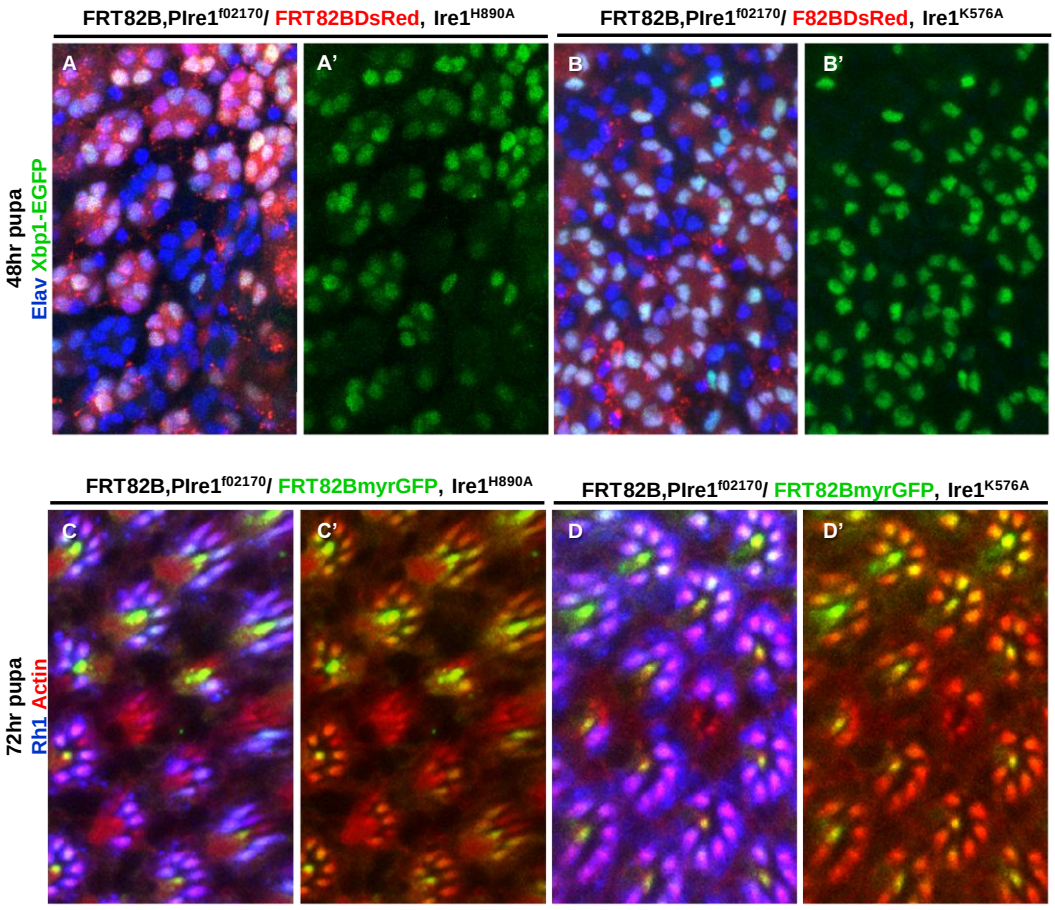

Figure 4.6 Ire1 RNase mutant (Ire1^{H890A}) and Ire1 kinase mutant (Ire1^{K576A}) fail to rescue Xbp1-EGFP expression and Rh1 localization to the rhabdomeres of PBac(WH)Ire1^{f02170} homozygous photoreceptors.

(A) Ire1^{H890A} and (B) Ire1^{K576A} fail to rescue expression of Xbp1-EGFP (green) in clones of *PBac{WH}Ire1^{f02170}* homozygous cells, labeled by the absence of DsRed. Elav is in blue.
(C) Ire1^{H890A} and (D) Ire1^{K576A} fail to rescue rhabdomeric localization of Rh1 (blue) in clones of *PBac{WH}Ire1^{f02170}* homozygous cells, labeled by the absence of myrGFP (green). Actin is in red.

Atf4 is up-regulated in *PBac{WH}Ire1^{f02170}* clones

We next investigated the role of Perk signaling and its target ATF4 during the development of the photoreceptors. ATF4 expression is up-regulated in

PBac{WH}Ire1^{f02170} mutant clones in the pupa, presumably due to a UPR compensatory mechanism (**Figure 4.7A**). Interestingly, ATF4 is not up-regulated in Excision79 (Xbp1^{exc79}) mutant clones (**Figure 4.7B**).

We down-regulated Perk and ATF4 expression by RNAi in the eye. In ATF4 RNAi mutants, the external morphology of the eye is normal and Rh1 is localizing to the rhabdomeres that show a regular arrangement and normal section (**Figure 4.7C,D**). Perk hypomorphs present a strong rough phenotype with extra-numerical cells in the eye consequence of an abnormal cell specification in the eye imaginal disc in the larva and reflecting the epistatic regulation of several cellular functions by Perk **Figure (4.7E,F**).

Discussion

Most previous studies on RIDD were performed in cultured cells, using RNAi knock-downs or knock-out lines and the real significance of RIDD at the level of the organism is still not understood. Here we showed that the poorly characterized branch of the UPR, RIDD, has a physiological role during photoreceptor differentiation in *Drosophila* using null mutants of Ire1 and Xbp1. In addition, we established a mechanism, wherein the control of Fatp expression through RIDD contributes to the regulation of the levels of phosphatidic acid, which is critical to the targeted delivery of proteins to the rhabdomere in the pupal eye. The main evidences supporting this mechanism are: a) Fatp mRNA and protein levels are elevated in Ire1 mutant *Drosophila* eyes; 2) Ire1 cleaves Fatp mRNA *in vitro*; 3) Phosphatidic acid levels are elevated in Ire1 mutant eyes; 4) Ire1 mutant Rh1 phenotype is rescued by Fatp RNAi and 5) over-expression of Lazaro, which lowers the levels of phosphatidic acid, also rescues Rh1 phenotype in Ire1 mutant photoreceptors.

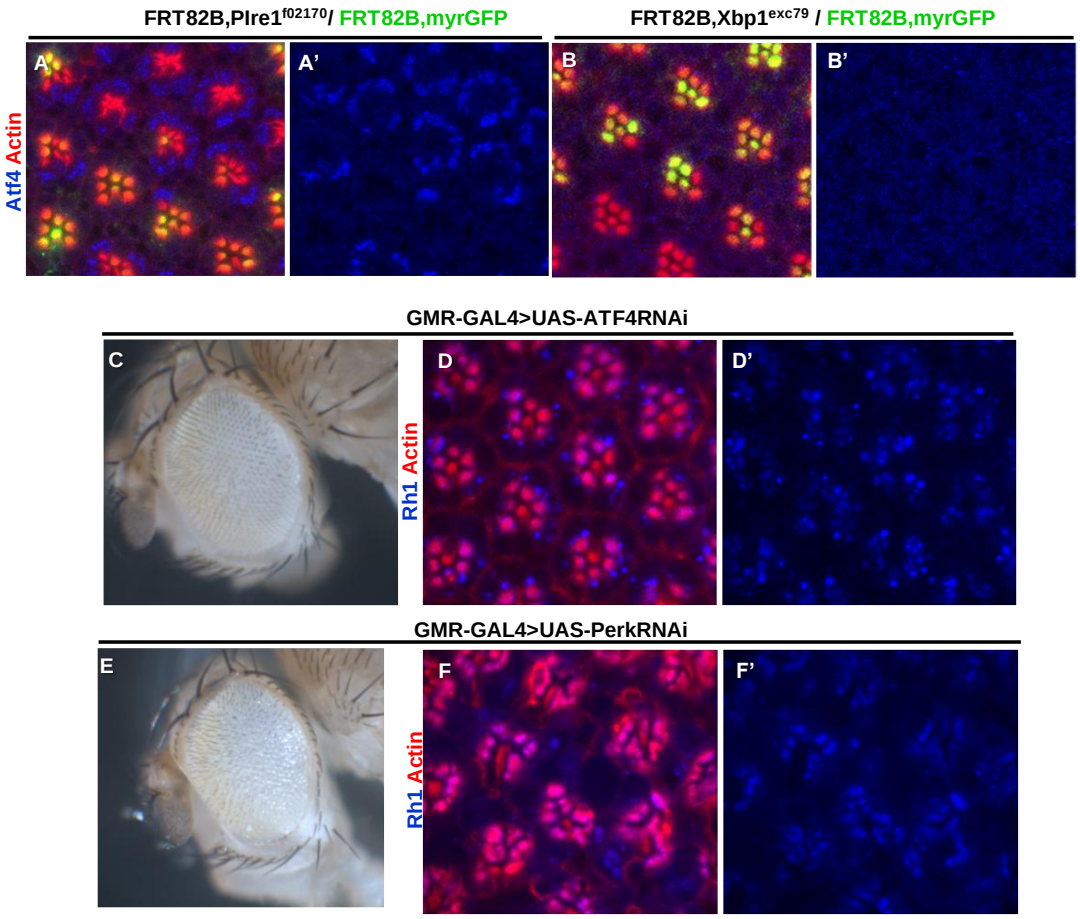

Figure 4.7 Analysis of Perk and ATF4 relevance for morphogenesis of the photoreceptors.

(A,B) ATF4 (blue) is up-regulated in (A) *PBac{WH}Ire1*^{f20170} homozygous clones but not in (B) Xbp1^{exc79} mutant homozygous clones. Mutant clones are marked by the absence of myrGFP, green. Actin is in red.
(C,D) GMR-GAL4>UAS-ATF4RNAi eye presents (C) normal external morphology and (D) normal loading of Rh1 (blue) into the rhabdomere (actin, red).
(E,F) GMR-GAL4>UAS-PERKRNAi causes (E) "rough" eye phenotype but (F) does not has a impact in the delivery of Rh1 (blue) to the rhabdomere (red).

Several RIDD targets were up-regulated in Ire1 mutant eyes and one of its targets, Fatp, has an import role in the regulation of Rh1 levels in photoreceptors. However we also observe increased levels of Fatp in the accessory cells of the lattice in Ire1 mutant eyes. We speculate if Fatp has any non cell-autonomous effect during the differentiation of photoreceptors in the pupa.

We also speculate about the general physiological contribution of RIDD for the photoreceptor differentiation. We assume that RIDD may perform two distinct roles: early reprogram of the ER repertoire or late maintenance of ER homeostasis. First role, RIDD may clear mRNAs from the translation and translocation machinery for the subsequent influx of new proteins synthesized during rhabdomere morphogenesis and induced by Xbp1spliced, for instance NinaA. Second role, RIDD may be necessary to alleviate severe ER stress in photoreceptors, resulting from the excessive load of Rh1, Spacemaker and other secretory proteins into the ER, thereafter counterbalancing Xbp1 splicing output. The rapid reduction of ER associated mRNAs by RIDD helps ensuring that proteins inside the ER can be properly folded and secreted. It would be interesting to detect the temporal activation of RIDD in the pupa.

Photoreceptors differentiation may resemble some aspects of pancreatic β-cells physiology, where Ire1 has a dual role depending on the amount/time of ER stress. In response to acute glucose stimulation, Ire1 is phosphorylated and increases insulin biosynthesis in β cells (Lipson et al., 2006; Lee et al., 2011) Conversely Ire1 degrades insulin mRNA under chronic exposure to high glucose conditions or severe ER stress (Lipson et al., 2008; Han et al., 2009). It would be interesting to analyze if proteins of the rhabdomere like Rh1 are targets of RIDD, as is the case of insulin.

Previous studies indicated Fatp to be a central regulator of Rh1 levels in the adult eye, but the mechanism was poorly understood (Dourlen et al., 2012). We discovered that Fatp is also a regulator of Rh1 levels in the pupa, taking into account that over-expression of Fatp disrupted the delivery of Rh1 to the rhabdomere. We propose that in Ire1 mutant retinas, higher expression of Fatp

increases the import of fatty acids into the cell, deregulating phosphatidic acid levels and consequently compromising secretory transport to the rhabdomere. In a yeast model of lipotoxicity induced by high cellular content of fatty acids, saturated phospholipids altered membrane properties with a directly impact on vesicular budding at later steps of the secretory pathway (trans-Golgi network) (Payet et al., 2013). These recent findings strongly corroborate our findings and establish fatty acids and phospholipids as key regulators of membrane trafficking.

In addition, in cell culture models it was shown that Perk is able to phosphorylate diacylglycerol and generate phosphatidic acid (Bobrovnikova-Marjon et al., 2012). As a matter of fact, we observed up-regulation of the Perk pathway mediator ATF4 in Ire1 mutant photoreceptors. It is possible that phosphatidic acid have another source besides up-regulation of Fatp, which relies on the branch of the UPR mediated by Perk. In conclusion, our results demonstrate the physiological relevance of Xbp1-independent mechanisms downstream of Ire1 in a developmental paradigm, photoreceptor differentiation in the *Drosophila* pupa.

Acknowledgments and author contribution

We would like to thank Bertrand Mollereau Eduardo Moreno, Padinjat Raghu, Don Ready, the Bloomington Stock Center, Pacmanfly and the Developmental Studies Hybridoma Bank for fly stocks, reagents, and antibodies. We thank Heather Harding for purified human Ire1, the 4m8C inhibitor and advice on the mRNA cleavage protocol. Fátima Cairrão did the *in vitro* cleavage assay and the qRT-PCR. Pedro M. Domingos, Elisabete Pires and Ana Varela Coelho performed the lipidomic analysis. Xiaomei Zeng and Hyung Don Ryoo obtained the Ire1 RNase and Kinase mutants.

References

Ali, M.M.U., Bagratuni, T., Davenport, E.L., Nowak, P.R., Silva-Santisteban, M.C., Hardcastle, A., McAndrews, C., Rowlands, M.G., Morgan, G.J., Aherne, W., et al. (2011). Structure of the Ire1 autophosphorylation complex and implications for the unfolded protein response. EMBO J. 30, 894–905.

Bertolotti, A., Zhang, Y., Hendershot, L.M., Harding, H.P., and Ron, D. (2000). Dynamic interaction of BiP and ER stress transducers in the unfolded-protein response. Nat. Cell Biol. 2, 326–332.

Bertolotti, A., Wang, X., Novoa, I., Jungreis, R., Schlessinger, K., Cho, J.H., West, A.B., and Ron, D. (2001). Increased sensitivity to dextran sodium sulfate colitis in IRE1beta-deficient mice. J. Clin. Invest. 107, 585–593.

Bobrovnikova-Marjon, E., Pytel, D., Riese, M.J., Vaites, L.P., Singh, N., Koretzky, G.A., Witze, E.S., and Diehl, J.A. (2012). PERK Utilizes Intrinsic Lipid Kinase Activity To Generate Phosphatidic Acid, Mediate Akt Activation, and Promote Adipocyte Differentiation. Mol. Cell. Biol. 32, 2268–2278.

Calfon, M., Zeng, H., Urano, F., Till, J.H., Hubbard, S.R., Harding, H.P., Clark, S.G., and Ron, D. (2002). IRE1 couples endoplasmic reticulum load to secretory capacity by processing the XBP-1 mRNA. Nature 415, 92–96.

Cox, J.S., and Walter, P. (1996). A novel mechanism for regulating activity of a transcription factor that controls the unfolded protein response. Cell 87, 391–404.

Cox, J.S., Shamu, C.E., and Walter, P. (1993). Transcriptional induction of genes encoding endoplasmic reticulum resident proteins requires a transmembrane protein kinase. Cell 73, 1197–1206.

Credle, J.J., Finer-Moore, J.S., Papa, F.R., Stroud, R.M., and Walter, P. (2005). On the mechanism of sensing unfolded protein in the endoplasmic reticulum. Proc. Natl. Acad. Sci. U. S. A. 102, 18773–18784.

Cross, B.C.S., Bond, P.J., Sadowski, P.G., Jha, B.K., Zak, J., Goodman, J.M., Silverman, R.H., Neubert, T.A., Baxendale, I.R., Ron, D., et al. (2012). PNAS Plus: The molecular basis for selective inhibition of unconventional mRNA splicing by an IRE1-binding small molecule. Proc. Natl. Acad. Sci. 109, E869–E878.

Dourlen, P., Bertin, B., Chatelain, G., Robin, M., Napoletano, F., Roux, M.J., and Mollereau, B. (2012). Drosophila Fatty Acid Transport Protein Regulates Rhodopsin-1 Metabolism and Is Required for Photoreceptor Neuron Survival. PLoS Genet. 8, e1002833.

Garcia-Murillas, I., Pettitt, T., Macdonald, E., Okkenhaug, H., Georgiev, P., Trivedi, D., Hassan, B., Wakelam, M., and Raghu, P. (2006). lazaro Encodes a Lipid Phosphate Phosphohydrolase that Regulates Phosphatidylinositol Turnover during Drosophila Phototransduction. Neuron 49, 533–546.

Golic, K.G. (1991). Site-specific recombination between homologous chromosomes in Drosophila. Science 252, 958–961.

Gonzalez, T.N., Sidrauski, C., Dörfler, S., and Walter, P. (1999). Mechanism of non-spliceosomal mRNA splicing in the unfolded protein response pathway. EMBO J. 18, 3119–3132.

Han, D., Lerner, A.G., Vande Walle, L., Upton, J.-P., Xu, W., Hagen, A., Backes, B.J., Oakes, S.A., and Papa, F.R. (2009). IRE1α Kinase Activation Modes Control Alternate Endoribonuclease Outputs to Determine Divergent Cell Fates. Cell 138, 562–575.

Hollien, J. (2006). Decay of Endoplasmic Reticulum-Localized mRNAs During the Unfolded Protein Response. Science 313, 104–107.

Hollien, J., Lin, J.H., Li, H., Stevens, N., Walter, P., and Weissman, J.S. (2009). Regulated Ire1-dependent decay of messenger RNAs in mammalian cells. J. Cell Biol. 186, 323–331.

Imagawa, Y., Hosoda, A., Sasaka, S.-I., Tsuru, A., and Kohno, K. (2008). RNase domains determine the functional difference between IRE1alpha and IRE1beta. FEBS Lett. 582, 656–660.

Kang, M.-J., and Ryoo, H.D. (2009). Suppression of retinal degeneration in Drosophila by stimulation of ER-associated degradation. Proc. Natl. Acad. Sci. U. S. A. 106, 17043–17048.

Kawahara, T., Yanagi, H., Yura, T., and Mori, K. (1997). Endoplasmic reticulum stress-induced mRNA splicing permits synthesis of transcription factor Hac1p/Ern4p that activates the unfolded protein response. Mol. Biol. Cell 8, 1845–1862.

Kimata, Y., Ishiwata-Kimata, Y., Ito, T., Hirata, A., Suzuki, T., Oikawa, D., Takeuchi, M., and Kohno, K. (2007). Two regulatory steps of ER-stress sensor Ire1 involving its cluster formation and interaction with unfolded proteins. J. Cell Biol. 179, 75–86.

Korennykh, A.V., Egea, P.F., Korostelev, A.A., Finer-Moore, J., Zhang, C., Shokat, K.M., Stroud, R.M., and Walter, P. (2008). The unfolded protein response signals through high-order assembly of Ire1. Nature 457, 687–693.

Korennykh, A.V., Korostelev, A.A., Egea, P.F., Finer-Moore, J., Stroud, R.M., Zhang, C., Shokat, K.M., and Walter, P. (2011). Structural and functional basis for RNA cleavage by Ire1. BMC Biol. 9, 47.

Lee, A.-H., Iwakoshi, N.N., and Glimcher, L.H. (2003). XBP-1 regulates a subset of endoplasmic reticulum resident chaperone genes in the unfolded protein response. Mol. Cell. Biol. 23, 7448–7459.

Lee, A.-H., Heidtman, K., Hotamisligil, G.S., and Glimcher, L.H. (2011). Dual and opposing roles of the unfolded protein response regulated by IRE1 and XBP1 in proinsulin processing and insulin secretion. Proc. Natl. Acad. Sci. 108, 8885–8890.

Lee, K.P.K., Dey, M., Neculai, D., Cao, C., Dever, T.E., and Sicheri, F. (2008). Structure of the Dual Enzyme Ire1 Reveals the Basis for Catalysis and Regulation in Nonconventional RNA Splicing. Cell 132, 89–100.

Li, B.X., Satoh, A.K., and Ready, D.F. (2007). Myosin V, Rab11, and dRip11 direct apical secretion and cellular morphogenesis in developing Drosophila photoreceptors. J. Cell Biol. 177, 659–669.

Li, H., Korennykh, A.V., Behrman, S.L., and Walter, P. (2010). Mammalian endoplasmic reticulum stress sensor IRE1 signals by dynamic clustering. Proc. Natl. Acad. Sci. 107, 16113–16118.

Lipson, K.L., Fonseca, S.G., Ishigaki, S., Nguyen, L.X., Foss, E., Bortell, R., Rossini, A.A., and Urano, F. (2006). Regulation of insulin biosynthesis in pancreatic beta cells by an endoplasmic reticulum-resident protein kinase IRE1. Cell Metab. 4, 245–254.

Lipson, K.L., Ghosh, R., and Urano, F. (2008). The Role of IRE1α in the Degradation of Insulin mRNA in Pancreatic β-Cells. PLoS ONE 3, e1648.

Mori, K., Ma, W., Gething, M.J., and Sambrook, J. (1993). A transmembrane protein with a cdc2+/CDC28-related kinase activity is required for signaling from the ER to the nucleus. Cell 74, 743–756.

Mori, K., Ogawa, N., Kawahara, T., Yanagi, H., and Yura, T. (2000). mRNA splicing-mediated C-terminal replacement of transcription factor Hac1p is required for efficient activation of the unfolded protein response. Proc. Natl. Acad. Sci. U. S. A. 97, 4660–4665.

Newsome, T.P., Asling, B., and Dickson, B.J. (2000). Analysis of Drosophila photoreceptor axon guidance in eye-specific mosaics. Dev. Camb. Engl. 127, 851–860.

Nishitoh, H., Matsuzawa, A., Tobiume, K., Saegusa, K., Takeda, K., Inoue, K., Hori, S., Kakizuka, A., and Ichijo, H. (2002). ASK1 is essential for endoplasmic reticulum stress-induced neuronal cell death triggered by expanded polyglutamine repeats. Genes Dev. 16, 1345–1355.

Payet, L.-A., Pineau, L., Snyder, E.C.R., Colas, J., Moussa, A., Vannier, B., Bigay, J., Clarhaut, J., Becq, F., Berjeaud, J.-M., et al. (2013). Saturated fatty acids alter the late secretory pathway by modulating membrane properties: SFA impact the late secretory pathway. Traffic.

Raghu, P., Coessens, E., Manifava, M., Georgiev, P., Pettitt, T., Wood, E., Garcia-Murillas, I., Okkenhaug, H., Trivedi, D., Zhang, Q., et al. (2009). Rhabdomere biogenesis in Drosophila photoreceptors is acutely sensitive to phosphatidic acid levels. J. Cell Biol. 185, 129–145.

Rüegsegger, U., Leber, J.H., and Walter, P. (2001). Block of HAC1 mRNA translation by long-range base pairing is released by cytoplasmic splicing upon induction of the unfolded protein response. Cell 107, 103–114.

Satoh, A.K. (2005). Rab11 mediates post-Golgi trafficking of rhodopsin to the photosensitive apical membrane of Drosophila photoreceptors. Development 132, 1487–1497.

Shamu, C.E., and Walter, P. (1996). Oligomerization and phosphorylation of the Ire1p kinase during intracellular signaling from the endoplasmic reticulum to the nucleus. EMBO J. 15, 3028–3039.

Sidrauski, C., and Walter, P. (1997). The transmembrane kinase Ire1p is a site-specific endonuclease that initiates mRNA splicing in the unfolded protein response. Cell 90, 1031–1039.

Sidrauski, C., Cox, J.S., and Walter, P. (1996). tRNA ligase is required for regulated mRNA splicing in the unfolded protein response. Cell 87, 405–413.

Sik Lee, Y. (2003). Making a better RNAi vector for Drosophila: use of intron spacers. Methods 30, 322–329.

Tirasophon, W., Welihinda, A.A., and Kaufman, R.J. (1998). A stress response pathway from the endoplasmic reticulum to the nucleus requires a novel bifunctional protein kinase/endoribonuclease (Ire1p) in mammalian cells. Genes Dev. 12, 1812–1824.

Travers, K.J., Patil, C.K., Wodicka, L., Lockhart, D.J., Weissman, J.S., and Walter, P. (2000). Functional and genomic analyses reveal an essential coordination between the unfolded protein response and ER-associated degradation. Cell 101, 249–258.

Urano, F., Wang, X., Bertolotti, A., Zhang, Y., Chung, P., Harding, H.P., and Ron, D. (2000). Coupling of stress in the ER to activation of JNK protein kinases by transmembrane protein kinase IRE1. Science 287, 664–666.

Welihinda, A.A., and Kaufman, R.J. (1996). The unfolded protein response pathway in Saccharomyces cerevisiae. Oligomerization and trans-phosphorylation of Ire1p (Ern1p) are required for kinase activation. J. Biol. Chem. 271, 18181–18187.

Yonamine, I., Bamba, T., Nirala, N.K., Jesmin, N., Kosakowska-Cholody, T., Nagashima, K., Fukusaki, E., Acharya, J.K., and Acharya, U. (2011). Sphingosine kinases and their metabolites modulate endolysosomal trafficking in photoreceptors. J. Cell Biol. 192, 557–567.

Yoshida, H., Matsui, T., Yamamoto, A., Okada, T., and Mori, K. (2001). XBP1 mRNA is induced by ATF6 and spliced by IRE1 in response to ER stress to produce a highly active transcription factor. Cell 107, 881–891.

Zhang, K., Wong, H.N., Song, B., Miller, C.N., Scheuner, D., and Kaufman, R.J. (2005). The unfolded protein response sensor IRE1alpha is required at 2 distinct steps in B cell lymphopoiesis. J. Clin. Invest. 115, 268–281.

Discussion

Chapter V

The UPR has been regarded as an emergency cellular response to the accumulation of misfolded proteins intrinsically associated with pathogenic conditions. However, the UPR activates processes as amino acid import and activation of transcription that may further challenge the folding capacity of the ER and its final outcome is not merely to combat ER stress. Instead the UPR reprograms the ER to increase the cell capacity to carry out secretion. The remodeling of the ER is achieved through the sequence in which UPR mechanisms are activated (Ron and Walter, 2007). The initial step of translation attenuation mediated by eiF2α phosphorylation helps to limit ER load and to liberate ribosomes and translation factors that can then be used to synthesize UPR-induced proteins. RIDD may also contribute to this resetting of the translational program. The UPR is essential during the differentiation and homeostasis of secretory cells and in B lymphocytes Xbp1 splicing seems to be induced as part of the developmental program (van Anken et al., 2003; Hu et al., 2009). In our study, activation of the XBP1-EGFP reporter occurs several hours before the defects of Spacemaker and Rh1 transport, suggesting that activation of the UPR anticipates the accumulation of misfolded proteins in the ER.

The UPR contributes to endomembrane homeostasis and biosynthesis of its lipidic components. Yeast UPR induces the expression of key enzymes of lipid synthesis, being essential in inositol production, a building block of phospholipids (Travers et al., 2000; Cox et al., 1997). Moreover, yeast Ire1 detects ER membrane abnormalities through an unknown mechanism, independent of its protein binding luminal domain (Promlek et al., 2011). Our findings further relate the UPR with endomembrane homeostasis and regulation of lipid metabolism. However we did not addressed how ER stress generated during the differentiation of photoreceptors is detected by Ire1, and for instance if the luminal domain of Ire1 is required to detect this stress. We think that ‘ER membrane stress’ is an interesting and new topic to be explored in the future that raises important questions.

Our work provides an example of the compensatory mechanisms between UPR pathways. The absence of Xbp1 in photoreceptors is probably compensated by other UPR branches that can activate ER chaperones and enzymes. The absence of Xbp1 has little impact on photoreceptors differentiation and we could only observe a very slight delay in the delivery of Rh1 to the rhabdomere, showing that the ER machinery is sufficient for photoreceptor differentiation in Xbp1 mutants.

The major contribution of this work is the identification of an Xbp1-independent physiological role of Ire1 during photoreceptor differentiation. We show that in the *Drosophila* eye, Ire1 signaling occurs through a mechanism independent of its canonical target Xbp1. In the recent years several studies demonstrated the activation of RIDD upon tissue specific deletion of Xbp1, which leads to over-activation of Ire1 in a feedback mechanism possibly due to exacerbated ER stress. Xbp1 liver deficiency provokes RIDD activation in mice, which contributes to a hypolipogenic phenotype with observation of reduced plasma cholesterol and triglycerides (So et al., 2012). Moreover, a comprehensive comparative microarray analysis identified 112 genes induced by Ire1α siRNA treatment in liver Xbp1-deficient mice, and the genes involved in lipid metabolism *angptl3* (angiopoietin-like protein 3), *ces1c*, *ces1d*, *ces1e*, *ces1f*, and *ces1g* were validated as RIDD substrates (So et al., 2012). Xbp1 liver specific deletion also protects against liver damage caused by the analgesic drug acetaminophen (ASAP) through RIDD degradation of Cyp1a2 and Cyp2e1 mRNAs, two P450 enzymes responsible for metabolizing the drug into an cytotoxic metabolite (Hur et al., 2012). Ire1α is also retro-activated by Xbp1 silencing in Min6 insulinoma cells and Ire1α reduces the levels of components of the insulin secretory pathway, namely PC1, PC2, and CPE enzymes, by cleaving its mRNAs (Lee et al., 2011). In this case, RIDD contributes to inefficient maturation of insulin in β-cells deficient for Xbp1.

These findings and others support the idea that RIDD is activated during severe or chronic ER stress conditions (Han et al., 2009; Hollien et al., 2009).

Along this line, RIDD may represent a broad and rapid mechanism for the cell to cope with ER stress. The model accepted at the moment suggests that chronic or severe ER stress contributes to the assembly of Ire1 oligomers, rather than dimmers, which attain a more loose conformation of the RNase active site and thus facilitate the broad degradation of mRNAs associated with the ER membrane (Han et al., 2009). It was shown that association with the ER membrane is necessary and sufficient for the degradation of RIDD targets and that Ire1 has a preference to cleave mRNAs at consensus sites similar to those flanking unconventional Xbp1 intron (Gaddam et al., 2013; Hollien and Weissman, 2006). Plasma membranes proteins are enriched among RIDD targets as expected, as they encode hydrophobic domains difficult to fold and are predict to stall during its translocation through the ER membrane. In the future, the conditions that activate preferentially RIDD to Xbp1 have to be clarified.

The pro-apoptotic program of Ire1 signaling also requires further attention in the future. The mediators are largely unknown and the switch signals that convert the Ire1 pro-survival response into a pro-apoptotic response are not understood. There is a debate about RIDD making part of this deleterious output of the UPR.

In summary we found that Ire1 mutation cause early degeneration of the retina in *Drosophila* due to severe morphological defects in the photosensitive cells, the photoreceptors, and Xbp1 mutation does not have eye phenotype but causes lethality of the organism during the second instar larval stage. Our results, demonstrate the physiological relevance of Xbp1-independent mechanisms downstream of Ire1 signaling using well-characterized genetic tools and a developmental paradigm.

References

Acosta-Alvear, D., Zhou, Y., Blais, A., Tsikitis, M., Lents, N.H., Arias, C., Lennon, C.J., Kluger, Y., and Dynlacht, B.D. (2007). XBP1 controls diverse cell type- and condition-specific transcriptional regulatory networks. Mol. Cell *27*, 53–66.

Ali, M.M.U., Bagratuni, T., Davenport, E.L., Nowak, P.R., Silva-Santisteban, M.C., Hardcastle, A., McAndrews, C., Rowlands, M.G., Morgan, G.J., Aherne, W., et al. (2011). Structure of the Ire1 autophosphorylation complex and implications for the unfolded protein response. EMBO J. *30*, 894–905.

Anfinsen, C.B., and Scheraga, H.A. (1975). Experimental and theoretical aspects of protein folding. Adv. Protein Chem. *29*, 205–300.

Van Anken, E., Romijn, E.P., Maggioni, C., Mezghrani, A., Sitia, R., Braakman, I., and Heck, A.J.R. (2003). Sequential waves of functionally related proteins are expressed when B cells prepare for antibody secretion. Immunity *18*, 243–253.

Aragón, T., van Anken, E., Pincus, D., Serafimova, I.M., Korennykh, A.V., Rubio, C.A., and Walter, P. (2009). Messenger RNA targeting to endoplasmic reticulum stress signalling sites. Nature *457*, 736–740.

Auf, G., Jabouille, A., Guérit, S., Pineau, R., Delugin, M., Bouchecareilh, M., Magnin, N., Favereaux, A., Maitre, M., Gaiser, T., et al. (2010). Inositol-requiring enzyme 1alpha is a key regulator of angiogenesis and invasion in malignant glioma. Proc. Natl. Acad. Sci. U. S. A. *107*, 15553–15558.

Bachmann, A., Schneider, M., Theilenberg, E., Grawe, F., and Knust, E. (2001). Drosophila Stardust is a partner of Crumbs in the control of epithelial cell polarity. Nature *414*, 638–643.

Bachmann, A., Grawe, F., Johnson, K., and Knust, E. (2008). Drosophila Lin-7 is a component of the Crumbs complex in epithelia and photoreceptor cells and prevents light-induced retinal degeneration. Eur. J. Cell Biol. *87*, 123–136.

Back, S.H., Scheuner, D., Han, J., Song, B., Ribick, M., Wang, J., Gildersleeve, R.D., Pennathur, S., and Kaufman, R.J. (2009). Translation attenuation through eIF2alpha phosphorylation prevents oxidative stress and maintains the differentiated state in beta cells. Cell Metab. *10*, 13–26.

Bagola, K., Mehnert, M., Jarosch, E., and Sommer, T. (2011). Protein dislocation from the ER. Biochim. Biophys. Acta *1808*, 925–936.

Bailey, D., and O'Hare, P. (2007). Transmembrane bZIP transcription factors in ER stress signaling and the unfolded protein response. Antioxid. Redox Signal. *9*, 2305–2321.

Baker, E.K., Colley, N.J., and Zuker, C.S. (1994). The cyclophilin homolog NinaA functions as a chaperone, forming a stable complex in vivo with its protein target rhodopsin. EMBO J. *13*, 4886–4895.

Bence, N.F., Sampat, R.M., and Kopito, R.R. (2001). Impairment of the ubiquitin-proteasome system by protein aggregation. Science *292*, 1552–1555.

Bernales, S., McDonald, K.L., and Walter, P. (2006). Autophagy counterbalances endoplasmic reticulum expansion during the unfolded protein response. PLoS Biol. *4*, e423.

Bernasconi, R., Pertel, T., Luban, J., and Molinari, M. (2008). A dual task for the Xbp1-responsive OS-9 variants in the mammalian endoplasmic reticulum: inhibiting secretion of misfolded protein conformers and enhancing their disposal. J. Biol. Chem. *283*, 16446–16454.

Bernasconi, R., Soldà, T., Galli, C., Pertel, T., Luban, J., and Molinari, M. (2010). Cyclosporine A-sensitive, cyclophilin B-dependent endoplasmic reticulum-associated degradation. PloS One *5*.

Beronja, S. (2005). Essential function of Drosophila Sec6 in apical exocytosis of epithelial photoreceptor cells. J. Cell Biol. *169*, 635–646.

Bertolotti, A., Zhang, Y., Hendershot, L.M., Harding, H.P., and Ron, D. (2000). Dynamic interaction of BiP and ER stress transducers in the unfolded-protein response. Nat. Cell Biol. *2*, 326–332.

Bertolotti, A., Wang, X., Novoa, I., Jungreis, R., Schlessinger, K., Cho, J.H., West, A.B., and Ron, D. (2001). Increased sensitivity to dextran sodium sulfate colitis in IRE1beta-deficient mice. J. Clin. Invest. *107*, 585–593.

Bhat, M.A., Izaddoost, S., Lu, Y., Cho, K.O., Choi, K.W., and Bellen, H.J. (1999). Discs Lost, a novel multi-PDZ domain protein, establishes and maintains epithelial polarity. Cell *96*, 833–845.

Blond-Elguindi, S., Cwirla, S.E., Dower, W.J., Lipshutz, R.J., Sprang, S.R., Sambrook, J.F., and Gething, M.J. (1993). Affinity panning of a library of peptides displayed on bacteriophages reveals the binding specificity of BiP. Cell *75*, 717–728.

Bobrovnikova-Marjon, E., Grigoriadou, C., Pytel, D., Zhang, F., Ye, J., Koumenis, C., Cavener, D., and Diehl, J.A. (2010). PERK promotes cancer cell proliferation and tumor growth by limiting oxidative DNA damage. Oncogene *29*, 3881–3895.

Brush, M.H., Weiser, D.C., and Shenolikar, S. (2003). Growth arrest and DNA damage-inducible protein GADD34 targets protein phosphatase 1 alpha to the endoplasmic reticulum and promotes dephosphorylation of the alpha subunit of eukaryotic translation initiation factor 2. Mol. Cell. Biol. *23*, 1292–1303.

Bush, K.T., Hendrickson, B.A., and Nigam, S.K. (1994). Induction of the FK506-binding protein, FKBP13, under conditions which misfold proteins in the endoplasmic reticulum. Biochem. J. *303 (Pt 3)*, 705–708.

Cagan, R.L., and Ready, D.F. (1989). The emergence of order in the Drosophila pupal retina. Dev. Biol. *136*, 346–362.

Calfon, M., Zeng, H., Urano, F., Till, J.H., Hubbard, S.R., Harding, H.P., Clark, S.G., and Ron, D. (2002). IRE1 couples endoplasmic reticulum load to secretory capacity by processing the XBP-1 mRNA. Nature *415*, 92–96.

Carvalho, P., Goder, V., and Rapoport, T.A. (2006). Distinct ubiquitin-ligase complexes define convergent pathways for the degradation of ER proteins. Cell *126*, 361–373.

Carvalho, P., Stanley, A.M., and Rapoport, T.A. (2010). Retrotranslocation of a misfolded luminal ER protein by the ubiquitin-ligase Hrd1p. Cell *143*, 579–591.

Chang, H.-Y. (2000). Rescue of Photoreceptor Degeneration in Rhodopsin-Null Drosophila Mutants by Activated Rac1. Science *290*, 1978–1980.

Chapman, R.E., and Walter, P. (1997). Translational attenuation mediated by an mRNA intron. Curr. Biol. CB *7*, 850–859.

Chevalier, M., Rhee, H., Elguindi, E.C., and Blond, S.Y. (2000). Interaction of murine BiP/GRP78 with the DnaJ homologue MTJ1. J. Biol. Chem. *275*, 19620–19627.

Christianson, J.C., Shaler, T.A., Tyler, R.E., and Kopito, R.R. (2008). OS-9 and GRP94 deliver mutant alpha1-antitrypsin to the Hrd1-SEL1L ubiquitin ligase complex for ERAD. Nat. Cell Biol. *10*, 272–282.

Chung, K.T., Shen, Y., and Hendershot, L.M. (2002). BAP, a mammalian BiP-associated protein, is a nucleotide exchange factor that regulates the ATPase activity of BiP. J. Biol. Chem. *277*, 47557–47563.

Claessen, J.H.L., Kundrat, L., and Ploegh, H.L. (2012). Protein quality control in the ER: balancing the ubiquitin checkbook. Trends Cell Biol. *22*, 22–32.

Clauss, I.M., Chu, M., Zhao, J.L., and Glimcher, L.H. (1996). The basic domain/leucine zipper protein hXBP-1 preferentially binds to and transactivates CRE-like sequences containing an ACGT core. Nucleic Acids Res. *24*, 1855–1864.

Clerc, S., Hirsch, C., Oggier, D.M., Deprez, P., Jakob, C., Sommer, T., and Aebi, M. (2009). Htm1 protein generates the N-glycan signal for glycoprotein degradation in the endoplasmic reticulum. J. Cell Biol. *184*, 159–172.

Connor, J.H., Weiser, D.C., Li, S., Hallenbeck, J.M., and Shenolikar, S. (2001). Growth arrest and DNA damage-inducible protein GADD34 assembles a novel signaling complex containing protein phosphatase 1 and inhibitor 1. Mol. Cell. Biol. *21*, 6841–6850.

Cook, T., and Desplan, C. (2001). Photoreceptor subtype specification: from flies to humans. Semin. Cell Dev. Biol. *12*, 509–518.

Cooper, G.M. (2000). The cell: a molecular approach (Washington, D.C.; Sunderland, Mass.: ASM Press ; Sinauer Associates).

Coss, M.C., Winterstein, D., Sowder, R.C., 2nd, and Simek, S.L. (1995). Molecular cloning, DNA sequence analysis, and biochemical characterization of a novel 65-kDa FK506-binding protein (FKBP65). J. Biol. Chem. *270*, 29336–29341.

Cox, J.S., and Walter, P. (1996). A novel mechanism for regulating activity of a transcription factor that controls the unfolded protein response. Cell *87*, 391–404.

Cox, J.S., Shamu, C.E., and Walter, P. (1993). Transcriptional induction of genes encoding endoplasmic reticulum resident proteins requires a transmembrane protein kinase. Cell *73*, 1197–1206.

Cox, J.S., Chapman, R.E., and Walter, P. (1997). The unfolded protein response coordinates the production of endoplasmic reticulum protein and endoplasmic reticulum membrane. Mol. Biol. Cell *8*, 1805–1814.

Credle, J.J., Finer-Moore, J.S., Papa, F.R., Stroud, R.M., and Walter, P. (2005). On the mechanism of sensing unfolded protein in the endoplasmic reticulum. Proc. Natl. Acad. Sci. U. S. A. *102*, 18773–18784.

Cunnea, P.M., Miranda-Vizuete, A., Bertoli, G., Simmen, T., Damdimopoulos, A.E., Hermann, S., Leinonen, S., Huikko, M.P., Gustafsson, J.-A., Sitia, R., et al. (2003). ERdj5, an endoplasmic reticulum (ER)-resident protein containing DnaJ and thioredoxin domains, is expressed in secretory cells or following ER stress. J. Biol. Chem. *278*, 1059–1066.

Delépine, M., Nicolino, M., Barrett, T., Golamaully, M., Lathrop, G.M., and Julier, C. (2000). EIF2AK3, encoding translation initiation factor 2-alpha kinase 3, is mutated in patients with Wolcott-Rallison syndrome. Nat. Genet. *25*, 406–409.

Denic, V., Quan, E.M., and Weissman, J.S. (2006). A luminal surveillance complex that selects misfolded glycoproteins for ER-associated degradation. Cell *126*, 349–359.

Dorner, A.J., Wasley, L.C., and Kaufman, R.J. (1990). Protein dissociation from GRP78 and secretion are blocked by depletion of cellular ATP levels. Proc. Natl. Acad. Sci. U. S. A. *87*, 7429–7432.

Ellgaard, L., and Helenius, A. (2003). Quality control in the endoplasmic reticulum. Nat. Rev. Mol. Cell Biol. *4*, 181–191.

Ferreiro, E., Resende, R., Costa, R., Oliveira, C.R., and Pereira, C.M.F. (2006). An endoplasmic-reticulum-specific apoptotic pathway is involved in prion and amyloid-beta peptides neurotoxicity. Neurobiol. Dis. *23*, 669–678.

Flynn, G.C., Pohl, J., Flocco, M.T., and Rothman, J.E. (1991). Peptide-binding specificity of the molecular chaperone BiP. Nature *353*, 726–730.

Frand, A.R., and Kaiser, C.A. (1998). The ERO1 gene of yeast is required for oxidation of protein dithiols in the endoplasmic reticulum. Mol. Cell *1*, 161–170.

Freedman, R.B. (1989). Protein disulfide isomerase: multiple roles in the modification of nascent secretory proteins. Cell *57*, 1069–1072.

Gaddam, D., Stevens, N., and Hollien, J. (2013). Comparison of mRNA localization and regulation during endoplasmic reticulum stress in Drosophila cells. Mol. Biol. Cell *24*, 14–20.

Gardner, B.M., and Walter, P. (2011). Unfolded proteins are Ire1-activating ligands that directly induce the unfolded protein response. Science *333*, 1891–1894.

Gardner, R.G., Swarbrick, G.M., Bays, N.W., Cronin, S.R., Wilhovsky, S., Seelig, L., Kim, C., and Hampton, R.Y. (2000). Endoplasmic reticulum degradation requires lumen to cytosol signaling. Transmembrane control of Hrd1p by Hrd3p. J. Cell Biol. *151*, 69–82.

Gauss, R., Sommer, T., and Jarosch, E. (2006a). The Hrd1p ligase complex forms a linchpin between ER-lumenal substrate selection and Cdc48p recruitment. EMBO J. *25*, 1827–1835.

Gauss, R., Jarosch, E., Sommer, T., and Hirsch, C. (2006b). A complex of Yos9p and the HRD ligase integrates endoplasmic reticulum quality control into the degradation machinery. Nat. Cell Biol. *8*, 849–854.

Haas, I.G., and Wabl, M. (1983). Immunoglobulin heavy chain binding protein. Nature *306*, 387–389.

Han, D., Lerner, A.G., Vande Walle, L., Upton, J.-P., Xu, W., Hagen, A., Backes, B.J., Oakes, S.A., and Papa, F.R. (2009). IRE1alpha kinase activation modes control alternate endoribonuclease outputs to determine divergent cell fates. Cell *138*, 562–575.

Hardie, R.C. (2012). Phototransduction mechanisms in Drosophila microvillar photoreceptors. Wiley Interdiscip. Rev. Membr. Transp. Signal. *1*, 162–187.

Harding, H.P., Zhang, Y., and Ron, D. (1999). Protein translation and folding are coupled by an endoplasmic-reticulum-resident kinase. Nature *397*, 271–274.

Harding, H.P., Novoa, I., Zhang, Y., Zeng, H., Wek, R., Schapira, M., and Ron, D. (2000). Regulated Translation Initiation Controls Stress-Induced Gene Expression in Mammalian Cells. Mol. Cell *6*, 1099–1108.

Harding, H.P., Zeng, H., Zhang, Y., Jungries, R., Chung, P., Plesken, H., Sabatini, D.D., and Ron, D. (2001). Diabetes mellitus and exocrine pancreatic dysfunction in perk-/- mice reveals a role for translational control in secretory cell survival. Mol. Cell *7*, 1153–1163.

Harding, H.P., Calfon, M., Urano, F., Novoa, I., and Ron, D. (2002). Transcriptional and translational control in the Mammalian unfolded protein response. Annu. Rev. Cell Dev. Biol. *18*, 575–599.

Harding, H.P., Zhang, Y., Zeng, H., Novoa, I., Lu, P.D., Calfon, M., Sadri, N., Yun, C., Popko, B., Paules, R., et al. (2003). An integrated stress response regulates amino acid metabolism and resistance to oxidative stress. Mol. Cell *11*, 619–633.

Haze, K., Yoshida, H., Yanagi, H., Yura, T., and Mori, K. (1999). Mammalian transcription factor ATF6 is synthesized as a transmembrane protein and activated by proteolysis in response to endoplasmic reticulum stress. Mol. Biol. Cell *10*, 3787–3799.

Helenius, A. (1994). How N-linked oligosaccharides affect glycoprotein folding in the endoplasmic reticulum. Mol. Biol. Cell *5*, 253–265.

Hetz, C. (2012). The unfolded protein response: controlling cell fate decisions under ER stress and beyond. Nat. Rev. Mol. Cell Biol. *13*, 89–102.

Hetz, C., and Glimcher, L.H. (2009). Fine-tuning of the unfolded protein response: Assembling the IRE1alpha interactome. Mol. Cell *35*, 551–561.

Hetz, C., Thielen, P., Matus, S., Nassif, M., Court, F., Kiffin, R., Martinez, G., Cuervo, A.M., Brown, R.H., and Glimcher, L.H. (2009). XBP-1 deficiency in the nervous system protects against amyotrophic lateral sclerosis by increasing autophagy. Genes Dev. *23*, 2294–2306.

Hirsch, C., Blom, D., and Ploegh, H.L. (2003). A role for N-glycanase in the cytosolic turnover of glycoproteins. EMBO J. *22*, 1036–1046.

Hollien, J. (2013). Evolution of the unfolded protein response. Biochim. Biophys. Acta *1833*, 2458–2463.

Hollien, J., and Weissman, J.S. (2006). Decay of endoplasmic reticulum-localized mRNAs during the unfolded protein response. Science *313*, 104–107.

Hollien, J., Lin, J.H., Li, H., Stevens, N., Walter, P., and Weissman, J.S. (2009). Regulated Ire1-dependent decay of messenger RNAs in mammalian cells. J. Cell Biol. *186*, 323–331.

Hong, M. (2004). Underglycosylation of ATF6 as a Novel Sensing Mechanism for Activation of the Unfolded Protein Response. J. Biol. Chem. *279*, 11354–11363.

Hong, Y., Ackerman, L., Jan, L.Y., and Jan, Y.-N. (2003). Distinct roles of Bazooka and Stardust in the specification of Drosophila photoreceptor membrane architecture. Proc. Natl. Acad. Sci. U. S. A. *100*, 12712–12717.

Hosokawa, N., Kamiya, Y., Kamiya, D., Kato, K., and Nagata, K. (2009). Human OS-9, a lectin required for glycoprotein endoplasmic reticulum-associated degradation, recognizes mannose-trimmed N-glycans. J. Biol. Chem. *284*, 17061–17068.

Hu, C.-C.A., Dougan, S.K., McGehee, A.M., Love, J.C., and Ploegh, H.L. (2009). XBP-1 regulates signal transduction, transcription factors and bone marrow colonization in B cells. EMBO J. *28*, 1624–1636.

Hu, P., Han, Z., Couvillon, A.D., Kaufman, R.J., and Exton, J.H. (2006). Autocrine tumor necrosis factor alpha links endoplasmic reticulum stress to the membrane death receptor pathway through IRE1alpha-mediated NF-kappaB activation and down-regulation of TRAF2 expression. Mol. Cell. Biol. *26*, 3071–3084.

Hubbard, S.C., and Ivatt, R.J. (1981). Synthesis and processing of asparagine-linked oligosaccharides. Annu. Rev. Biochem. *50*, 555–583.

Van Huizen, R. (2003). P58IPK, a Novel Endoplasmic Reticulum Stress-inducible Protein and Potential Negative Regulator of eIF2alpha Signaling. J. Biol. Chem. *278*, 15558–15564.

Hur, K.Y., So, J.-S., Ruda, V., Frank-Kamenetsky, M., Fitzgerald, K., Koteliansky, V., Iwawaki, T., Glimcher, L.H., and Lee, A.-H. (2012). IRE1α activation protects mice against acetaminophen-induced hepatotoxicity. J. Exp. Med. *209*, 307–318.

Husain, N., Pellikka, M., Hong, H., Klimentova, T., Choe, K.-M., Clandinin, T.R., and Tepass, U. (2006). The Agrin/Perlecan-Related Protein Eyes Shut Is Essential for Epithelial Lumen Formation in the Drosophila Retina. Dev. Cell *11*, 483–493.

Iwakoshi, N.N., Lee, A.-H., Vallabhajosyula, P., Otipoby, K.L., Rajewsky, K., and Glimcher, L.H. (2003). Plasma cell differentiation and the unfolded protein response intersect at the transcription factor XBP-1. Nat. Immunol. *4*, 321–329.

Iwawaki, T., Akai, R., and Kohno, K. (2010). IRE1α disruption causes histological abnormality of exocrine tissues, increase of blood glucose level, and decrease of serum immunoglobulin level. PloS One *5*, e13052.

Izaddoost, S., Nam, S.-C., Bhat, M.A., Bellen, H.J., and Choi, K.-W. (2002). Drosophila Crumbs is a positional cue in photoreceptor adherens junctions and rhabdomeres. Nature *416*, 178–183.

Jiang, H.-Y., Wek, S.A., McGrath, B.C., Lu, D., Hai, T., Harding, H.P., Wang, X., Ron, D., Cavener, D.R., and Wek, R.C. (2004). Activating Transcription Factor 3 Is Integral to the Eukaryotic Initiation Factor 2 Kinase Stress Response. Mol. Cell. Biol. *24*, 1365–1377.

Johnson, K., Grawe, F., Grzeschik, N., and Knust, E. (2002). Drosophila crumbs is required to inhibit light-induced photoreceptor degeneration. Curr. Biol. CB *12*, 1675–1680.

Jousse, C., Oyadomari, S., Novoa, I., Lu, P., Zhang, Y., Harding, H.P., and Ron, D. (2003). Inhibition of a constitutive translation initiation factor 2alpha phosphatase, CReP, promotes survival of stressed cells. J. Cell Biol. *163*, 767–775.

Kadowaki, H., Nishitoh, H., Urano, F., Sadamitsu, C., Matsuzawa, A., Takeda, K., Masutani, H., Yodoi, J., Urano, Y., Nagano, T., et al. (2005). Amyloid beta induces neuronal cell death through ROS-mediated ASK1 activation. Cell Death Differ. *12*, 19–24.

Kalies, K.-U., Allan, S., Sergeyenko, T., Kröger, H., and Römisch, K. (2005). The protein translocation channel binds proteasomes to the endoplasmic reticulum membrane. EMBO J. *24*, 2284–2293.

Kaser, A., Lee, A.-H., Franke, A., Glickman, J.N., Zeissig, S., Tilg, H., Nieuwenhuis, E.E.S., Higgins, D.E., Schreiber, S., Glimcher, L.H., et al. (2008). XBP1 links ER stress to intestinal inflammation and confers genetic risk for human inflammatory bowel disease. Cell *134*, 743–756.

Katz, B. (2009). Drosophila Photoreceptors and Signaling Mechanisms. Front. Cell. Neurosci. *3*.

Kimata, Y., Kimata, Y.I., Shimizu, Y., Abe, H., Farcasanu, I.C., Takeuchi, M., Rose, M.D., and Kohno, K. (2003). Genetic evidence for a role of BiP/Kar2 that regulates Ire1 in response to accumulation of unfolded proteins. Mol. Biol. Cell *14*, 2559–2569.

Kimata, Y., Ishiwata-Kimata, Y., Ito, T., Hirata, A., Suzuki, T., Oikawa, D., Takeuchi, M., and Kohno, K. (2007). Two regulatory steps of ER-stress sensor Ire1 involving its cluster formation and interaction with unfolded proteins. J. Cell Biol. *179*, 75–86.

Kimmig, P., Diaz, M., Zheng, J., Williams, C.C., Lang, A., Aragón, T., Li, H., and Walter, P. (2012). The unfolded protein response in fission yeast modulates stability of select mRNAs to maintain protein homeostasis. eLife *1*, e00048.

Kirschfeld, K. (1967). [The projection of the optical environment on the screen of the rhabdomere in the compound eye of the Musca]. Exp. Brain Res. Exp. Hirnforsch. Expérimentation Cérébrale *3*, 248–270.

Kirschfeld, K. (1973). [Neural superposition eye]. Fortschr. Zool. *21*, 229–257.

Kirschfeld, K., and Snyder, A.W. (1976). Measurement of a photoreceptor's characteristic waveguide parameter. Vision Res. *16*, 775–778.

Kock, I., Bulgakova, N.A., Knust, E., Sinning, I., and Panneels, V. (2009). Targeting of Drosophila rhodopsin requires helix 8 but not the distal C-terminus. PloS One *4*, e6101.

Koizumi, N., Martinez, I.M., Kimata, Y., Kohno, K., Sano, H., and Chrispeels, M.J. (2001). Molecular characterization of two Arabidopsis Ire1 homologs, endoplasmic reticulum-located transmembrane protein kinases. Plant Physiol. *127*, 949–962.

Kokame, K. (2000). Identification of ERSE-II, a New cis-Acting Element Responsible for the ATF6-dependent Mammalian Unfolded Protein Response. J. Biol. Chem. *276*, 9199–9205.

Korennykh, A., and Walter, P. (2012). Structural basis of the unfolded protein response. Annu. Rev. Cell Dev. Biol. *28*, 251–277.

Korennykh, A.V., Egea, P.F., Korostelev, A.A., Finer-Moore, J., Zhang, C., Shokat, K.M., Stroud, R.M., and Walter, P. (2009). The unfolded protein response signals through high-order assembly of Ire1. Nature *457*, 687–693.

Korennykh, A.V., Korostelev, A.A., Egea, P.F., Finer-Moore, J., Stroud, R.M., Zhang, C., Shokat, K.M., and Walter, P. (2011a). Structural and functional basis for RNA cleavage by Ire1. BMC Biol. *9*, 47.

Korennykh, A.V., Egea, P.F., Korostelev, A.A., Finer-Moore, J., Stroud, R.M., Zhang, C., Shokat, K.M., and Walter, P. (2011b). Cofactor-mediated conformational control in the bifunctional kinase/RNase Ire1. BMC Biol. *9*, 48.

Kornfeld, R., and Kornfeld, S. (1985). Assembly of asparagine-linked oligosaccharides. Annu. Rev. Biochem. *54*, 631–664.

Kumar, J.P., and Ready, D.F. (1995). Rhodopsin plays an essential structural role in Drosophila photoreceptor development. Dev. Camb. Engl. *121*, 4359–4370.

Kumar, J.P., Bowman, J., O'Tousa, J.E., and Ready, D.F. (1997). Rhodopsin replacement rescues photoreceptor structure during a critical developmental window. Dev. Biol. *188*, 43–47.

Land, M.F., and Fernald, R.D. (1992). The evolution of eyes. Annu. Rev. Neurosci. *15*, 1–29.

Laprise, P., Beronja, S., Silva-Gagliardi, N.F., Pellikka, M., Jensen, A.M., McGlade, C.J., and Tepass, U. (2006). The FERM protein Yurt is a negative regulatory component of the Crumbs complex that controls epithelial polarity and apical membrane size. Dev. Cell *11*, 363–374.

Lee, A.-H., Iwakoshi, N.N., and Glimcher, L.H. (2003). XBP-1 regulates a subset of endoplasmic reticulum resident chaperone genes in the unfolded protein response. Mol. Cell. Biol. *23*, 7448–7459.

Lee, A.-H., Chu, G.C., Iwakoshi, N.N., and Glimcher, L.H. (2005). XBP-1 is required for biogenesis of cellular secretory machinery of exocrine glands. EMBO J. *24*, 4368–4380.

Lee, A.-H., Scapa, E.F., Cohen, D.E., and Glimcher, L.H. (2008a). Regulation of hepatic lipogenesis by the transcription factor XBP1. Science *320*, 1492–1496.

Lee, A.-H., Heidtman, K., Hotamisligil, G.S., and Glimcher, L.H. (2011). Dual and opposing roles of the unfolded protein response regulated by IRE1 and XBP1 in proinsulin processing and insulin secretion. Proc. Natl. Acad. Sci. *108*, 8885–8890.

Lee, A.S., Bell, J., and Ting, J. (1984). Biochemical characterization of the 94- and 78-kilodalton glucose-regulated proteins in hamster fibroblasts. J. Biol. Chem. *259*, 4616–4621.

Lee, K.P.K., Dey, M., Neculai, D., Cao, C., Dever, T.E., and Sicheri, F. (2008b). Structure of the dual enzyme Ire1 reveals the basis for catalysis and regulation in nonconventional RNA splicing. Cell *132*, 89–100.

Leonard, D.S., Bowman, V.D., Ready, D.F., and Pak, W.L. (1992). Degeneration of photoreceptors in rhodopsin mutants of Drosophila. J. Neurobiol. *23*, 605–626.

Li, B.X., Satoh, A.K., and Ready, D.F. (2007). Myosin V, Rab11, and dRip11 direct apical secretion and cellular morphogenesis in developing Drosophila photoreceptors. J. Cell Biol. *177*, 659–669.

Li, H., Korennykh, A.V., Behrman, S.L., and Walter, P. (2010). Mammalian endoplasmic reticulum stress sensor IRE1 signals by dynamic clustering. Proc. Natl. Acad. Sci. U. S. A. *107*, 16113–16118.

Lin, J.H., Walter, P., and Yen, T.S.B. (2008). Endoplasmic Reticulum Stress in Disease Pathogenesis. Annu. Rev. Pathol. Mech. Dis. *3*, 399–425.

Lipson, K.L., Fonseca, S.G., Ishigaki, S., Nguyen, L.X., Foss, E., Bortell, R., Rossini, A.A., and Urano, F. (2006). Regulation of insulin biosynthesis in pancreatic beta cells by an endoplasmic reticulum-resident protein kinase IRE1. Cell Metab. *4*, 245–254.

Lipson, K.L., Ghosh, R., and Urano, F. (2008). The Role of IRE1α in the Degradation of Insulin mRNA in Pancreatic β-Cells. PLoS ONE *3*, e1648.

Liu, C.Y., Schröder, M., and Kaufman, R.J. (2000). Ligand-independent dimerization activates the stress response kinases IRE1 and PERK in the lumen of the endoplasmic reticulum. J. Biol. Chem. *275*, 24881–24885.

Liu, C.Y., Wong, H.N., Schauerte, J.A., and Kaufman, R.J. (2002). The protein kinase/endoribonuclease IRE1alpha that signals the unfolded protein response has a luminal N-terminal ligand-independent dimerization domain. J. Biol. Chem. *277*, 18346–18356.

Lu, P.D., Harding, H.P., and Ron, D. (2004). Translation reinitiation at alternative open reading frames regulates gene expression in an integrated stress response. J. Cell Biol. *167*, 27–33.

Lütcke, H. (1995). Signal recognition particle (SRP), a ubiquitous initiator of protein translocation. Eur. J. Biochem. FEBS *228*, 531–550.

Ma, Y., and Hendershot, L.M. (2003). Delineation of a negative feedback regulatory loop that controls protein translation during endoplasmic reticulum stress. J. Biol. Chem. *278*, 34864–34873.

Ma, Y., and Hendershot, L.M. (2004). The role of the unfolded protein response in tumour development: friend or foe? Nat. Rev. Cancer *4*, 966–977.

Ma, K., Vattem, K.M., and Wek, R.C. (2002a). Dimerization and release of molecular chaperone inhibition facilitate activation of eukaryotic initiation factor-2 kinase in response to endoplasmic reticulum stress. J. Biol. Chem. *277*, 18728–18735.

Ma, Y., Brewer, J.W., Alan Diehl, J., and Hendershot, L.M. (2002b). Two Distinct Stress Signaling Pathways Converge Upon the CHOP Promoter During the Mammalian Unfolded Protein Response. J. Mol. Biol. *318*, 1351–1365.

Malhotra, J.D., and Kaufman, R.J. (2007). The endoplasmic reticulum and the unfolded protein response. Semin. Cell Dev. Biol. *18*, 716–731.

Mauro, C., Crescenzi, E., De Mattia, R., Pacifico, F., Mellone, S., Salzano, S., de Luca, C., D'Adamio, L., Palumbo, G., Formisano, S., et al. (2006). Central role of the scaffold protein tumor necrosis factor receptor-associated factor 2 in regulating endoplasmic reticulum stress-induced apoptosis. J. Biol. Chem. *281*, 2631–2638.

Molinari, M., Calanca, V., Galli, C., Lucca, P., and Paganetti, P. (2003). Role of EDEM in the release of misfolded glycoproteins from the calnexin cycle. Science *299*, 1397–1400.

Mollereau, B., and Domingos, P.M. (2005). Photoreceptor differentiation in Drosophila: from immature neurons to functional photoreceptors. Dev. Dyn. Off. Publ. Am. Assoc. Anat. *232*, 585–592.

Montell, C. (2012). Drosophila visual transduction. Trends Neurosci. *35*, 356–363.

Moore, K.A., and Hollien, J. (2012). The unfolded protein response in secretory cell function. Annu. Rev. Genet. *46*, 165–183.

Moore, K.A., Plant, J.J., Gaddam, D., Craft, J., and Hollien, J. (2013). Regulation of Sumo mRNA during Endoplasmic Reticulum Stress. PLoS ONE *8*, e75723.

Mori, K., Sant, A., Kohno, K., Normington, K., Gething, M.J., and Sambrook, J.F. (1992). A 22 bp cis-acting element is necessary and sufficient for the induction of the yeast KAR2 (BiP) gene by unfolded proteins. EMBO J. *11*, 2583–2593.

Mori, K., Ma, W., Gething, M.J., and Sambrook, J. (1993). A transmembrane protein with a cdc2+/CDC28-related kinase activity is required for signaling from the ER to the nucleus. Cell *74*, 743–756.

Mori, K., Kawahara, T., Yoshida, H., Yanagi, H., and Yura, T. (1996). Signalling from endoplasmic reticulum to nucleus: transcription factor with a basic-leucine zipper motif is

required for the unfolded protein-response pathway. Genes Cells Devoted Mol. Cell. Mech. *1*, 803–817.

Mori, K., Ogawa, N., Kawahara, T., Yanagi, H., and Yura, T. (1998). Palindrome with spacer of one nucleotide is characteristic of the cis-acting unfolded protein response element in Saccharomyces cerevisiae. J. Biol. Chem. *273*, 9912–9920.

Moses, K. (2006). Evolutionary biology: fly eyes get the whole picture. Nature *443*, 638–639.

Munro, S., and Pelham, H.R. (1986). An Hsp70-like protein in the ER: identity with the 78 kd glucose-regulated protein and immunoglobulin heavy chain binding protein. Cell *46*, 291–300.

Nadanaka, S., Okada, T., Yoshida, H., and Mori, K. (2007). Role of disulfide bridges formed in the luminal domain of ATF6 in sensing endoplasmic reticulum stress. Mol. Cell. Biol. *27*, 1027–1043.

Nagai, A., Kadowaki, H., Maruyama, T., Takeda, K., Nishitoh, H., and Ichijo, H. (2009). USP14 inhibits ER-associated degradation via interaction with IRE1alpha. Biochem. Biophys. Res. Commun. *379*, 995–1000.

Nedelsky, N.B., Todd, P.K., and Taylor, J.P. (2008). Autophagy and the ubiquitin-proteasome system: collaborators in neuroprotection. Biochim. Biophys. Acta *1782*, 691–699.

Nekrutenko, A., and He, J. (2006). Functionality of unspliced XBP1 is required to explain evolution of overlapping reading frames. Trends Genet. TIG *22*, 645–648.

Ng, D.T., Brown, J.D., and Walter, P. (1996). Signal sequences specify the targeting route to the endoplasmic reticulum membrane. J. Cell Biol. *134*, 269–278.

Ng, W., Sergeyenko, T., Zeng, N., Brown, J.D., and Römisch, K. (2007). Characterization of the proteasome interaction with the Sec61 channel in the endoplasmic reticulum. J. Cell Sci. *120*, 682–691.

Nikawa, J., Akiyoshi, M., Hirata, S., and Fukuda, T. (1996). Saccharomyces cerevisiae IRE2/HAC1 is involved in IRE1-mediated KAR2 expression. Nucleic Acids Res. *24*, 4222–4226.

Nishitoh, H., Matsuzawa, A., Tobiume, K., Saegusa, K., Takeda, K., Inoue, K., Hori, S., Kakizuka, A., and Ichijo, H. (2002). ASK1 is essential for endoplasmic reticulum stress-induced neuronal cell death triggered by expanded polyglutamine repeats. Genes Dev. *16*, 1345–1355.

Niwa, M., Patil, C.K., DeRisi, J., and Walter, P. (2005). Genome-scale approaches for discovering novel nonconventional splicing substrates of the Ire1 nuclease. Genome Biol. *6*, R3.

Novoa, I., Zeng, H., Harding, H.P., and Ron, D. (2001). Feedback inhibition of the unfolded protein response by GADD34-mediated dephosphorylation of eIF2alpha. J. Cell Biol. *153*, 1011–1022.

Novoa, I., Zhang, Y., Zeng, H., Jungreis, R., Harding, H.P., and Ron, D. (2003). Stress-induced gene expression requires programmed recovery from translational repression. EMBO J. *22*, 1180–1187.

Oda, Y., Hosokawa, N., Wada, I., and Nagata, K. (2003). EDEM as an acceptor of terminally misfolded glycoproteins released from calnexin. Science *299*, 1394–1397.

Ogata, M., Hino, S., Saito, A., Morikawa, K., Kondo, S., Kanemoto, S., Murakami, T., Taniguchi, M., Tanii, I., Yoshinaga, K., et al. (2006). Autophagy is activated for cell survival after endoplasmic reticulum stress. Mol. Cell. Biol. *26*, 9220–9231.

Oikawa, D., Kimata, Y., Kohno, K., and Iwawaki, T. (2009). Activation of mammalian IRE1alpha upon ER stress depends on dissociation of BiP rather than on direct interaction with unfolded proteins. Exp. Cell Res. *315*, 2496–2504.

Oikawa, D., Tokuda, M., Hosoda, A., and Iwawaki, T. (2010). Identification of a consensus element recognized and cleaved by IRE1. Nucleic Acids Res. *38*, 6265–6273.

Okamura, K., Kimata, Y., Higashio, H., Tsuru, A., and Kohno, K. (2000). Dissociation of Kar2p/BiP from an ER sensory molecule, Ire1p, triggers the unfolded protein response in yeast. Biochem. Biophys. Res. Commun. *279*, 445–450.

Okuda-Shimizu, Y., and Hendershot, L.M. (2007). Characterization of an ERAD pathway for nonglycosylated BiP substrates, which require Herp. Mol. Cell *28*, 544–554.

Omori, Y., and Malicki, J. (2006). oko meduzy and related crumbs genes are determinants of apical cell features in the vertebrate embryo. Curr. Biol. CB *16*, 945–957.

Ozcan, U., Cao, Q., Yilmaz, E., Lee, A.-H., Iwakoshi, N.N., Ozdelen, E., Tuncman, G., Görgün, C., Glimcher, L.H., and Hotamisligil, G.S. (2004). Endoplasmic reticulum stress links obesity, insulin action, and type 2 diabetes. Science *306*, 457–461.

Ozcan, U., Yilmaz, E., Ozcan, L., Furuhashi, M., Vaillancourt, E., Smith, R.O., Görgün, C.Z., and Hotamisligil, G.S. (2006). Chemical chaperones reduce ER stress and restore glucose homeostasis in a mouse model of type 2 diabetes. Science *313*, 1137–1140.

Papa, F.R., Zhang, C., Shokat, K., and Walter, P. (2003). Bypassing a kinase activity with an ATP-competitive drug. Science *302*, 1533–1537.

Pattingre, S., Bauvy, C., Carpentier, S., Levade, T., Levine, B., and Codogno, P. (2009). Role of JNK1-dependent Bcl-2 phosphorylation in ceramide-induced macroautophagy. J. Biol. Chem. *284*, 2719–2728.

Paulsen, R., and Schwemer, J. (1979). Vitamin A deficiency reduces the concentration of visual pigment protein within blowfly photoreceptor membranes. Biochim. Biophys. Acta *557*, 385–390.

Pellikka, M., Tanentzapf, G., Pinto, M., Smith, C., McGlade, C.J., Ready, D.F., and Tepass, U. (2002). Crumbs, the Drosophila homologue of human CRB1/RP12, is essential for photoreceptor morphogenesis. Nature *416*, 143–149.

Pichaud, F., and Desplan, C. (2002). A new view oh photoreceptors. Nature *416*, 139–140.

Pinal, N., and Pichaud, F. (2011). Dynamin- and Rab5-dependent endocytosis is required to prevent Drosophila photoreceptor degeneration. J. Cell Sci. *124*, 1564–1570.

Pinal, N., Goberdhan, D.C.I., Collinson, L., Fujita, Y., Cox, I.M., Wilson, C., and Pichaud, F. (2006). Regulated and Polarized PtdIns(3,4,5)P3 Accumulation Is Essential for Apical Membrane Morphogenesis in Photoreceptor Epithelial Cells. Curr. Biol. *16*, 140–149.

Price, E.R., Zydowsky, L.D., Jin, M.J., Baker, C.H., McKeon, F.D., and Walsh, C.T. (1991). Human cyclophilin B: a second cyclophilin gene encodes a peptidyl-prolyl isomerase with a signal sequence. Proc. Natl. Acad. Sci. U. S. A. *88*, 1903–1907.

Promlek, T., Ishiwata-Kimata, Y., Shido, M., Sakuramoto, M., Kohno, K., and Kimata, Y. (2011). Membrane aberrancy and unfolded proteins activate the endoplasmic reticulum stress sensor Ire1 in different ways. Mol. Biol. Cell *22*, 3520–3532.

Quan, E.M., Kamiya, Y., Kamiya, D., Denic, V., Weibezahn, J., Kato, K., and Weissman, J.S. (2008). Defining the glycan destruction signal for endoplasmic reticulum-associated degradation. Mol. Cell *32*, 870–877.

Raghu, P., Coessens, E., Manifava, M., Georgiev, P., Pettitt, T., Wood, E., Garcia-Murillas, I., Okkenhaug, H., Trivedi, D., Zhang, Q., et al. (2009). Rhabdomere biogenesis in Drosophila photoreceptors is acutely sensitive to phosphatidic acid levels. J. Cell Biol. *185*, 129–145.

Rasheva, V.I., and Domingos, P.M. (2009). Cellular responses to endoplasmic reticulum stress and apoptosis. Apoptosis *14*, 996–1007.

Ready, D.F., Hanson, T.E., and Benzer, S. (1976). Development of the Drosophila retina, a neurocrystalline lattice. Dev. Biol. *53*, 217–240.

Reimold, A.M., Etkin, A., Clauss, I., Perkins, A., Friend, D.S., Zhang, J., Horton, H.F., Scott, A., Orkin, S.H., Byrne, M.C., et al. (2000). An essential role in liver development for transcription factor XBP-1. Genes Dev. *14*, 152–157.

Reimold, A.M., Iwakoshi, N.N., Manis, J., Vallabhajosyula, P., Szomolanyi-Tsuda, E., Gravallese, E.M., Friend, D., Grusby, M.J., Alt, F., and Glimcher, L.H. (2001). Plasma cell differentiation requires the transcription factor XBP-1. Nature *412*, 300–307.

Riemer, J., Appenzeller-Herzog, C., Johansson, L., Bodenmiller, B., Hartmann-Petersen, R., and Ellgaard, L. (2009). A luminal flavoprotein in endoplasmic reticulum-associated degradation. Proc. Natl. Acad. Sci. U. S. A. *106*, 14831–14836.

Robson, A., and Collinson, I. (2006). The structure of the Sec complex and the problem of protein translocation. EMBO Rep. *7*, 1099–1103.

Romero-Ramirez, L., Cao, H., Nelson, D., Hammond, E., Lee, A.-H., Yoshida, H., Mori, K., Glimcher, L.H., Denko, N.C., Giaccia, A.J., et al. (2004). XBP1 is essential for survival under hypoxic conditions and is required for tumor growth. Cancer Res. *64*, 5943–5947.

Ron, D., and Walter, P. (2007a). Signal integration in the endoplasmic reticulum unfolded protein response. Nat. Rev. Mol. Cell Biol. *8*, 519–529.

Rosenbaum, E.E., Hardie, R.C., and Colley, N.J. (2006). Calnexin is essential for rhodopsin maturation, Ca2+ regulation, and photoreceptor cell survival. Neuron *49*, 229–241.

Rubio, C., Pincus, D., Korennykh, A., Schuck, S., El-Samad, H., and Walter, P. (2011). Homeostatic adaptation to endoplasmic reticulum stress depends on Ire1 kinase activity. J. Cell Biol. *193*, 171–184.

Ruddock, L.W., and Molinari, M. (2006). N-glycan processing in ER quality control. J. Cell Sci. *119*, 4373–4380.

Rüegsegger, U., Leber, J.H., and Walter, P. (2001). Block of HAC1 mRNA translation by long-range base pairing is released by cytoplasmic splicing upon induction of the unfolded protein response. Cell *107*, 103–114.

Rutkowski, D.T., Wu, J., Back, S.-H., Callaghan, M.U., Ferris, S.P., Iqbal, J., Clark, R., Miao, H., Hassler, J.R., Fornek, J., et al. (2008). UPR pathways combine to prevent hepatic steatosis caused by ER stress-mediated suppression of transcriptional master regulators. Dev. Cell *15*, 829–840.

Ryoo, H.D., Domingos, P.M., Kang, M.-J., and Steller, H. (2007). Unfolded protein response in a Drosophila model for retinal degeneration. EMBO J. *26*, 242–252.

Salvini-Plawen, L.V., and Mayr, E. (1977). On the evolution of photoreceptors and eyes. Evol. Biol. 207–263.

Satoh, A.K. (2005). Rab11 mediates post-Golgi trafficking of rhodopsin to the photosensitive apical membrane of Drosophila photoreceptors. Development *132*, 1487–1497.

Scheuner, D., Song, B., McEwen, E., Liu, C., Laybutt, R., Gillespie, P., Saunders, T., Bonner-Weir, S., and Kaufman, R.J. (2001). Translational control is required for the unfolded protein response and in vivo glucose homeostasis. Mol. Cell *7*, 1165–1176.

Scheuner, D., Vander Mierde, D., Song, B., Flamez, D., Creemers, J.W.M., Tsukamoto, K., Ribick, M., Schuit, F.C., and Kaufman, R.J. (2005). Control of mRNA translation preserves endoplasmic reticulum function in beta cells and maintains glucose homeostasis. Nat. Med. *11*, 757–764.

Schlenstedt, G., Harris, S., Risse, B., Lill, R., and Silver, P.A. (1995). A yeast DnaJ homologue, Scj1p, can function in the endoplasmic reticulum with BiP/Kar2p via a conserved domain that specifies interactions with Hsp70s. J. Cell Biol. *129*, 979–988.

Shaffer, A.L., Shapiro-Shelef, M., Iwakoshi, N.N., Lee, A.-H., Qian, S.-B., Zhao, H., Yu, X., Yang, L., Tan, B.K., Rosenwald, A., et al. (2004). XBP1, downstream of Blimp-1, expands the secretory apparatus and other organelles, and increases protein synthesis in plasma cell differentiation. Immunity *21*, 81–93.

Shamu, C.E., and Walter, P. (1996). Oligomerization and phosphorylation of the Ire1p kinase during intracellular signaling from the endoplasmic reticulum to the nucleus. EMBO J. *15*, 3028–3039.

Shen, J., Chen, X., Hendershot, L., and Prywes, R. (2002). ER stress regulation of ATF6 localization by dissociation of BiP/GRP78 binding and unmasking of Golgi localization signals. Dev. Cell *3*, 99–111.

Shen, X., Ellis, R.E., Lee, K., Liu, C.Y., Yang, K., Solomon, A., Yoshida, H., Morimoto, R., Kurnit, D.M., Mori, K., et al. (2001). Complementary signaling pathways regulate the unfolded protein response and are required for C. elegans development. Cell *107*, 893–903.

Shoulders, M.D., Ryno, L.M., Genereux, J.C., Moresco, J.J., Tu, P.G., Wu, C., Yates, J.R., 3rd, Su, A.I., Kelly, J.W., and Wiseman, R.L. (2013). Stress-independent activation of XBP1s and/or ATF6 reveals three functionally diverse ER proteostasis environments. Cell Rep. *3*, 1279–1292.

Sidrauski, C., and Walter, P. (1997). The transmembrane kinase Ire1p is a site-specific endonuclease that initiates mRNA splicing in the unfolded protein response. Cell *90*, 1031–1039.

Sidrauski, C., Cox, J.S., and Walter, P. (1996). tRNA ligase is required for regulated mRNA splicing in the unfolded protein response. Cell *87*, 405–413.

Smith, M.H., Ploegh, H.L., and Weissman, J.S. (2011). Road to Ruin: Targeting Proteins for Degradation in the Endoplasmic Reticulum. Science *334*, 1086–1090.

So, J.-S., Hur, K.Y., Tarrio, M., Ruda, V., Frank-Kamenetsky, M., Fitzgerald, K., Koteliansky, V., Lichtman, A.H., Iwawaki, T., Glimcher, L.H., et al. (2012). Silencing of Lipid Metabolism Genes through IRE1α-Mediated mRNA Decay Lowers Plasma Lipids in Mice. Cell Metab. *16*, 487–499.

Sone, M., Zeng, X., Larese, J., and Ryoo, H.D. (2013). A modified UPR stress sensing system reveals a novel tissue distribution of IRE1/XBP1 activity during normal Drosophila development. Cell Stress Chaperones *18*, 307–319.

Souid, S., Lepesant, J.-A., and Yanicostas, C. (2007). The xbp-1 gene is essential for development in Drosophila. Dev. Genes Evol. *217*, 159–167.

Spik, G., Haendler, B., Delmas, O., Mariller, C., Chamoux, M., Maes, P., Tartar, A., Montreuil, J., Stedman, K., and Kocher, H.P. (1991). A novel secreted cyclophilin-like protein (SCYLP). J. Biol. Chem. *266*, 10735–10738.

Sriburi, R., Jackowski, S., Mori, K., and Brewer, J.W. (2004). XBP1: a link between the unfolded protein response, lipid biosynthesis, and biogenesis of the endoplasmic reticulum. J. Cell Biol. *167*, 35–41.

Stamnes, M.A., Shieh, B.H., Chuman, L., Harris, G.L., and Zuker, C.S. (1991). The cyclophilin homolog ninaA is a tissue-specific integral membrane protein required for the proper synthesis of a subset of Drosophila rhodopsins. Cell *65*, 219–227.

Von Stein, W., Ramrath, A., Grimm, A., Müller-Borg, M., and Wodarz, A. (2005). Direct association of Bazooka/PAR-3 with the lipid phosphatase PTEN reveals a link between the PAR/aPKC complex and phosphoinositide signaling. Dev. Camb. Engl. *132*, 1675–1686.

Stolz, A., Hilt, W., Buchberger, A., and Wolf, D.H. (2011). Cdc48: a power machine in protein degradation. Trends Biochem. Sci. *36*, 515–523.

Tepass, U., Theres, C., and Knust, E. (1990). crumbs encodes an EGF-like protein expressed on apical membranes of Drosophila epithelial cells and required for organization of epithelia. Cell *61*, 787–799.

Tirasophon, W., Welihinda, A.A., and Kaufman, R.J. (1998). A stress response pathway from the endoplasmic reticulum to the nucleus requires a novel bifunctional protein kinase/endoribonuclease (Ire1p) in mammalian cells. Genes Dev. *12*, 1812–1824.

Travers, K.J., Patil, C.K., Wodicka, L., Lockhart, D.J., Weissman, J.S., and Walter, P. (2000). Functional and genomic analyses reveal an essential coordination between the unfolded protein response and ER-associated degradation. Cell *101*, 249–258.

Urano, F., Wang, X., Bertolotti, A., Zhang, Y., Chung, P., Harding, H.P., and Ron, D. (2000). Coupling of stress in the ER to activation of JNK protein kinases by transmembrane protein kinase IRE1. Science *287*, 664–666.

Ushioda, R., Hoseki, J., Araki, K., Jansen, G., Thomas, D.Y., and Nagata, K. (2008). ERdj5 is required as a disulfide reductase for degradation of misfolded proteins in the ER. Science *321*, 569–572.

Vattem, K.M., and Wek, R.C. (2004). Reinitiation involving upstream ORFs regulates ATF4 mRNA translation in mammalian cells. Proc. Natl. Acad. Sci. U. S. A. *101*, 11269–11274.

Vecchi, C., Montosi, G., Zhang, K., Lamberti, I., Duncan, S.A., Kaufman, R.J., and Pietrangelo, A. (2009). ER stress controls iron metabolism through induction of hepcidin. Science *325*, 877–880.

Wang, S., and Kaufman, R.J. (2012). The impact of the unfolded protein response on human disease. J. Cell Biol. *197*, 857–867.

Wang, X.Z., Harding, H.P., Zhang, Y., Jolicoeur, E.M., Kuroda, M., and Ron, D. (1998). Cloning of mammalian Ire1 reveals diversity in the ER stress responses. EMBO J. *17*, 5708–5717.

Wang, Y., Shen, J., Arenzana, N., Tirasophon, W., Kaufman, R.J., and Prywes, R. (2000). Activation of ATF6 and an ATF6 DNA binding site by the endoplasmic reticulum stress response. J. Biol. Chem. *275*, 27013–27020.

Webel, R., Menon, I., O'Tousa, J.E., and Colley, N.J. (2000). Role of asparagine-linked oligosaccharides in rhodopsin maturation and association with its molecular chaperone, NinaA. J. Biol. Chem. *275*, 24752–24759.

Welihinda, A.A., and Kaufman, R.J. (1996). The unfolded protein response pathway in Saccharomyces cerevisiae. Oligomerization and trans-phosphorylation of Ire1p (Ern1p) are required for kinase activation. J. Biol. Chem. *271*, 18181–18187.

Wickner, W., and Schekman, R. (2005). Protein translocation across biological membranes. Science *310*, 1452–1456.

Wiseman, R.L., Zhang, Y., Lee, K.P.K., Harding, H.P., Haynes, C.M., Price, J., Sicheri, F., and Ron, D. (2010). Flavonol Activation Defines an Unanticipated Ligand-Binding Site in the Kinase-RNase Domain of IRE1. Mol. Cell *38*, 291–304.

Wolf, T., and Ready, D.F. (1993). Pattern formation in the Drosophila retina. In The Development of Drosophila Melanogaster, M. Bate, and A.M. Arias, eds. (New York: Cold Spring Harbor Laboratory Press), pp. 1277–1325.

Yamamoto, K., Sato, T., Matsui, T., Sato, M., Okada, T., Yoshida, H., Harada, A., and Mori, K. (2007). Transcriptional induction of mammalian ER quality control proteins is mediated by single or combined action of ATF6alpha and XBP1. Dev. Cell *13*, 365–376.

Yan, W., Frank, C.L., Korth, M.J., Sopher, B.L., Novoa, I., Ron, D., and Katze, M.G. (2002). Control of PERK eIF2 kinase activity by the endoplasmic reticulum stress-induced molecular chaperone P58IPK. Proc. Natl. Acad. Sci. *99*, 15920–15925.

Yanagitani, K., Imagawa, Y., Iwawaki, T., Hosoda, A., Saito, M., Kimata, Y., and Kohno, K. (2009). Cotranslational targeting of XBP1 protein to the membrane promotes cytoplasmic splicing of its own mRNA. Mol. Cell *34*, 191–200.

Yanagitani, K., Kimata, Y., Kadokura, H., and Kohno, K. (2011). Translational pausing ensures membrane targeting and cytoplasmic splicing of XBP1u mRNA. Science *331*, 586–589.

Ye, J., Rawson, R.B., Komuro, R., Chen, X., Davé, U.P., Prywes, R., Brown, M.S., and Goldstein, J.L. (2000). ER stress induces cleavage of membrane-bound ATF6 by the same proteases that process SREBPs. Mol. Cell *6*, 1355–1364.

Yoshida, H. (1998). Identification of the cis-Acting Endoplasmic Reticulum Stress Response Element Responsible for Transcriptional Induction of Mammalian Glucose-regulated Proteins. INVOLVEMENT OF BASIC LEUCINE ZIPPER TRANSCRIPTION FACTORS. J. Biol. Chem. *273*, 33741–33749.

Yoshida, H., Okada, T., Haze, K., Yanagi, H., Yura, T., Negishi, M., and Mori, K. (2000). ATF6 Activated by Proteolysis Binds in the Presence of NF-Y (CBF) Directly to the cis-Acting Element Responsible for the Mammalian Unfolded Protein Response. Mol. Cell. Biol. *20*, 6755–6767.

Yoshida, H., Matsui, T., Yamamoto, A., Okada, T., and Mori, K. (2001). XBP1 mRNA is induced by ATF6 and spliced by IRE1 in response to ER stress to produce a highly active transcription factor. Cell *107*, 881–891.

Yoshida, H., Matsui, T., Hosokawa, N., Kaufman, R.J., Nagata, K., and Mori, K. (2003). A Time-Dependent Phase Shift in the Mammalian Unfolded Protein Response. Dev. Cell *4*, 265–271.

Yoshida, H., Oku, M., Suzuki, M., and Mori, K. (2006). pXBP1(U) encoded in XBP1 pre-mRNA negatively regulates unfolded protein response activator pXBP1(S) in mammalian ER stress response. J. Cell Biol. *172*, 565–575.

Zelhof, A.C., Hardy, R.W., Becker, A., and Zuker, C.S. (2006). Transforming the architecture of compound eyes. Nature *443*, 696–699.

Zhang, C., Wang, G., Zheng, Z., Maddipati, K.R., Zhang, X., Dyson, G., Williams, P., Duncan, S.A., Kaufman, R.J., and Zhang, K. (2012). Endoplasmic reticulum-tethered transcription factor cAMP responsive element-binding protein, hepatocyte specific, regulates hepatic lipogenesis, fatty acid oxidation, and lipolysis upon metabolic stress in mice. Hepatology *55*, 1070–1082.

Zhang, K., Wong, H.N., Song, B., Miller, C.N., Scheuner, D., and Kaufman, R.J. (2005). The unfolded protein response sensor IRE1α is required at 2 distinct steps in B cell lymphopoiesis. J. Clin. Invest. *115*, 268–281.

Zhang, K., Shen, X., Wu, J., Sakaki, K., Saunders, T., Rutkowski, D.T., Back, S.H., and Kaufman, R.J. (2006). Endoplasmic reticulum stress activates cleavage of CREBH to induce a systemic inflammatory response. Cell *124*, 587–599.

Zhang, P., McGrath, B., Li, S., Frank, A., Zambito, F., Reinert, J., Gannon, M., Ma, K., McNaughton, K., and Cavener, D.R. (2002). The PERK eukaryotic initiation factor 2 alpha kinase is required for the development of the skeletal system, postnatal growth, and the function and viability of the pancreas. Mol. Cell. Biol. *22*, 3864–3874.

Zhou, J., Liu, C.Y., Back, S.H., Clark, R.L., Peisach, D., Xu, Z., and Kaufman, R.J. (2006). The crystal structure of human IRE1 luminal domain reveals a conserved dimerization interface required for activation of the unfolded protein response. Proc. Natl. Acad. Sci. U. S. A. *103*, 14343–14348.